SOMATOMOTOR FUNCTIONING IN MARMOSETS AND THE EVOLUTION OF SPINAL CORDS IN PRIMATES

By

Mark J. Burish

Dissertation

Submitted to the Faculty of the

Graduate School of Vanderbilt University

in partial fulfillment of the requirements

for the degree of

DOCTOR OF PHILOSOPHY

in

Neuroscience

August, 2008

Nashville, Tennessee

Approved:

Dr. Jon H. Kaas

Dr. Kenneth C. Catania

Dr. Troy A. Hackett

Dr. Anna W. Roe

ACKNOWLEDGMENTS

I first thank Dr. Jon Kaas for his role as my advisor and mentor. To his students Jon is truly always available, he is incredibly supportive, and he gives an extraordinary amount of independence. Jon encouraged me to pursue several collaborations, let me get involved in teaching opportunities, and allowed me to make my own mistakes, all of which helped me develop more fully as an academic scientist. Jon was very generous in taking a chance on an MD/PhD student with demands from a second program, and I am grateful for that. He fostered my scientific and personal growth in ways I could never have imagined. I credit him with expanding my knowledge, curiosity, and analytical abilities.

The lab members have been similarly supportive, and I could not have asked for a better laboratory environment. I especially thank Mike Remple and Iwona Stepniewska, my mentors within the lab who got me on my feet and continue to give me advice. Special thanks also go to Omar Gharbawie, Huixin Qi, Charnese Bowes, and Klint Peebles, who helped me continue my research and provided me with a great deal of time, energy, and skill. And thanks to Peiyan Wong, who joined Jon's lab with me, shared an office with me, and has generally put up with me over the years.

For the spinal cord scaling project I am grateful for the expertise of Christine Collins from the Kaas lab and Suzana Herculano-Houzel from the Universidade Federal do Rio de Janeiro. For the marmoset studies I am grateful for the expertise of Mary Feurtado, Laura Trice, and Mary Varghese. I thank another collaborator, James Massey from the University of Louisville, who pushed me to investigate squirrel monkeys and

therapeutics, and who gave me a lot of helpful med school advice. Within the lab I thank Jamie Reed, Corrie Camalier, Lisa de la Mothe, and Peter Kaskan, who I would occasionally bother for wisdom, and Mary Baldwin and Christina Cerkevich, who I would occasionally bother for help with experiments.

I also thank my committee members Ken Catania, Troy Hackett, and Anna Roe. They have been very understanding of my added medical school requirements, and integral in keeping me on track. More importantly, they have gone out of their way between committee meetings to be involved in my research, offering advice, technical support, and the occasional tissue sample for the spinal cord project.

Finally I thank my parents for everything. They gave me every opportunity in the world and they believed in me; that's a powerful combination.

TABLE OF CONTENTS

Page

LIST OF TABLES

LIST OF FIGURES

LIST OF ABBREVIATIONS

Cortical Areas

1/2	Areas 1 and 2
3a	Area 3a
3b	Area 3b (primary somatosensory cortex)
6d	Area 6d
6dr	Area 6dr
6m	Area 6m
6v	Area 6v
M1	Primary motor cortex
PMD	Premotor dorsal area
PMV	Premotor ventral area
PV	Parietal ventral area
SMA	Supplementary motor area
SII or S2	Secondary somatosensory cortex

Evoked movements

A	Ankle
b (prefix)	bilateral
C	Cheek
d (prefix)	distal
D	Digit (finger)
D5	Digit 5 (pinky)
do (prefix)	dorsal
Ea	Ear
Ed	Eyelid
El	Elbow
FA	Face (Chapter II) or Forearm (Chapter III)
FL	Forelimb
H	Hip
HA	Hand
HL	Hindlimb
i (prefix)	ipsilateral
J	Jaw
K	Knee
LL	Lower lip
LT	Lower trunk
m (prefix)	middle
Ne	Neck
No	Nose
p (prefix)	proximal
P	Pad on hand
Pa	Palm
PTh	Thenar pad
PH	Hypothenar pad
ra (prefix)	Radial
S	Shoulder
Ta	Tail
Th	Throat
To	Toe (Chapter II) or Tongue (Chapter III)
Tr	Trunk

Evoked movements (continued)

UL	Upper lip
UT	Upper trunk
V	Vibrissa
W or Wr	Wrist

Spinal scaling

BO	Body
BS/Thal	All parts of brain except cortex and cerebellum
Cbl	Cerebellum
Ctx	Cortex
D	Density
M	Mass
N	Number or spinal neurons
NN	Spinal non-neurons
SC	Spinal cord

CHAPTER I

INTRODUCTION

Overview

Our understanding of the central nervous system in humans is based in large part on studies of the CNS in other primates. The more species that show a specific trait (such as the existence of primary motor cortex) or proportionality (such as the ratio of brain size to body size), the more confident we are that the trait or proportionality has been evolutionarily preserved and may be present in all primates. For this comparative approach to understanding evolution we prefer to investigate a range of well-studied animals throughout the phylogenic tree, as opposed to concentrating on a few intensely-studied model species (Preuss, 2000).

With the comparative approach in mind, this dissertation is divided into three projects presented in three different chapters. The first two are investigations of marmoset frontoparietal cortex: firstly the normal organization, measured by intracortical microstimulation (chapter two), and secondly the abnormal organization after spinal cord lesion, measured by multiunit recordings (chapter three). During the examination of spinal cord lesions, there were questions about how the spinal cord was organized, how marmoset spinal cords compared to other primates. Since physiologic studies of the spinal cord have proven difficult both in personal experience (unpublished) and in a previous primate study (Moritz et al., 2007), I instead turned my attention to a more general examination of spinal cords. Thus the third project is a comparative

analysis of the cellular organization of spinal cords in several primate species (chapter four).

A brief overview of the three projects is provided in this introduction, with a more detailed introduction provided within each chapter. The final chapter of the dissertation is a summary of the findings for all three projects.

Frontoparietal cortex

For the purposes of this dissertation, frontoparietal cortex is defined as the cortical region between prefrontal cortex (Brodmann's areas 8, 45 and all frontal areas rostral to it) and posterior parietal cortex (Brodmann's area 5 and all parietal areas caudal to it) (Brodmann, 1909). It is composed essentially of Brodmann's areas 6, 4, 3, 1, and 2, several motor and somatosensory areas surrounding the central sulcus or dimple in primates. The motor areas rostral to the central sulcus or dimple include two regions. The first is primary motor cortex, a single highly excitable area encoding late-stage movements (Kaas and Stepniewska, 2002; Umilta et al., 2007). The second is a collection of premotor areas, which can be divided into at least three areas (Luppino and Rizzolatti, 2000): the supplementary motor area, involved in movement planning (Donoghue and Sanes, 1994); the premotor dorsal area, involved in reaching and the combination of spatial, visual, and somatosensory inputs (Wise et al., 1997); and the premotor ventral area, involved in grasping and control of the hand (Kurata, 2007). The somatosensory areas caudal to the central sulcus or dimple include at least three regions. The first is area 3a, which mainly encodes proprioceptive information from muscle spindle and other deep receptors (Kaas, 2004b). The second is area 3b, which mainly

encodes tactile or cutaneous information (Kaas, 1983). The third is a region caudal to area 3b which, depending on the species, may be a combination of area 1, which responds to cutaneous stimulation, and area 2, which responds to proprioceptive stimulation (Kaas, 1983; Padberg et al., 2007). Frontoparietal cortex can be expanded slightly to include other areas, such as the frontal eye field and the lateral somatosensory areas S2 and PV, but these areas are not the focus of chapters two and three.

Marmoset cortex

Common marmosets (*Callithrix jacchus*) are small primates belonging to the New World monkey branch of arthopoid primates (Fig. 1), and are in an interesting evolutionary position because of their size. Marmosets are smaller than most primates, ranging from 100-750g (Fleagle, 1999). Older reports view marmosets as monkeys that might resemble the size and features of the original primate ancestor (Herschkovitz 1977, Beattie 1927, Le Gros Clark 1937). However, the majority of recent reports view marmosets as a dwarfed species, having reduced in size from a larger primate ancestor (Bloch and Boyer, 2002; Ford and Davis, 1992; Sussman and Kinzey, 1984). In dwarfed species, the reduction in body size leads to a corresponding decrease in brain size (Jerison, 1973). This reduction in brain size may in turn lead to modifications in cortical organization. Modifications can occur in a number of ways including: 1) changes in the amount of cortex devoted to a particular system such as the motor system, 2) changes in the amount of cortex devoted a particular body part within a system, 3) changes in the number of cortical areas, 4) changes in the types of cortical and subcortical connections, and 5) the addition/subtraction of modules (Krubitzer and Kaas, 2005).

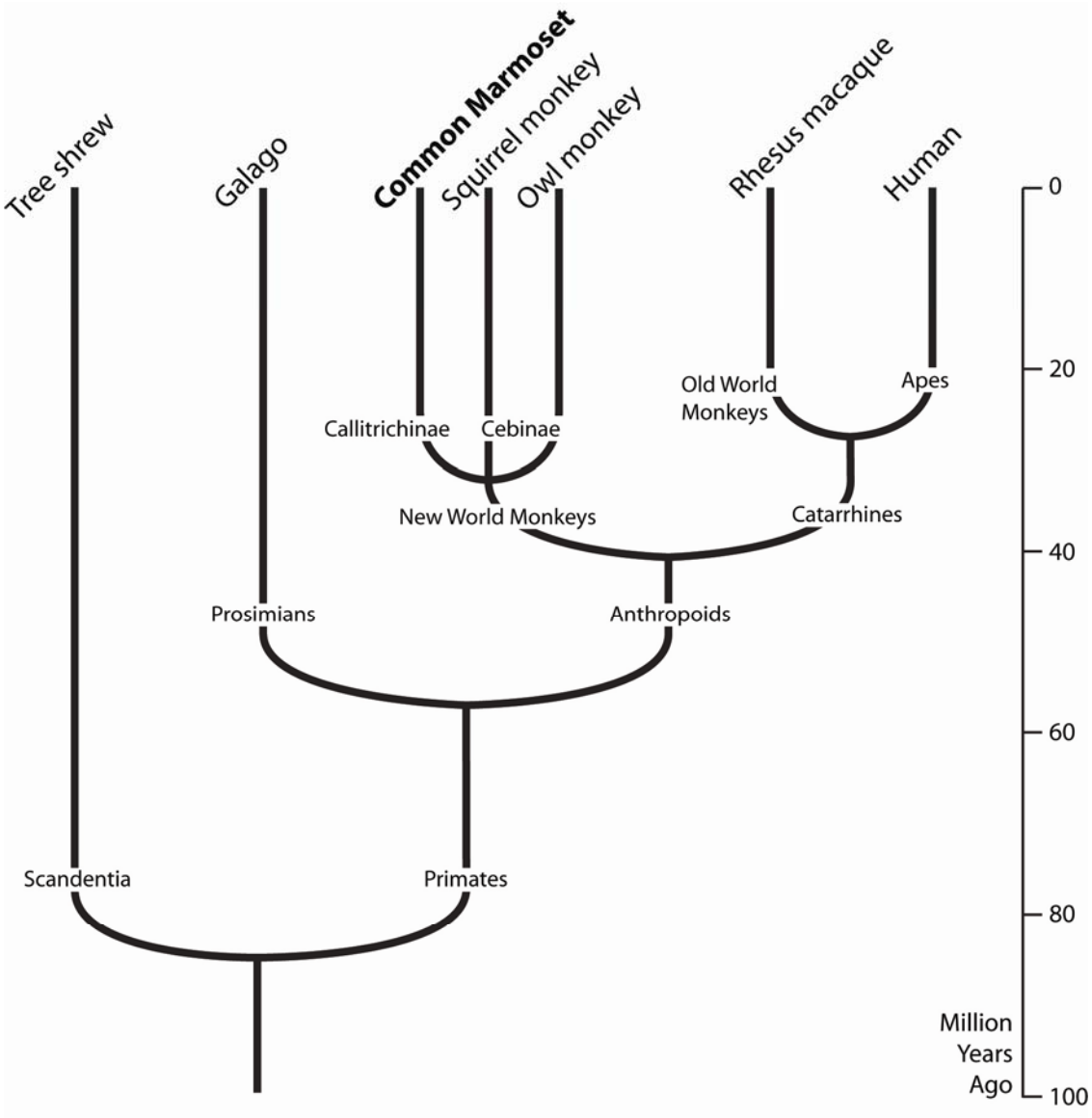

Figure 1. Phylogeny of primates and tree shrews, based on Purvis (1995) and Murphy et al. (2001).

Motor cortex has undergone a significant amount of modification between the earliest mammals, who appear to lack a primary motor cortex (Beck et al., 1996; Frost et al., 2000), rodents and tree shrews, who appear to have two motor areas (Donoghue and Wise, 1982; Neafsey and Sievert, 1982; Remple et al., 2006; Remple et al., 2007), prosimian and New World monkeys, who have several motor areas (Kaas, 2004a; Stepniewska et al., 1993; Wu and Kaas, 2003), and Old World monkeys, who have several motor areas (Matelli et al., 1985; Matelli et al., 1991; Rizzolatti et al., 1998) and have subdivisions within each motor area (Preuss et al., 1997; Stepniewska et al., 2006). Somatosensory cortex has likewise undergone a great deal of modification between the earliest mammals, with five somatosensory areas and parallel thalamic projections, rodents, with a primary somatosensory area but no identifiable areas 3a, 1, or 2 (Kaas, 1983), and New World and Old World monkeys, with areas 3b, 3a, 1, 2, and serial processing from the thalamus (Kaas, 2004a). Due to this variability in somatomotor systems across mammals, the organization of motor cortex in a dwarfed primate, as well as somatosensory reorganization following dorsal column injury, is of particular interest.

Common marmosets are one of the few well-studied members of the Callithricidae family of marmosets and tamarins (Fleagle, 1999; Murphy et al., 2001; Purvis, 1995). Many aspects of visual cortex (Fritsches and Rosa, 1996; Lui et al., 2006; Lyon and Kaas, 2001; Rosa and Elston, 1998; Rosa et al., 1997; Rosa et al., 2005; Sengpiel et al., 1996), somatosensory cortex (Huffman and Krubitzer, 2001a; Huffman and Krubitzer, 2001b; Krubitzer and Kaas, 1990; Krubitzer and Kaas, 1992; Qi et al., 2002), and auditory cortex (Aitkin et al., 1988; Aitkin et al., 1986; de la Mothe et al., 2006a; de la Mothe et al., 2006b; Kajikawa et al., 2005; Kajikawa et al., 2008; Philibert et

al., 2005) have been explored in this species, as well as some aspects of the prefrontal cortex (Burman et al., 2006; Dias et al., 1996; Roberts and Wallis, 2000). Their sociality and behavior have been observed (Addessi et al., 2007; Burkart et al., 2007; Kaplan and Rogers, 2006; Lazaro-Perea et al., 2004; Przybyszewski et al., 2007), and marmosets have been used as models of spinal injury (Iwanami et al., 2005) and Parkinsonism (Jenner, 2004; Jenner et al., 1984; Kupsch et al., 2001; Nomoto et al., 1986). Despite all of these investigations, the normal organization of the motor system in marmosets largely has not been examined. While studies of connectivity (Huffman and Krubitzer, 2001a; Huffman and Krubitzer, 2001b; Krubitzer and Kaas, 1990; Qi et al., 2002), and brief examinations of architecture (Burman et al., 2006; Huffman and Krubitzer, 2001a) have been performed, motor physiology has been studied only in one older paper (Mott et al., 1909), and the methods of cortical stimulation have since been refined. I focused on the physiology and architecture of frontoparietal cortex, which is the region of cortex with the majority of corticospinal projections (Canedo, 1997; Nudo and Masterton, 1988; Nudo et al., 1995). Our investigation (Burish et al., 2008), along with an investigation published concurrently (Burman et al., 2008), provides a more complete picture of how the somatomotor cortical system of marmosets is arranged.

After understanding the normal organization of frontoparietal cortex, I was interested in how cortical organization changes following injury. Cortical zones that lose peripheral input, such as the arm representation in somatosensory cortex after limb amputation, do not remain silent. Instead cortical plasticity occurs, and cortical zones adjacent to the arm such as the face and trunk enlarge to fill in the silent zone. Previous work on this type of cortical reorganization in primates has been performed following a

range of injuries, such as nerve cuts (Garraghty et al., 1994; Garraghty and Kaas, 1991; Kolarik et al., 1994; Merzenich et al., 1983a; Merzenich et al., 1983b; Silva et al., 1996), amputations (Florence and Kaas, 1995; Florence et al., 1998; Merzenich et al., 1984), rhizotomies or dorsal root cuts (Darian-Smith, 2004; Darian-Smith and Brown, 2000; Pons et al., 1991), and dorsal column lesions (Jain et al., 1997). Little work, however, has been performed in the Callithricidae family. Our method examined injury to the dorsal columns of the spinal cord, the major spinal pathway conveying somatosensory information to the cortex about fine touch, vibration, and proprioception (the position of the limbs in space). Previous work on dorsal column injury has been limited, investigated only in rats (Jain et al., 1995) and owl monkeys (Jain et al., 1997), and observed in humans (Moore et al., 2000). Recovery from such an injury has important implications for several human disorders that target the dorsal columns: traumatic injury (Jackson et al., 2004), autoimmune disorders such as multiple sclerosis (Ropper et al., 2005), congenital diseases such as Friedreich ataxia (Kasper and Harrison, 2005), metabolic diseases such as vitamin B_{12} deficency (Ropper et al., 2005), and infections such as HIV (Petito et al., 1985), HTLV-1 (Osame et al., 1986), and syphilis (Kasper and Harrison, 2005). As such, it is important for us to improve our understanding of the dorsal column injury in animal models.

Spinal cord scaling

There are certain relationships, such as brain size to body size (Jerison, 1973) or cortical gray matter volume to cortical neuron density (Prothero, 1997), which are relatively constant in mammals. Animals with larger bodies have larger brains, and

animals with more gray matter have a lower neuron density. Using the known ratios for these relationships, for example, it is possible to predict a given species' neuron density if we know its gray matter volume. Interesting cases arise when animals deviate significantly from the standard ratio. Primates, for example, have abnormally large brains for their body size.

These relationships can be expressed mathematically as straight lines on logarithmic plots. The mathematical plots of biological relationships are called allometric scaling rules, as they seem to dictate certain proportionalities in all mammals. The mathematical plots offer no biological explanations and so are open to interpretation. For example, the abnormally large brains of primates, and of humans in particular, have been proposed as a source of increased intelligence and social complexity (Barton and Dunbar, 1997).

In terms of the central nervous system, many allometric scaling rules have been proposed (Changizi, 2001). These rules generally focus on the brain, especially the cortex. In comparison, there has been much less investigation into scaling rules of the spinal cord.

References

Addessi E, Chiarotti F, Visalberghi E, Anzenberger G. 2007. Response to novel food and the role of social influences in common marmosets (Callithrix jacchus) and Goeldi's monkeys (Callimico goeldii). Am J Primatol 69(11):1210-1222.

Aitkin LM, Kudo M, Irvine DR. 1988. Connections of the primary auditory cortex in the common marmoset, Callithrix jacchus jacchus. J Comp Neurol 269(2):235-248.

Aitkin LM, Merzenich MM, Irvine DR, Clarey JC, Nelson JE. 1986. Frequency representation in auditory cortex of the common marmoset (Callithrix jacchus jacchus). J Comp Neurol 252(2):175-185.

Barton RA, Dunbar RIM. 1997. Evolution of the social brain. In: Whiten AW, Byrne RW, editors. Machiavellian Intelligence II: Evaluations and Extenstions. New York: Cambridge University Press. p 240-263.

Beck PD, Pospichal MW, Kaas JH. 1996. Topography, architecture, and connections of somatosensory cortex in opossums: evidence for five somatosensory areas. J Comp Neurol 366(1):109-133.

Bloch JI, Boyer DM. 2002. Grasping primate origins. Science 298(5598):1606-1610.

Brodmann, 1909. Vergleichende Lokalisationslehre der Grosshirnrhinde. Leipzig: Barth. Translated by Garey LJ, 1994, as "Localisation in the Cerebral Cortex"; London: Smith-Gorden.

Burish MJ, Stepniewska I, Kaas JH. 2008. Microstimulation and architectonics of frontoparietal cortex in common marmosets (Callithrix jacchus). J Comp Neurol 507(2):1151-1168.

Burkart JM, Fehr E, Efferson C, van Schaik CP. 2007. Other-regarding preferences in a non-human primate: common marmosets provision food altruistically. Proc Natl Acad Sci U S A 104(50):19762-19766.

Burman KJ, Palmer SM, Gamberini M, Rosa MG. 2006. Cytoarchitectonic subdivisions of the dorsolateral frontal cortex of the marmoset monkey (Callithrix jacchus), and their projections to dorsal visual areas. J Comp Neurol 495(2):149-172.

Burman KJ, Palmer SM, Gamberini M, Spitzer MW, Rosa MG. 2008. Anatomical and physiological definition of the motor cortex of the marmoset monkey. J Comp Neurol 506(5):860-876.

Canedo A. 1997. Primary motor cortex influences on the descending and ascending systems. Prog Neurobiol 51(3):287-335.

Changizi MA. 2001. Principles underlying mammalian neocortical scaling. Biol Cybern 84(3):207-215.

Darian-Smith C. 2004. Primary afferent terminal sprouting after a cervical dorsal rootlet section in the macaque monkey. J Comp Neurol 470(2):134-150.

Darian-Smith C, Brown S. 2000. Functional changes at periphery and cortex following dorsal root lesions in adult monkeys. Nat Neurosci 3(5):476-481.

de la Mothe LA, Blumell S, Kajikawa Y, Hackett TA. 2006a. Cortical connections of the auditory cortex in marmoset monkeys: core and medial belt regions. J Comp Neurol 496(1):27-71.

de la Mothe LA, Blumell S, Kajikawa Y, Hackett TA. 2006b. Thalamic connections of the auditory cortex in marmoset monkeys: core and medial belt regions. J Comp Neurol 496(1):72-96.

Dias R, Robbins TW, Roberts AC. 1996. Dissociation in prefrontal cortex of affective and attentional shifts. Nature 380(6569):69-72.

Donoghue JP, Sanes JN. 1994. Motor areas of the cerebral cortex. J Clin Neurophysiol 11(4):382-396.

Donoghue JP, Wise SP. 1982. The motor cortex of the rat: cytoarchitecture and microstimulation mapping. J Comp Neurol 212(1):76-88.

Fleagle JG. 1999. Primate adaptation and evolution. San Diego: Academic Press. xvii, 596 p. p.

Florence SL, Kaas JH. 1995. Large-scale reorganization at multiple levels of the somatosensory pathway follows therapeutic amputation of the hand in monkeys. J Neurosci 15(12):8083-8095.

Florence SL, Taub HB, Kaas JH. 1998. Large-scale sprouting of cortical connections after peripheral injury in adult macaque monkeys. Science 282(5391):1117-1121.

Ford SM, Davis LC. 1992. Systematics and body size: implications for feeding adaptations in New World monkeys. Am J Phys Anthropol 88(4):415-468.

Fritsches KA, Rosa MG. 1996. Visuotopic organisation of striate cortex in the marmoset monkey (Callithrix jacchus). J Comp Neurol 372(2):264-282.

Frost SB, Milliken GW, Plautz EJ, Masterton RB, Nudo RJ. 2000. Somatosensory and motor representations in cerebral cortex of a primitive mammal (Monodelphis domestica): a window into the early evolution of sensorimotor cortex. J Comp Neurol 421(1):29-51.

Garraghty PE, Hanes DP, Florence SL, Kaas JH. 1994. Pattern of peripheral deafferentation predicts reorganizational limits in adult primate somatosensory cortex. Somatosens Mot Res 11(2):109-117.

Garraghty PE, Kaas JH. 1991. Large-scale functional reorganization in adult monkey cortex after peripheral nerve injury. Proc Natl Acad Sci U S A 88(16):6976-6980.

Huffman KJ, Krubitzer L. 2001a. Area 3a: topographic organization and cortical connections in marmoset monkeys. Cereb Cortex 11(9):849-867.

Huffman KJ, Krubitzer L. 2001b. Thalamo-cortical connections of areas 3a and M1 in marmoset monkeys. J Comp Neurol 435(3):291-310.

Iwanami A, Yamane J, Katoh H, Nakamura M, Momoshima S, Ishii H, Tanioka Y, Tamaoki N, Nomura T, Toyama Y, Okano H. 2005. Establishment of graded spinal cord injury model in a nonhuman primate: the common marmoset. J Neurosci Res 80(2):172-181.

Jackson AB, Dijkers M, Devivo MJ, Poczatek RB. 2004. A demographic profile of new traumatic spinal cord injuries: change and stability over 30 years. Arch Phys Med Rehabil 85(11):1740-1748.

Jain N, Catania KC, Kaas JH. 1997. Deactivation and reactivation of somatosensory cortex after dorsal spinal cord injury. Nature 386(6624):495-498.

Jain N, Florence SL, Kaas JH. 1995. Limits on plasticity in somatosensory cortex of adult rats: hindlimb cortex is not reactivated after dorsal column section. J Neurophysiol 73(4):1537-1546.

Jenner P. 2004. Preclinical evidence for neuroprotection with monoamine oxidase-B inhibitors in Parkinson's disease. Neurology 63(7 Suppl 2):S13-22.

Jenner P, Rupniak NM, Rose S, Kelly E, Kilpatrick G, Lees A, Marsden CD. 1984. 1-Methyl-4-phenyl-1,2,3,6-tetrahydropyridine-induced parkinsonism in the common marmoset. Neurosci Lett 50(1-3):85-90.

Jerison HJ. 1973. Evolution of the brain and intelligence. New York: Academic Press. xiv, 482 p. p.

Kaas JH. 1983. What, if anything, is SI? Organization of first somatosensory area of cortex. Physiol Rev 63(1):206-231.

Kaas JH. 2004a. Evolution of somatosensory and motor cortex in primates. Anat Rec A Discov Mol Cell Evol Biol 281(1):1148-1156.

Kaas JH. 2004b. Somatosensory Systen. In: Paxinos G, Mai JK, editors. The human nervous system. 2nd ed. Amsterdam; Boston: Elsevier Academic Press. p xvii, 1366 p.

Kaas JH, Stepniewska I. 2002. Motor Cortex. Ramachandran VS, editor. San Diego: Academic Press.

Kajikawa Y, de La Mothe L, Blumell S, Hackett TA. 2005. A comparison of neuron response properties in areas A1 and CM of the marmoset monkey auditory cortex: tones and broadband noise. J Neurophysiol 93(1):22-34.

Kajikawa Y, de la Mothe LA, Blumell S, Sterbing-D'Angelo SJ, D'Angelo W, Camalier CR, Hackett TA. 2008. Coding of FM sweep trains and twitter calls in area CM of marmoset auditory cortex. Hear Res.

Kaplan G, Rogers LJ. 2006. Head-cocking as a form of exploration in the common marmoset and its development. Dev Psychobiol 48(7):551-560.

Kasper DL, Harrison TR. 2005. Harrison's principles of internal medicine. New York: McGraw-Hill, Medical Pub. Division. 2 v. p.

Kolarik RC, Rasey SK, Wall JT. 1994. The consistency, extent, and locations of early-onset changes in cortical nerve dominance aggregates following injury of nerves to primate hands. J Neurosci 14(7):4269-4288.

Krubitzer L, Kaas J. 2005. The evolution of the neocortex in mammals: how is phenotypic diversity generated? Curr Opin Neurobiol 15(4):444-453.

Krubitzer LA, Kaas JH. 1990. The organization and connections of somatosensory cortex in marmosets. J Neurosci 10(3):952-974.

Krubitzer LA, Kaas JH. 1992. The somatosensory thalamus of monkeys: cortical connections and a redefinition of nuclei in marmosets. J Comp Neurol 319(1):123-140.

Kupsch A, Sautter J, Gotz ME, Breithaupt W, Schwarz J, Youdim MB, Riederer P, Gerlach M, Oertel WH. 2001. Monoamine oxidase-inhibition and MPTP-induced neurotoxicity in the non-human primate: comparison of rasagiline (TVP 1012) with selegiline. J Neural Transm 108(8-9):985-1009.

Kurata K. 2007. Laterality of movement-related activity reflects transformation of coordinates in ventral premotor cortex and primary motor cortex of monkeys. J Neurophysiol 98(4):2008-2021.

Lazaro-Perea C, M DEFA, Snowdon CT. 2004. Grooming as a reward? Social function of grooming between females in cooperatively breeding marmosets. Anim Behav 67(4):627-636.

Lui LL, Bourne JA, Rosa MG. 2006. Functional response properties of neurons in the dorsomedial visual area of New World monkeys (Callithrix jacchus). Cereb Cortex 16(2):162-177.

Luppino G, Rizzolatti G. 2000. The Organization of the Frontal Motor Cortex. News Physiol Sci 15:219-224.

Lyon DC, Kaas JH. 2001. Connectional and architectonic evidence for dorsal and ventral V3, and dorsomedial area in marmoset monkeys. J Neurosci 21(1):249-261.

Matelli M, Luppino G, Rizzolatti G. 1985. Patterns of cytochrome oxidase activity in the frontal agranular cortex of the macaque monkey. Behav Brain Res 18(2):125-136.

Matelli M, Luppino G, Rizzolatti G. 1991. Architecture of superior and mesial area 6 and the adjacent cingulate cortex in the macaque monkey. J Comp Neurol 311(4):445-462.

Merzenich MM, Kaas JH, Wall J, Nelson RJ, Sur M, Felleman D. 1983a. Topographic reorganization of somatosensory cortical areas 3b and 1 in adult monkeys following restricted deafferentation. Neuroscience 8(1):33-55.

Merzenich MM, Kaas JH, Wall JT, Sur M, Nelson RJ, Felleman DJ. 1983b. Progression of change following median nerve section in the cortical representation of the hand in areas 3b and 1 in adult owl and squirrel monkeys. Neuroscience 10(3):639-665.

Merzenich MM, Nelson RJ, Stryker MP, Cynader MS, Schoppmann A, Zook JM. 1984. Somatosensory cortical map changes following digit amputation in adult monkeys. J Comp Neurol 224(4):591-605.

Moore CI, Stern CE, Dunbar C, Kostyk SK, Gehi A, Corkin S. 2000. Referred phantom sensations and cortical reorganization after spinal cord injury in humans. Proc Natl Acad Sci U S A 97(26):14703-14708.

Moritz CT, Lucas TH, Perlmutter SI, Fetz EE. 2007. Forelimb movements and muscle responses evoked by microstimulation of cervical spinal cord in sedated monkeys. J Neurophysiol 97(1):110-120.

Mott FW, Schuster E, Halliburton WD. 1909. Cortical lamination and localization in the brain of the marmoset. Proc Soc London, series B 82:124-134.

Murphy WJ, Eizirik E, O'Brien SJ, Madsen O, Scally M, Douady CJ, Teeling E, Ryder OA, Stanhope MJ, de Jong WW, Springer MS. 2001. Resolution of the early placental mammal radiation using Bayesian phylogenetics. Science 294(5550):2348-2351.

Neafsey EJ, Sievert C. 1982. A second forelimb motor area exists in rat frontal cortex. Brain Res 232(1):151-156.

Nomoto M, Jenner P, Marsden CD. 1986. Alterations in motor behaviour produced by the isomers of 3-PPP in the MPTP-treated marmoset. Eur J Pharmacol 121(1):123-128.

Nudo RJ, Masterton RB. 1988. Descending pathways to the spinal cord: a comparative study of 22 mammals. J Comp Neurol 277(1):53-79.

Nudo RJ, Sutherland DP, Masterton RB. 1995. Variation and evolution of mammalian corticospinal somata with special reference to primates. J Comp Neurol 358(2):181-205.

Osame M, Usuku K, Izumo S, Ijichi N, Amitani H, Igata A, Matsumoto M, Tara M. 1986. HTLV-I associated myelopathy, a new clinical entity. Lancet 1(8488):1031-1032.

Padberg J, Franca JG, Cooke DF, Soares JG, Rosa MG, Fiorani M, Jr., Gattass R, Krubitzer L. 2007. Parallel evolution of cortical areas involved in skilled hand use. J Neurosci 27(38):10106-10115.

Petito CK, Navia BA, Cho ES, Jordan BD, George DC, Price RW. 1985. Vacuolar myelopathy pathologically resembling subacute combined degeneration in patients with the acquired immunodeficiency syndrome. N Engl J Med 312(14):874-879.

Philibert B, Beitel RE, Nagarajan SS, Bonham BH, Schreiner CE, Cheung SW. 2005. Functional organization and hemispheric comparison of primary auditory cortex in the common marmoset (Callithrix jacchus). J Comp Neurol 487(4):391-406.

Pons TP, Garraghty PE, Ommaya AK, Kaas JH, Taub E, Mishkin M. 1991. Massive cortical reorganization after sensory deafferentation in adult macaques. Science 252(5014):1857-1860.

Preuss TM. 2000. Taking the measure of diversity: comparative alternatives to the model-animal paradigm in cortical neuroscience. Brain Behav Evol 55(6):287-299.

Preuss TM, Stepniewska I, Jain N, Kaas JH. 1997. Multiple divisions of macaque precentral motor cortex identified with neurofilament antibody SMI-32. Brain Res 767(1):148-153.

Prothero J. 1997. Scaling of cortical neuron density and white matter volume in mammals. J Hirnforsch 38(4):513-524.

Przybyszewski AW, Sosale S, Chaudhuri A. 2007. Activity of common marmosets (Callithrix jacchus) in limited spaces: hand movement characteristics. J Comp Psychol 121(3):332-344.

Purvis A. 1995. A composite estimate of primate phylogeny. Philos Trans R Soc Lond B Biol Sci 348(1326):405-421.

Qi HX, Lyon DC, Kaas JH. 2002. Cortical and thalamic connections of the parietal ventral somatosensory area in marmoset monkeys (Callithrix jacchus). J Comp Neurol 443(2):168-182.

Remple MS, Reed JL, Stepniewska I, Kaas JH. 2006. Organization of frontoparietal cortex in the tree shrew (Tupaia belangeri). I. Architecture, microelectrode maps, and corticospinal connections. J Comp Neurol 497(1):133-154.

Remple MS, Reed JL, Stepniewska I, Lyon DC, Kaas JH. 2007. The organization of frontoparietal cortex in the tree shrew (Tupaia belangeri): II. Connectional evidence for a frontal-posterior parietal network. J Comp Neurol 501(1):121-149.

Rizzolatti G, Luppino G, Matelli M. 1998. The organization of the cortical motor system: new concepts. Electroencephalogr Clin Neurophysiol 106(4):283-296.

Roberts AC, Wallis JD. 2000. Inhibitory control and affective processing in the prefrontal cortex: neuropsychological studies in the common marmoset. Cereb Cortex 10(3):252-262.

Ropper AH, Adams RD, Victor M, Brown RH, Victor M. 2005. Adams and Victor's principles of neurology. New York: McGraw-Hill, Medical Pub. Division. x, 1382 p. p.

Rosa MG, Elston GN. 1998. Visuotopic organisation and neuronal response selectivity for direction of motion in visual areas of the caudal temporal lobe of the marmoset monkey (Callithrix jacchus): middle temporal area, middle temporal crescent, and surrounding cortex. J Comp Neurol 393(4):505-527.

Rosa MG, Fritsches KA, Elston GN. 1997. The second visual area in the marmoset monkey: visuotopic organisation, magnification factors, architectonical boundaries, and modularity. J Comp Neurol 387(4):547-567.

Rosa MG, Palmer SM, Gamberini M, Tweedale R, Pinon MC, Bourne JA. 2005. Resolving the organization of the New World monkey third visual complex: the dorsal extrastriate cortex of the marmoset (Callithrix jacchus). J Comp Neurol 483(2):164-191.

Sengpiel F, Troilo D, Kind PC, Graham B, Blakemore C. 1996. Functional architecture of area 17 in normal and monocularly deprived marmosets (Callithrix jacchus). Vis Neurosci 13(1):145-160.

Silva AC, Rasey SK, Wu X, Wall JT. 1996. Initial cortical reactions to injury of the median and radial nerves to the hands of adult primates. J Comp Neurol 366(4):700-716.

Stepniewska I, Preuss TM, Kaas JH. 1993. Architectonics, somatotopic organization, and ipsilateral cortical connections of the primary motor area (M1) of owl monkeys. J Comp Neurol 330(2):238-271.

Stepniewska I, Preuss TM, Kaas JH. 2006. Ipsilateral cortical connections of dorsal and ventral premotor areas in New World owl monkeys. J Comp Neurol 495(6):691-708.

Sussman RW, Kinzey WG. 1984. The ecological role of the callitrichidae: a review. Am J Phys Anthropol 64(4):419-449.

Umilta MA, Brochier T, Spinks RL, Lemon RN. 2007. Simultaneous recording of macaque premotor and primary motor cortex neuronal populations reveals different functional contributions to visuomotor grasp. J Neurophysiol 98(1):488-501.

Wise SP, Boussaoud D, Johnson PB, Caminiti R. 1997. Premotor and parietal cortex: corticocortical connectivity and combinatorial computations. Annu Rev Neurosci 20:25-42.

Wu CW, Kaas JH. 2003. Somatosensory cortex of prosimian Galagos: physiological recording, cytoarchitecture, and corticocortical connections of anterior parietal cortex and cortex of the lateral sulcus. J Comp Neurol 457(3):263-292.

CHAPTER II

MICROSTIMULATION AND ARCHITECTONICS OF FRONTOPARIETAL CORTEX IN COMMON MARMOSETS (*CALLITHRIX JACCHUS*)

This chapter is reproduced from the published work by Burish MJ, Stepniewska I, and Kaas JH. 2008. Microstimulation and architectonics of frontoparietal cortex in common marmosets (*Callithrix jacchus*). J Comp Neurol 507(2):1151-1168. It is unaltered except for deletion of the abstract and addition of an addendum at the end, which compares our work to a similar paper released concurrently.

Introduction

In this study, we compared patterns of cortically evoked movements with cortical architecture to define and characterize subdivisions of frontoparietal sensorimotor cortex in marmosets. In other primates (Dum and Strick, 1991; Preuss et al., 1996; Rizzolatti et al., 1998; Wu and Kaas, 1999), motor cortex is commonly divided into a primary motor area (M1), dorsal (PMD) and ventral (PMV) premotor areas, and a supplementary motor area (SMA). M1 is sometimes divided further into rostral and caudal divisions, as are both the dorsal and ventral premotor areas. A frontal eye field is included as a visuomotor area, and two or more motor areas have been defined in cingulate cortex of the medial wall of the cerebral hemisphere. Movements can also be elicited by electrical stimulation of area 3a of anterior parietal cortex, and sometimes of other areas of somatosensory cortex as well. The purpose of the present study was to see to what extent

the organization of motor functions in frontoparietal cortex of marmosets resembles that of other primates.

Marmosets and tamarins belong to the Callitrichidae family of New World monkeys. There are several reasons to consider the possibility that their frontoparietal motor systems differ in organization from those of other studied primates. First, Callitrichines are one of the oldest branches of the radiation of New World monkeys, diverging from the Cebinae radiation (squirrel, cebus, and owl monkeys) over 30 million years ago; another early branch led to the Atelidae family of howler, woolly, and spider monkeys (Fleagle, 1999; Purvis, 1995). It is surprising that we know very little about the cortical motor network in any member of this Callitrichine radiation, although visual (Fritsches and Rosa, 1996; Lui et al., 2006; Lyon and Kaas, 2001; Rosa and Elston, 1998; Rosa et al., 1997; Rosa et al., 2005; Sengpiel et al., 1996), auditory (Aitkin et al., 1988; Aitkin et al., 1986; de la Mothe et al., 2006a; de la Mothe et al., 2006b; Kajikawa et al., 2005; Philibert et al., 2005), and somatosensory (Huffman and Krubitzer, 2001a; Huffman and Krubitzer, 2001b; Krubitzer and Kaas, 1990b; Krubitzer and Kaas, 1992; Qi et al., 2002) cortical areas have been well studied. More importantly, marmosets are unusual primates. They are the smallest of the New World monkeys (100-750g) and have small brains (Fleagle, 1999; Herculano-Houzel et al., 2007). As brain functions and organization are related to brain size (Jerison, 1973; Kaas, 2000), one wonders what sorts of adjustments occurred in the brain as this line of primates evolved. We already know that the somatosensory cortex of Callitrichines is unusual in that the cortex caudal to area 3b is relatively unresponsive to somatosensory stimuli, at least in anesthetized animals, and there is no clear evidence for an area 2 representation (Carlson et al., 1986; Krubitzer

and Kaas, 1990b). Finally, Callitrichines have unusual locomotor adaptations. In particular, all digits except the great toe have claws rather than nails (Fleagle, 1999; Sussman and Kinzey, 1984), allowing them to cling to the sides of trees like squirrels (Cartmill, 1974). These and other features of the Callitrichine adaptation make them interesting primates for further investigation.

In this report, we focus on the somatotopy and architecture of primary motor cortex (M1) in marmosets. We also identify motor and architectural characteristics of other areas of frontoparietal cortex. A preliminary description of this research has been presented elsewhere (Burish et al., 2006).

Materials and methods

We performed intracortical microstimulation and architectural analysis on five adult common marmosets (*Callithrix jacchus jacchus*). We limited our electrode penetrations to the left hemispheres, leaving the right hemispheres unexposed and unperturbed during the microstimulation session (Table 1). All ten hemispheres were examined histologically. All procedures were approved by the Vanderbilt University Institutional Animal Care and Use Committee and followed National Institutes of Health guidelines.

Surgery and Microstimulation. Anesthesia was induced with an intramuscular injection of ketamine (30 mg/kg) and xylazine (1-2 mg/kg) followed temporarily by 2% isoflurane gas for surgical preparation and alignment in stereotaxic frame, and transferred to an intravenous ketamine infusion (20 mg/ml maintaining a surgical anesthetic level) supplemented with intramuscular xylazine (5 mg/kg). In three animals (cases 06-02,

TABLE 1. Summary of intracortical microstimulation cases[1]

Case	Plane of section	Total ICMS sites	Premotor	M1	Area 3a	Area 3b
06-35	Sagittal	172	16(23)	45(6)	18(4)	18(15)
06-27	Flat	224	15(28)	54(9)	27(3)	33(30)
06-48	Flat	226	20(31)	55(5)	36(5)	24(38)
06-13	Flat	209	16(26)	75(7)	33(5)	13(25)
06-02	Flat	150	0(9)	55(59)	6(21)	0(0)

[1]Case numbers are ordered as they appear in the paper. Weights (Wt.) are reported in grams, and Plane represents the plane of tissue sectioning. Numbers for Premotor, M1, area 3a, and area 3b represent responsive and (non-responsive) penetration points for each area of the left hemisphere. ICMS, intracortical microstimulation.

06-13, and 06-27), additional oxygen was delivered via tracheal intubation tube. In all animals, a portion of the scalp, cranium, and dura was removed over the frontal and parietal lobes in the left hemisphere and covered periodically either with saline or silicone oil to prevent desiccation.

Intracortical microstimulation was performed with low-impedance tungsten microelectrodes (Microprobe Inc., Potomac, MD). The electrode penetration sites were marked on a high resolution photograph of the exposed cortex. Individual electrode penetrations were placed into the cortex perpendicular to the pial surface at a depth of 1.6-1.8 mm, as this depth was optimal in preliminary experiments and is similar to optimal depths in other New World monkeys (Gould et al., 1986; Stepniewska et al., 1993; Wu and Kaas, 1999). For many electrode sites a range of depths were tested, from as superficial as 1.5 mm to as deep as 2.4 mm.

As marmosets have no central sulcus or dimple, the location of primary motor cortex was estimated based on bone landmarks and cortical surface vasculature, as well as on the quality of motor responses that could be elicited. Multiple penetrations were made in a grid pattern with 0.2 mm to 1.0 mm between penetration sites, avoiding surface blood vessels. The stimulus consisted of a short monophasic train of 60 msec with a single pulse duration of 0.2 msec and a frequency of 300 Hz, as in previous microstimulation studies in New World monkeys (Gould et al., 1986; Stepniewska et al., 1993; Wu and Kaas, 1999). The stimulus was delivered using a Master-8 Stimulator (A.M.P.I., Jerusalem, Israel) connected to a stimulus isolation unit (Bak Electronics Inc., Mount Airy, MD).

During the experimental session, evoked movements were observed by at least two individuals and broadly classified into four body regions: facial movements (jaw, lips, nose, cheek, vibrissae, eyelid, ear, and some neck movements), forelimb movements (digit, wrist, elbow, and shoulder movements), trunk movements (lower trunk, upper trunk, and some neck movements), and hindlimb movements (toe, ankle, knee, hip, and tail movements). Movements of the pharynx/larynx were not examined, although some movements classified as 'neck' could possibly reflect pharyngeal or upper trunk movements. Movements of the tongue and eyes were examined but not observed in any of the cases. A minority of stimulation sites evoked weak movements that were difficult to classify; these ambiguous sites were noted more generally such as 'shoulder/upper trunk' or 'forelimb'. To be classified as a multi-joint site, such as 'hip&toe,' the site must have elicited more than one joint or facial movement at the threshold current. Threshold current was defined as the lowest value of current in which visible movements were observed repeatedly (on almost every trial); for each penetration we recorded the depth from which the lowest threshold movement was evoked. Stimulation first occurred at 50-120 μA, levels suspected to be above threshold, then decreased as necessary. Unresponsive penetration points were defined as points that did not elicit visible movements at 120 μA or less. The limit of 120 μA was chosen as a trade-off between: 1) identifying motor areas requiring higher thresholds, and 2) restricting the current spread to approximately 300 μm (Stoney et al., 1968). At the conclusion of the microstimulation session, microlesions of 10 μA direct current were placed at some penetration sites to mark physiologic borders.

Perfusion and Histology. At the end of the microstimulation session each animal was given a lethal dose of sodium pentobarbital, and when areflexive, the heart was exposed, an incision made in the right atrium, and a needle inserted into the left ventricle at the apex for perfusion. The animals were perfused with 0.9% phosphate-buffered saline (PBS, pH 7.4), followed by 2-4% paraformaldehyde in PBS, followed by paraformaldehyde and 10% sucrose in PBS. For sectioning, in most cases cortex was separated from the rest of the brain, flattened, postfixed overnight in paraformaldehyde and 10% sucrose in PBS, and transferred to 30% sucrose in PBS. The next day tissue was cut parallel to the surface in 40 μm sections. In one case (06-35) the brain was cut into a block then cut in the sagittal plane in 40 μm sections. The following stains were used: 1) Nissl substance, using cresyl violet, 2) cytochrome oxidase (Wong-Riley, 1979), 3) acetylcholinesterase (Geneser-Jensen and Blackstad, 1971), 4) Gallyas myelin stain (Gallyas, 1979), and 5) immunohistochemistry using the antibody SMI-32, a mouse monoclonal antibody to non-phosphorylated neurofilament H (Covance Inc., Princeton, New Jersey; Lee et al., 1988; Sternberger and Sternberger, 1983). SMI-32 immunohistochemistry has previously been used to identify cortical motor areas in tree shrews (Remple et al., 2006) and macaques (Gabernet et al., 1999; Geyer et al., 2000; Preuss et al., 1997), and our pattern of SMI-32 staining is consistent with these works. For SMI-32 reactions, sections were incubated in 0.3% hydrogen peroxide for 30 minutes at room temperature, washed with 0.25% Triton in Tris-buffered saline (Tx/TBS, pH 7.5), and incubated with a 1:2000 dilution of SMI-32 primary antibody in 3% normal horse serum and Tx/TBS for 48 hours at 4 ℃. Sections were washed and processed using the Vectastain Elite ABC kit (Vector Laboratories, Burlingame, CA), involving a

1:200 dilution of biotinylated secondary antibody in Tx/TBS at room temperature for 2 hours, followed by a 1:100 dilution of ABC reagent in Tx/TBS at room temperature for 1 hour. Sections were developed using the VIP substrate kit (Vector Laboratories).

Anatomic reconstructions were performed using brain sections cut parallel to the surface of manually flattened cortex (4 cases) or sections cut in the sagittal plane (1 case). The tangential sections were divided into two or three series, with the first series stained for myelin, the second for cytochrome oxidase, and in one case a third series stained for acetylcholinesterase. Sagittal sections were divided into four series, with one-of-every-four processed for Nissl, myelin, and SMI-32 antibody, and one-of-every-eight stained for acetylcholinesterase or cytochrome oxidase. Sections were photographed on a Nikon DXM1200F digital camera attached to a Nikon Eclipse E800 microscope (Nikon Corporation, Melville, NY). JPEG images were generated directly using the Nikon ACT-1 software. Tissue images were not altered except for uniform changes in contrast via the Adobe Photoshop levels command (Adobe Systems Incorporated, San Jose, CA). Images were imported into Adobe Illustrator (Adobe Systems Incorporated, San Jose, CA), and borders of sensory and motor areas were outlined. For flattened sections in cases 06-02, 06-27, and 06-48, microlesions visible in the tissue were used to align multiple tissue sections with each other, as well as with the physiologic data. For flattened sections in one case (06-13), the microlesions were not visible, and alignment of histological sections with the physiologic map was approximated based on anatomic landmarks (medial wall and lateral sulcus) and the quality of the physiologic responses. For sagittal sections, microlesions were used to align the physiologic map, and both microlesions and

surface vasculature were used to align tissue sections; the myelin, Nissl, and SMI-32 sections were most useful in identifying borders.

Quantitative analysis. Threshold values for evoked movements were separated by area (M1, 3a, 3b, and premotor) and analyzed. Premotor cortex was combined for quantitative analysis, and included all parts of area 6 (encompassing SMA, PMD, and PMV). Areas S2, PV, 1, and 2 were excluded from the analysis due to the paucity of evoked movements. Calculations include threshold values from four cases (06-13, 06-27, 06-35, and 06-48). The fifth case (06-02) was excluded from the calculations due to the paucity of evoked responses. For M1 and area 3a, threshold values were further analyzed and compared between: 1) different body representations (hindlimb, trunk, forelimb, and face movements), and 2) proximal (shoulder, elbow, trunk, hip, knee, and tail) and distal (wrist, digits, ankle, toes) movements. Values corresponding to ambiguous movements were excluded from the comparisons of body representations and proximal versus distal movements. Finally, M1 was also analyzed and compared between rostral, central, and caudal M1 regions (either rostral and caudal halves or rostral, intermediate, and caudal thirds). To evaluate differences between the areas, nonparametric statistical tests (Siegel and Castellan, 1988) were calculated using Matlab (The MathWorks, Inc., Natick, MA) and SPSS (SPSS Inc., Chicago, IL). Homogeneity of variance was tested using Levene's test. When homogeneous, Mann-Whitney U tests were used for comparisons between two groups and Kruskal-Wallis tests for comparisons of more than two groups. When not homogeneous, Kolmogorov-Smirnov tests were used for comparisons between two groups.

Results

Microstimulation mapping

We extensively stimulated the frontoparietal cortex involving motor, premotor, and somatosensory areas in marmosets with intracortical microelectrodes and correlated microstimulation results with the architectonic features of stimulated cortex. Our focus was primary motor cortex, but we observed body movements from eight areas of sensorimotor cortex (Fig. 1). Whereas movements were consistently evoked from M1 (and area 3a) with low current thresholds, premotor and most somatosensory areas were much less excitable, as thresholds lower than or equal to 120 μA evoked fewer movements from these areas.

Microstimulation of sites in frontoparietal cortex at near threshold current typically evoked contralateral movements of a single joint or a single location on the face: very rarely multi-joint or ipsilateral movements were elicited. Threshold values varied from 2 to 120 μA and were generally lowest 1.6-1.8 mm from the pial surface. The same movement could be evoked throughout the depth of the cortex at a single electrode penetration site. When an electrode site was retested at a later time in the experiment, the same movement as initially recorded was evoked.

Motor cortex

M1. Maps of primary motor cortex were obtained in five cases. Two of these maps were incomplete (case 06-13 and case 06-02, not shown), but the results were consistent with

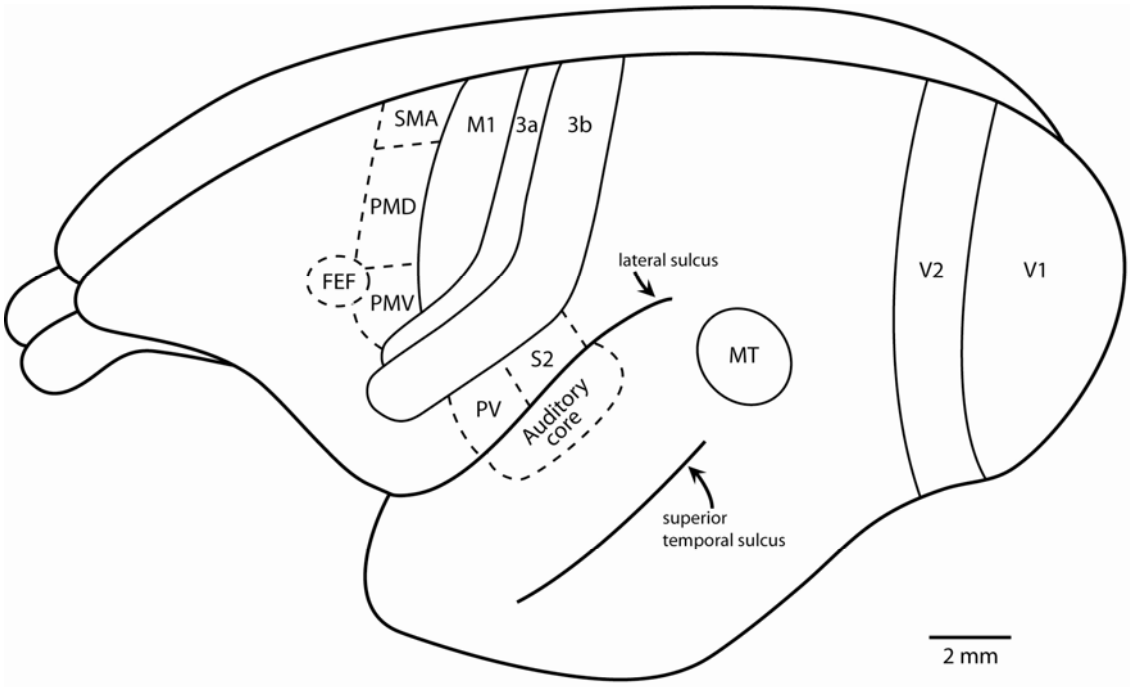

Fig. 1. Proposed organization of frontoparietal cortex in the common marmoset. The location of primary motor cortex is based on the electrophysiologic maps and cytoarchitecture of this study. The locations of somatosensory areas were based on our results as well as previous studies of primary somatosensory area 3b (Krubitzer and Kaas, 1990b), somatosensory area 3a (Huffman and Krubitzer, 2001a), and the lateral somatosensory areas PV and S2 (Krubitzer and Kaas, 1990b; Qi et al., 2002). Locations of SMA, PMD, and PMV are based on our results as well as the previous subdivisions of 6m, 6d, and 6v from Burman et al. (2006). The relative locations of the frontal eye field (Krubitzer and Kaas, 1990a), the auditory core (de la Mothe et al., 2006a; de la Mothe et al., 2006b) and three visual areas V1, V2, and MT (Fritsches and Rosa, 1996; Rosa and Elston, 1998; Rosa et al., 1997; Sengpiel et al., 1996) are also shown but were not examined in this study.

the more extensive findings from the other cases. M1 occupies an area of frontal cortex above the rostral portion of the lateral sulcus, extending approximately 2 mm rostrocaudally and 10 mm mediolaterally. The median threshold value for evoked movements at sites in M1 was 55 μA. Compared to other frontoparietal areas, current thresholds for evoking movements from M1 were significantly lower than for premotor cortex (median 80 μA, Mann-Whitney U-test, $p=0.00007$) and area 3b (median 75 μA, Mann-Whitney U-test, $p=0.0003$), but not significantly different than for area 3a (median 60 μA, Mann-Whitney U-test, $p=0.11$).

Examination of body movements in M1 evoked by microstimulation revealed a gross topographic representation from head to toe (Figs. 2-5). An orderly mediolateral progression was apparent in all cases, with hindlimb movements evoked most medially, followed by trunk, forelimb, and finally facial movements most laterally. There were, however, a few exceptions to the mediolateral progression, with the hindlimb region containing a single forelimb movement (Fig. 5), the trunk region containing shoulder, elbow, and wrist movements (Fig. 4-5), and the face region containing elbow movements (Fig. 4).

In the medial portion of M1, stimulation predominantly evoked movements of the hindlimb. Hip movements were the most common, representing 80% of all penetration points in this region, although the knee (2%), ankle (2%), toes (2%), and tail (4%) were also represented in the medial M1 region. No ipsilateral movements were seen, and only one multijoint movement could be clearly identified: one point eliciting hip and toe movements in the rostromedial portion of M1 (Fig. 2). Electrode penetrations were not

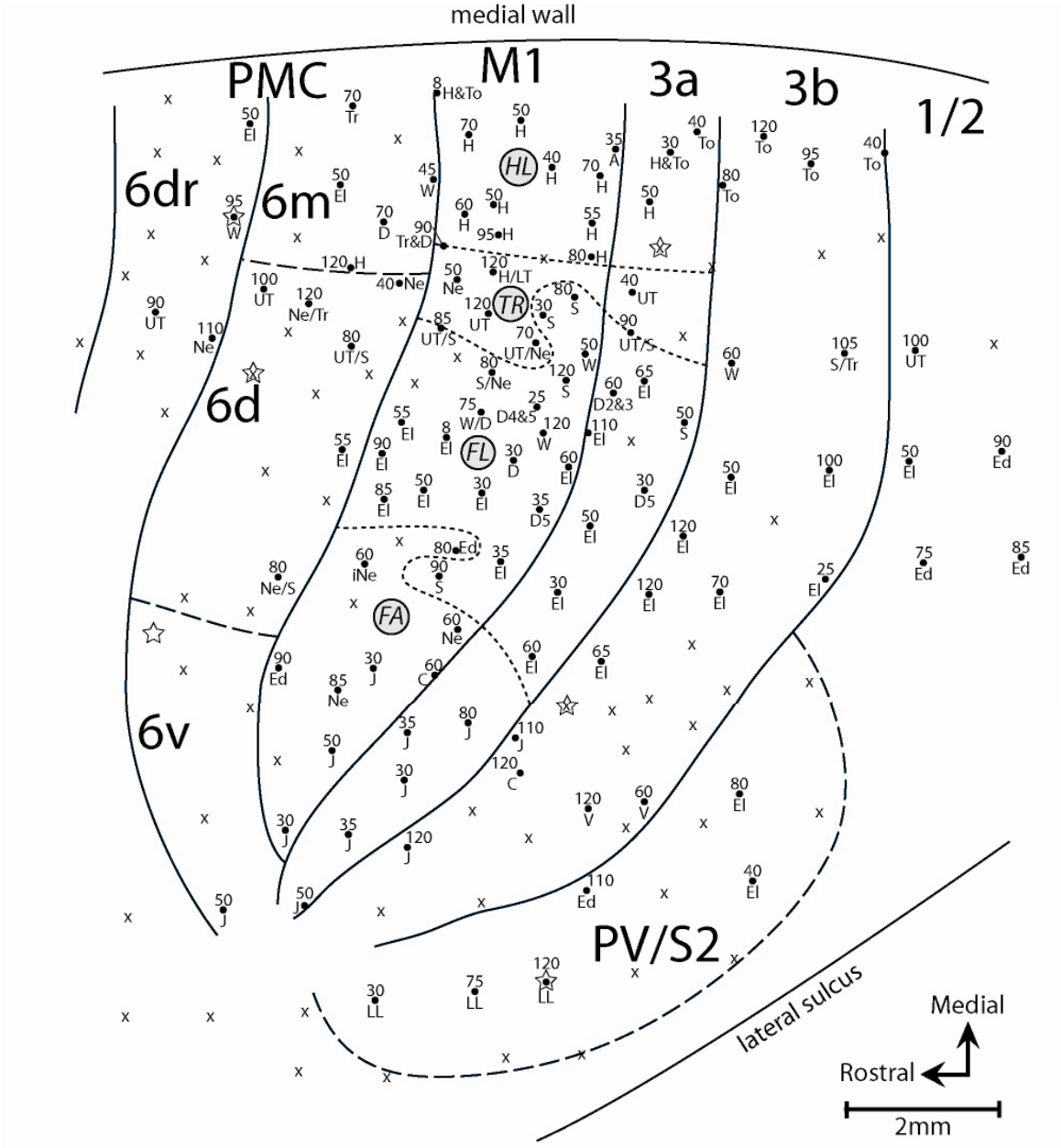

Fig. 2. Results of microstimuation mapping in the frontoparietal cortex of case 06-35. Solid lines indicate architectonic borders (reconstructed from sagittal sections) and anatomic boundaries (medial wall and lateral sulcus). A long dashed line indicates the approximate location of the lateral somatosensory areas (PV and S2). Short dashed lines spanning M1 and area 3a indicate physiologic borders between the hindlimb (HL), trunk (TR), forelimb (FL), and face (FA) regions, while dashed lines in premotor cortex show the approximate architectural borders of 6m, 6d, and 6v. Black dots represent the locations of responsive penetration points, with threshold currents (in μA) and specific evoked movements (see abbreviations) shown above and below each point. "X's" represent the locations of penetration points that did not evoke movements at 120μA or below. Stars mark the location of lesions. Orientation and scale are at bottom right.

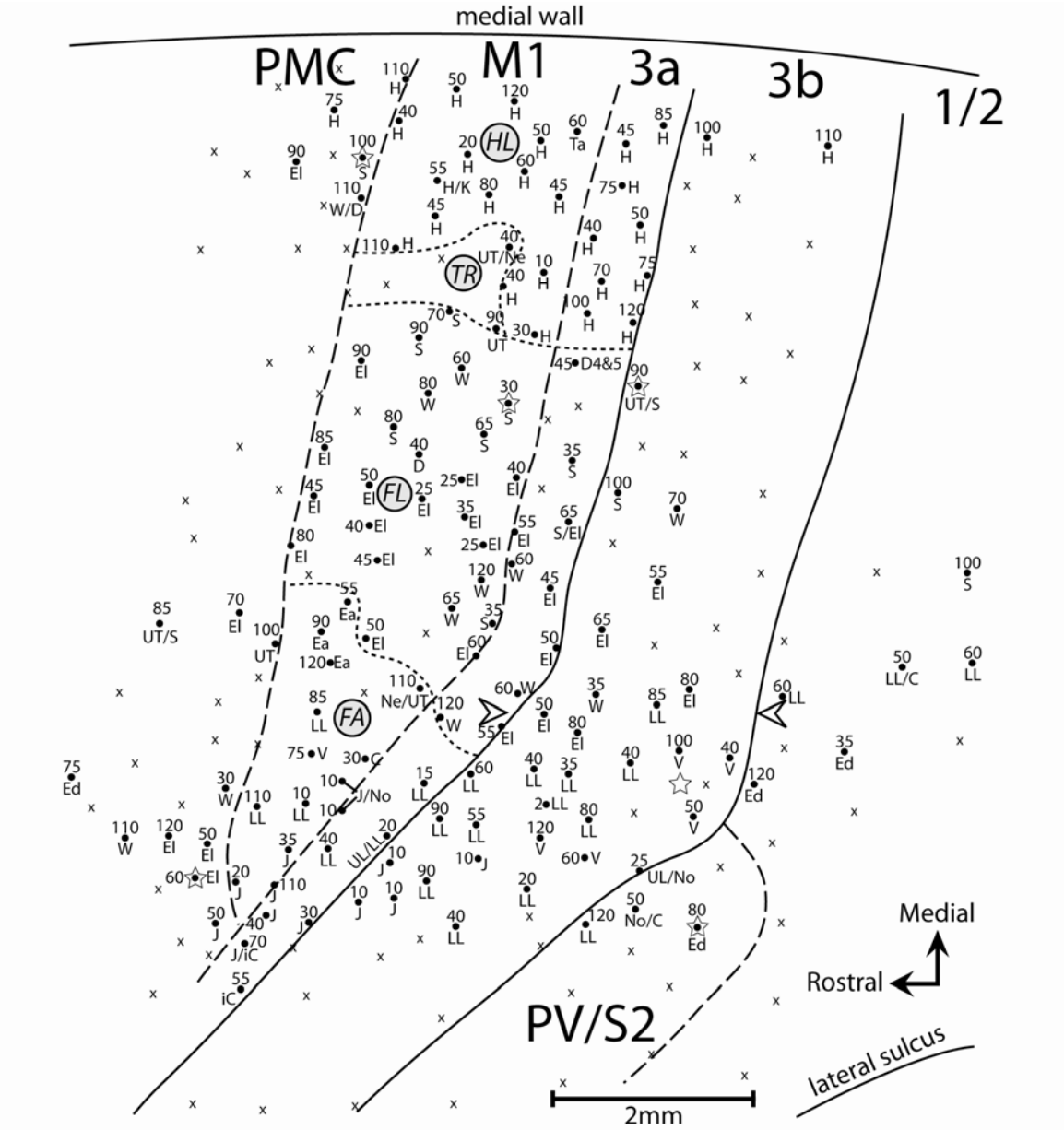

Fig. 3. Results of microstimuation mapping in the frontoparietal cortex of case 06-27. Solid lines indicate architectonic borders (reconstructed from flattened sections) and anatomic boundaries. The dashed lines running mediolaterally between PMC, M1, and area 3a indicate the approximate architectural borders. Dotted lines spanning rostrocaudally across M1 and area 3a indicate physiologic borders: note that the trunk regions in this case are small, with two responsive points in M1 and none in area 3a. Black dots, "X's", and stars represent the locations of responsive penetration points, unresponsive penetration points, and lesions. Threshold values (in μA) and movements (see abbreviations) are shown. Two arrowheads near the 3b bend mark the location of a myelin-light septum seen in histological sections. Scale and orientation are at bottom right.

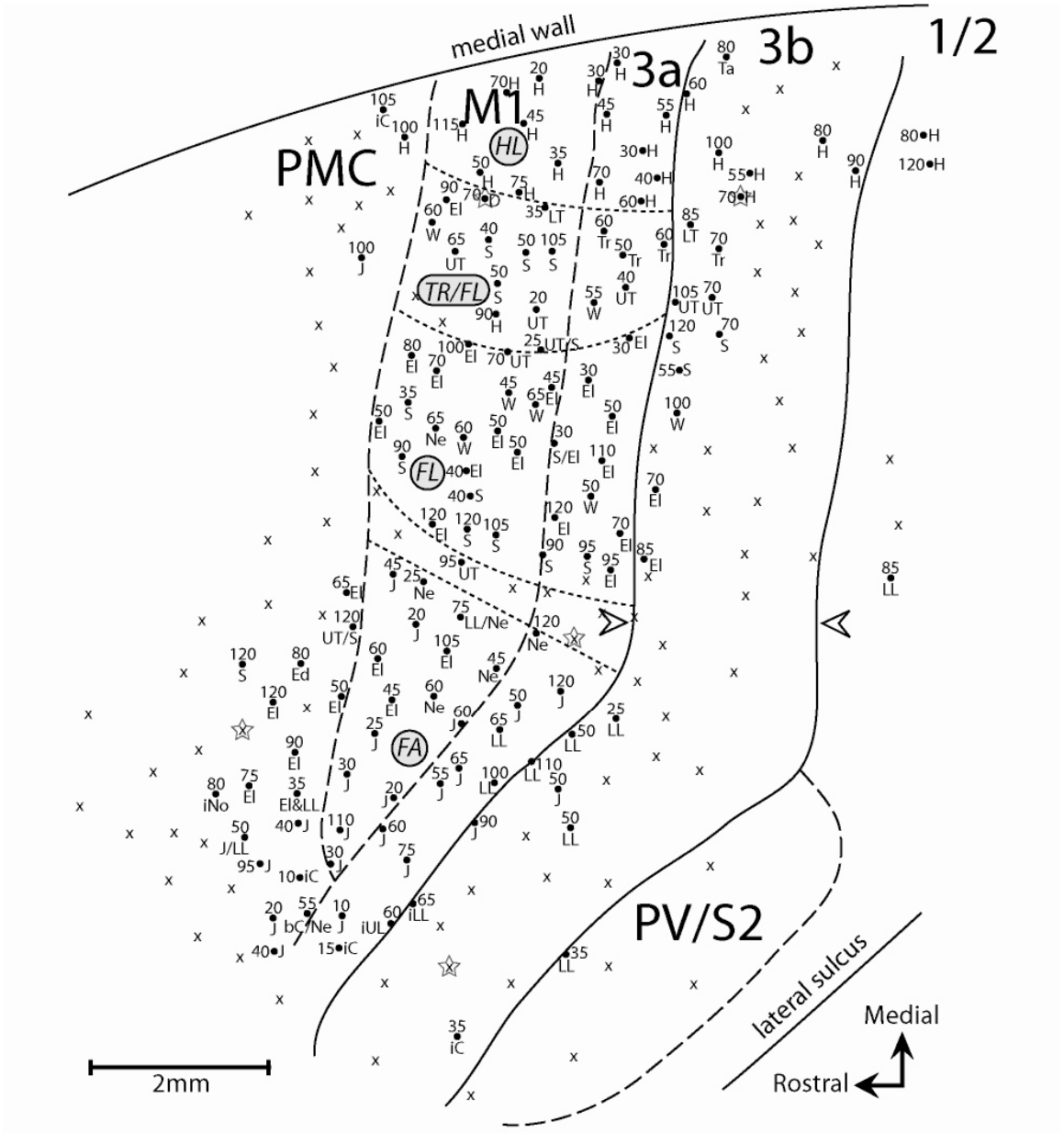

Fig. 4. Results of microstimuation mapping in the frontoparietal cortex of case 06-48. Solid lines indicate architectonic borders for area 3b (reconstructed from flattened sections) and anatomic boundaries. Long dashed lines show the approximate architectural borders for M1 and the lateral somatosensory areas (PV/S2). Short dotted lines spanning rostrocaudally across M1 and area 3a indicate physiologic borders between the body regions. Note that in the M1 trunk region of this case there is a collection of forelimb (and one hindlimb) movements, while in the M1 face region there is a collection of forelimb movements in the middle. Additionally, there appears to be a zone between the forelimb and face regions that is largely unresponsive, with one trunk movement. Black circles, "X's", and stars represent the locations of responsive penetration points, unresponsive penetration points, and lesions. Threshold values (in μA) and movements (see abbreviations) are shown. Two arrowheads near the 3b bend mark the location of a myelin-light septum seen in histological sections. Scale and orientation are at bottom.

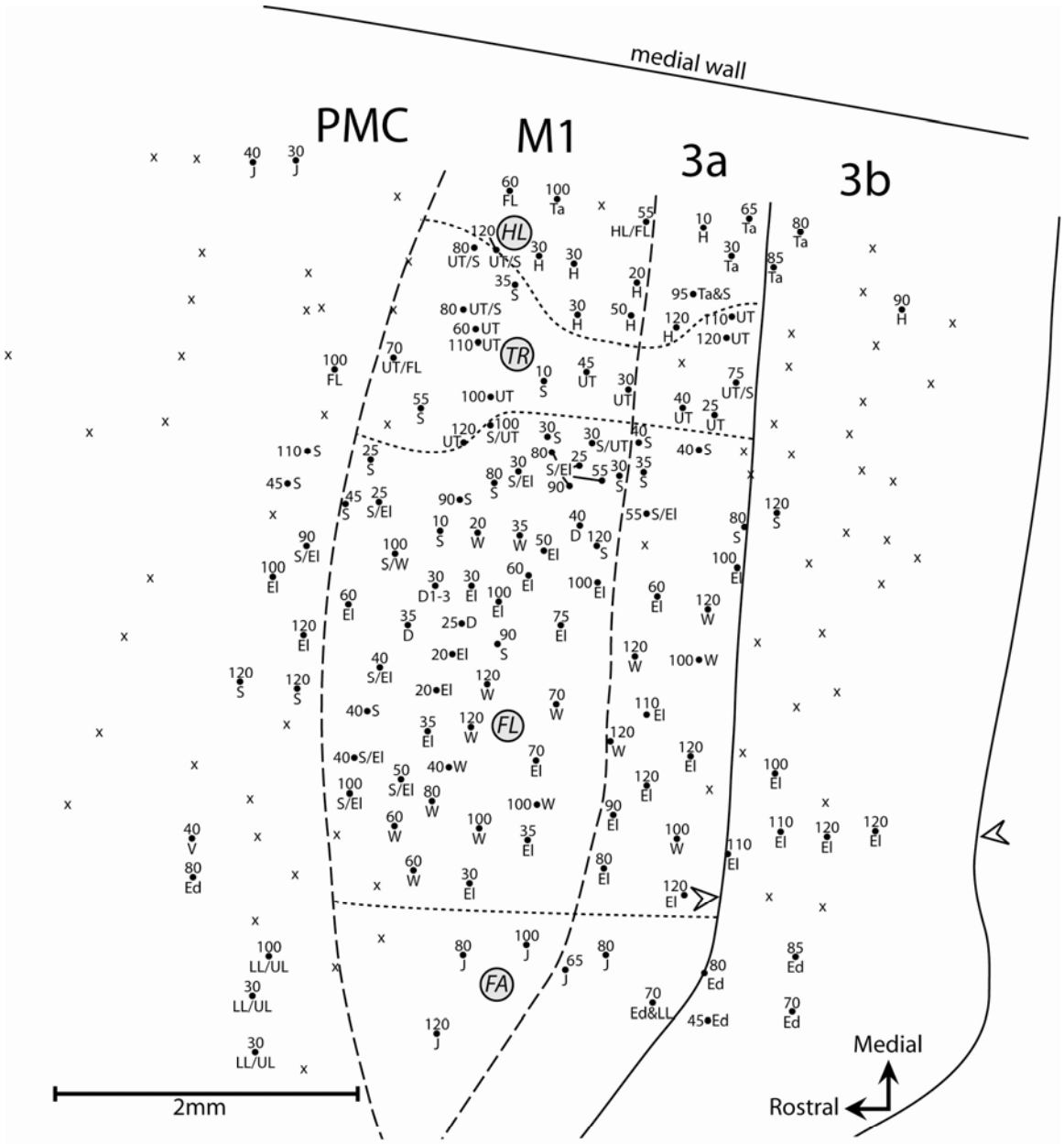

Fig. 5. Results of microstimuation mapping in the frontoparietal cortex of case 06-13. Solid lines indicate architectonic borders (reconstructed from flattened sections) and anatomic boundaries. Long dashed lines running mediolaterally show the approximate architectural borders for M1. Dotted lines spanning rostrocaudally across M1 and area 3a indicate physiologic borders between the body regions. The forearm/face border can be identified but microstimulation of the face region was incomplete. Ten penetration points were cropped so that the figure could be enlarged: five unresponsive points in a line extending 3 mm rostrally from the rostral-most "FL" site, and five points (3 jaw and 2 unresponsive) in a line extending 4 mm lateral to the lateral-most jaw site. Black dots and "X's" represent the locations of responsive and unresponsive penetration points, respectively. Threshold values (in μA) and movements (see abbreviations) are shown. Two arrowheads near the 3b bend mark the location of a myelin-light septum seen in histological sections. Scale and orientation are at bottom.

made in the medial-most portions of cortex near the superior sagittal sinus. Thus the hindlimb representation of M1 may extend into cortex of the medial wall.

Trunk movements were evoked from a region of cortex immediately lateral to the hindlimb representation in M1. This region was more variable in composition than the parts of M1 devoted to hindlimb, forelimb, and face movements. It differed greatly in size, being smaller in some cases (Figs. 2-3) and larger in others (Figs. 4-5). Microstimulation sites in this region evoked mainly upper trunk movements (46% of all penetration points in this region) as well as lower trunk (5%) and neck (8%) movements. However, many non-trunk movements, such as shoulder (28%) and hip (5%) were evoked, and some unresponsive sites were also found in this region. Many of the trunk movements were bilateral, with the contralateral movement stronger than the ipsilateral movement. Only one clear multijoint movement was seen (Fig. 2). Because of this variability in evoked movements, the borders of the trunk representation of M1 with hindlimb and forelimb were difficult to define. In the caudal half of M1, the hindlimb representation even bordered directly with the forelimb (Fig. 3). A poorly defined trunk region of M1, with interspersed forelimb movements and direct hindlimb/forelimb borders, has also been observed in owl monkeys (Gould et al., 1986; Stepniewska et al., 1993).

Forelimb movements were evoked from a large region of cortex lateral to the trunk representation. No hindlimb or face movements were evoked from this region, and no case had more than two sites eliciting movements of the trunk. Movements from the contralateral shoulder, elbow, wrist, and digits were observed, including movement of a single digit (Fig. 2). No ipsilateral movements were seen. Movements of proximal

forelimb joints were more common than those of the distal joints (shoulder 33% and elbow 46% of all penetration points tested, versus wrist 16% and digits 7%). The only obvious multijoint movements were those of multiple digits, usually all 5 digits, but in one case just digits 4 and 5 (Fig. 2) and in another case digits 1, 2, and 3 (Fig. 5). No mediolateral somatotopy was apparent within the forelimb region, as types of movements such as wrist (Fig. 3) were evoked from sites scattered across the region.

Face movements were evoked from a region of cortex just lateral to the region where forelimb movements were evoked. Occasionally, forelimb movements were also elicited from this territory. The majority of movements elicited from this region were movements of the jaw (40% of all tested points) and neck (18%), although we also observed movements of the lower lip (9%), cheek (7%), ear (7%), eyelid (4%), vibrissae (2%), and nose (2%). No movements of the tongue or eyes were observed. One ipsilateral movement of the neck (Fig. 2) and one dual movement of the eyelid and lower lip (Fig. 5) were observed. As in the forelimb region, no mediolateral organization was apparent, and movements of specific locations of the face such as the jaw (Fig. 4) were scattered within the face region.

No significant differences in threshold values were found between points evoking hindlimb, trunk, forelimb, and face movements in M1 (Kruskal-Wallis test, $p=0.28$), or between points evoking proximal or distal movements (Mann-Whitney U-test, $p=0.88$). Rostrocaudally, there was no significant difference in threshold values for evoked movements between the rostral and caudal halves of M1 (Mann-Whitney U-test, $p=0.11$). Additionally, there was no significant difference in M1 movement thresholds between the rostral third and the intermediate third (Kolmogorov-Smirnov test, $p=0.46$). However,

thresholds for the caudal third of M1 (median 50 μA) were significantly lower than those of the intermediate third (median 65 μA, Kolmogorov-Smirnov test, p=0.008) and those of the rostral third (median 60 μA, Mann-Whitney U-test, p=0.027). This could reflect lower thresholds for sites along the caudal border of M1.

Premotor cortex. We examined all cortex immediately rostral to M1, equivalent to SMA, PMD, and PMV in other primates. Movements at thresholds of 120 μA or less in this premotor cortex (PMC) were most reliably evoked in a 1 mm band adjacent to M1. The majority of sites in the regions of cortex presumed to be premotor cortex were unresponsive. Generally a physiologic border between M1 and PMC could be distinguished by higher threshold values in PMC and by the types of body movements evoked (especially in the medial part of PMC). Due to the unresponsive sites in rostral PMC, no physiologic border between premotor and prefrontal cortex was determined.

Movements were elicited throughout the mediolateral extent of PMC. In the medial-most portion, movements of the hindlimb, trunk, forelimb, and face were evoked. Studies in other primates have found a rostrocaudal organization of body movements in this region, with hindlimb movements being most caudal and face movements most rostral (Brinkman and Porter, 1979; Gould et al., 1986; Preuss et al., 1996; Welker et al., 1957; Woolsey et al., 1952), but no obvious pattern was apparent in marmosets from the few responsive sites in this study. The middle portion of PMC evoked movements of the trunk and proximal forelimb; no movements of the wrist or digits were observed. The lateral-most portion of PMC evoked movements of the face, including ipsilateral and bilateral movements, as well as movements of the forelimb, including proximal and distal

musculature. Finally, a few higher-threshold responses from area 6dr ((Burman et al., 2006); Fig. 2), including forelimb and trunk, could be elicited.

Somatosensory cortex

Area 3a. Area 3a is located immediately caudal to M1 and extends approximately 1 mm rostrocaudally and 10 mm mediolaterally. Significantly lower currents were necessary to evoke threshold movements from area 3a than from premotor cortex (Mann-Whitney U-test, $p=0.018$) and area 3b (Mann-Whitney U-test, $p=0.041$).

Body movements in area 3a were somatotopically represented in a mediolateral order similar to that in M1, with hindlimb movements located most medially, followed by trunk, forelimb, and then face most laterally. Borders between the hindlimb, trunk, forelimb, and face representations were generally in similar locations in both area 3a and M1, such that a continuous line could be drawn across the two areas. Mainly hip movements (77% of all penetration sites tested) were evoked from the hindlimb region of area 3a. Some toe (8%) and tail (12%) movements were evoked, with no knee or ankle movements and only one non-hindlimb movement (Fig. 5). The 3a trunk region, like the M1 trunk region, was highly variable and contained both trunk and forelimb movements. In one case (Fig. 3) no trunk movements were elicited, and stimulation sites where hindlimb movements were evoked directly bordered those where forelimb movements were evoked. Only forelimb movements were evoked from the 3a forelimb region, including a single digit movement (Fig. 2). The majority of penetration sites in the 3a forelimb region elicited elbow movements (50% of tested sites), followed by shoulder (20%), wrist (16%) and finally digit movements (5%). The 3a face region consisted

entirely of sites where face movements were evoked, predominantly of the lower face (jaw 58% of tested sites, lower lip 23%) although other face movements were also seen (cheek 13%, eyelid 6%, upper lip 6%, neck 3%, nose 3%). No movements of the tongue, eyes, or ears were seen. Ipsilateral face movements were seen in two cases (Figs. 3-4), suggesting that area 3a may contain a motor representation of the ipsilateral face in its most lateral portion (Iyengar et al., 2007; Kaas et al., 2006). As area 3a is narrow compared to the adjacent areas M1 and 3b, we had fewer electrode penetration sites in area 3a, but, at our electrode spacing, no mediolateral or rostrocaudal organization was apparent within the hindlimb, trunk, forelimb, or face regions of area 3a. No significant differences in threshold values were found between hindlimb, trunk, forelimb, and face movements in area 3a or between proximal and distal movements (Kruskal-Wallis test, $p=0.18$ and Mann-Whitney U-test, $p=0.26$, respectively).

Area 3b. Area 3b is similar in width to M1, spanning approximately 2 mm rostrocaudally. Mediolaterally area 3b is much longer, however, extending approximately 8 mm lateral to the midline before bending rostrally and extending 6 mm further. No significant difference in currents evoking threshold movements was seen between area 3b and premotor cortex (Mann-Whitney U-test, $p=0.55$). In our experiments, stimulation of 3b sometimes yielded high threshold movements from the hindlimb, trunk, forelimb, and face. Area 3b had a mediolateral motor organization similar to that of M1 and area 3a, and one that matches its somatosensory representation (Krubitzer and Kaas, 1990b). However, the majority of sites tested were unresponsive, and the detailed organization of area 3b could not be determined from our stimulation data.

Other somatosensory areas. Previous studies in marmosets have revealed at least two somatosensory areas near the lateral sulcus: area PV and area S2 (Krubitzer and Kaas, 1990b; Qi et al., 2002). In our study the majority of stimulation sites in PV and S2 were unresponsive. However, high threshold face movements were evoked from both areas, including movements of the lower lip, eyelid, and nose. In one case (Fig. 2), elbow movements were evoked from the caudal portion, presumably area S2. No trunk or hindlimb movements were seen in these lateral somatosensory areas.

Responses to cutaneous stimuli have also been identified in cortex caudal to area 3b in marmosets (Huffman and Krubitzer, 2001a; Krubitzer and Kaas, 1990b). There is some debate on whether this cortex corresponds to area 1, area 2, area 5, or some combination of these areas of other primates (Padberg et al., 2005). In the present study this cortex was largely unresponsive to stimulation. However, a variety of movements were evoked from this cortex at high current levels, including medial hindlimb movements (hip and tail), a more lateral upper trunk movement, even more lateral forelimb movements (shoulder and elbow), and face movements (eyelid and lower lip) most laterally (Figs. 2-4). Even these few penetration sites suggest a mediolateral organization of the caudal somatosensory area that is similar to that of area 3b.

Architectural mapping

Our architectonic material is based on six sagittal preparations (one left hemisphere, five right hemispheres) and four flattened cortices (all left hemispheres).

Sagittal sections

Motor cortex. The characteristic features of primary motor cortex, including large pyramidal cells in layer V and an indistinct or missing layer IV, were observed in Nissl-stained and SMI-32-immunoreacted sections in marmosets (Fig 6A-B). The sizes of layer V pyramidal cells decreased in rostral M1 and more so in PMC. Within M1, pyramidal cells were generally largest in medial sections and smallest in lateral sections, making the PMC/M1 border more difficult to define laterally in Nissl-stained and SMI-32-immunoreacted sections. In sections stained for myelin, M1 generally stained more darkly in layers V and VI than either PMC or area 3a (Fig. 6C).

The primary motor cortex of marmosets was generally homogeneous in appearance. Although previous studies have suggested that two (owl monkeys) or even three (macaques) architectonic subdivisions exist within M1 (Preuss et al., 1997; Stepniewska et al., 1993), we did not observe such divisions in marmosets. In our Nissl- and acetylcholinesterase-stained sections of marmoset M1, no sharp change in pyramidal cell size occurred between caudal and rostral M1, although there was a tendency for pyramidal cell size to be larger in caudal portions of M1 and to decrease gradually near the PMC border. Differences in SMI-32 immunoreactivity were not evident in marmoset M1.

PMC in marmosets has recently been subdivided into three areas (6m, 6d, and 6v) based on the pattern of myelination; a fourth region (6dr) has also been identified which contains architectural features of both premotor and prefrontal regions (Burman et al., 2006). The borders between subdivisions of area 6 could be distinguished in sagittal and coronal sections (not shown). Although not always visible, a thin myelin-light region

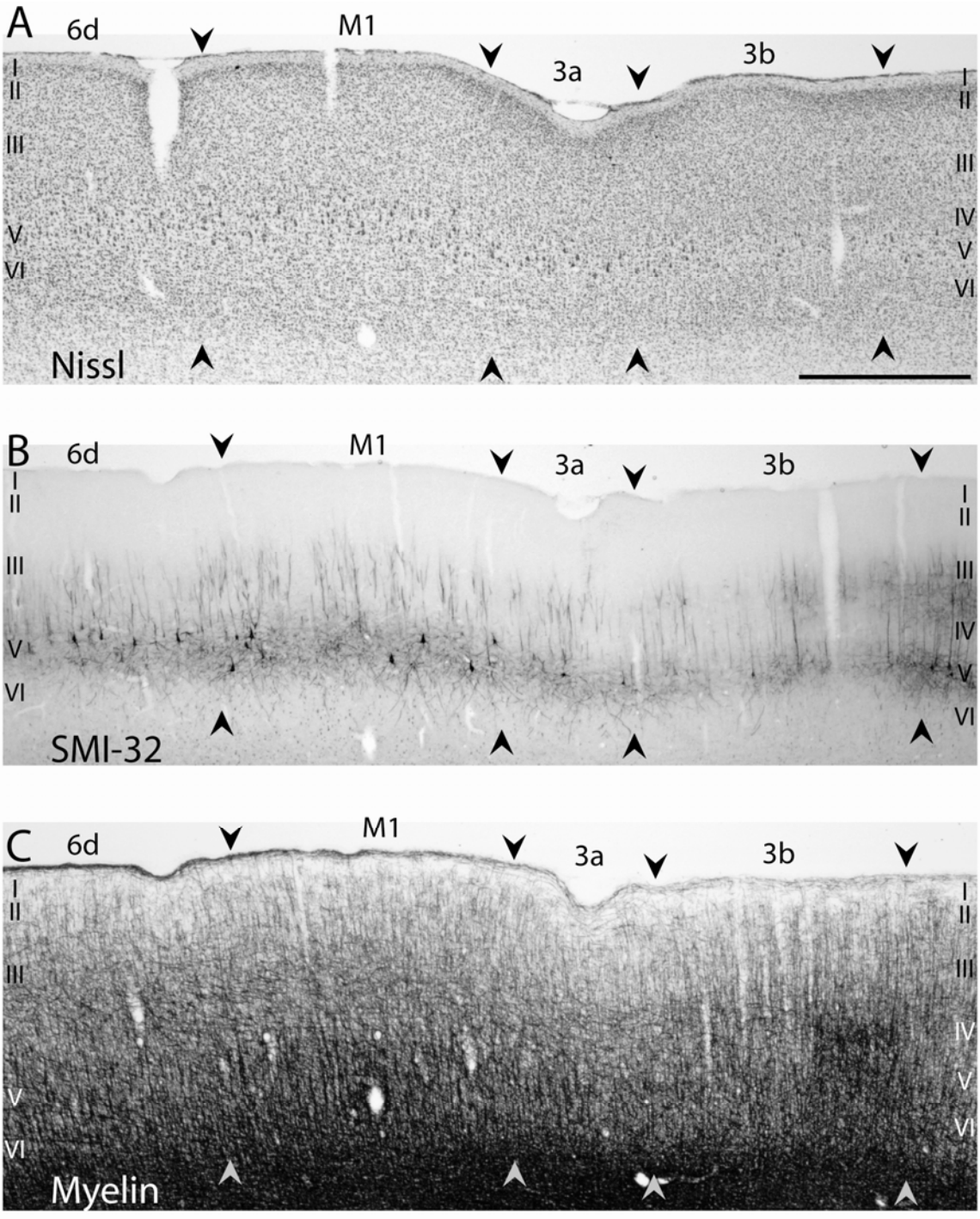

Fig. 6. Architecture of sagittal sections in the right hemisphere of case 06-02. Adjacent sections were stained with cresyl violet (Nissl) (A), immunoreacted with SMI-32 antibody (B), or stained for myelinated fibers (C). Arrowheads mark boundaries between areas. Rostral is to the left. Scale bar = 1 mm and applies to all sections.

between the bands of Baillarger could be identified in areas 6m and 6v of some sections that was absent in 6d, as previously described (Burman et al., 2006).

Somatosensory cortex. The characteristic features of area 3b, including well-defined layers IV and VI surrounding a thin layer V with small pyramidal cells, were apparent in our Nissl-stained sections (Fig. 6A). In SMI-32-immunoreacted sections the thinness of layer V was especially apparent, and layer IV was weakly immunoreactive for SMI-32 antibody (Fig. 6B). In myelin-stained sections, the deeper layers of area 3b stained more darkly than the surrounding areas (Fig. 6C).

Area 3a, located adjacent to M1 rostrally and area 3b caudally, had characteristics that were intermediate between those of M1 and 3b in Nissl-stained and SMI-32-immunoreacted sections. Area 3a had both large layer V pyramidal cells, a characteristic of M1 that can best be seen in the Nissl stained section (Fig. 6A), as well as an identifiable layer IV, a characteristic of area 3b best seen as an SMI-32 light region between the darker layers III and V (Fig. 6B). In myelin-stained sections, area 3a generally stained more lightly than either area 3b or M1. Area 3a was also thinner rostrocaudally, being approximately half the length of either M1 or 3b.

Cortex immediately caudal to area 3b was characterized by a prominent layer IV and a well-defined layer V in Nissl-stained and SMI-32-immunoreactive sections. Moreover, in SMI-32 sections layers III and V were more immunoreactive than in area 3b. In myelin-stained sections this caudal area generally stained more lightly than area 3b. Previous investigators have been uncertain whether cortex immediately caudal to area 3b in marmosets more clearly resembles area 1, area 2, or area 5 of other primates (Padberg et al., 2005), as the identities of these areas can be difficult to define based on

architectonics alone (see Qi et al., 2007). By position, the cortex is area 1. As expected for area 1, it does receive dense projections from area 3b (Krubitzer and Kaas, 1990b).

Sections of flattened cortex

Architectonic subdivisions of sensorimotor cortex reconstructed for flattened cortices were made by identifying architectonic boundaries in individual sections cut parallel to the surface and reacted for myelinated fibers, cytochrome oxidase, or, in one case, acetylcholinesterase. The borders determined in individual sections were then compared and superimposed to yield the composite border. Area 3b was the most distinct area in all the preparations, identified as a myelin, cytochrome oxidase (Fig. 7), and acetylcholinesterase-dense region extending from the medial wall toward the lateral sulcus and angling rostrally above the lateral sulcus. Myelin staining was patchy along the mediolateral length of area 3b, as in previous descriptions (Huffman and Krubitzer, 2001a; Krubitzer and Kaas, 1990b). Several patches of lightly myelinated fibers were observed in all of our cases, especially in the lateral part of area 3b. Above the 3b bend a myelin-light septum was observed (Fig. 7C) near the forearm-face border (Fang et al., 2002; Krubitzer and Kaas, 1990b). Below the 3b bend several myelin-light patches could be seen, reflecting the modular arrangement of contralateral and ipsilateral face in this area (Kaas et al., 2006). These lighter septal regions were less obvious in sections reacted for cytochrome oxidase (Fig. 7D-F).

In sagittal sections stained for myelin both M1 and 3b were darker than the surrounding areas, suggesting that area 3a represents a myelin-light band between the two areas. A light band could be seen in some cortical sections cut parallel to the surface,

Fig. 7. Architecture of flattened sections reacted for myelinated fibers and cytochrome oxidase. A: Schematic outline of borders identified in case 06-13. Dashed lines in A and D represent borders that were not visualized in all sections. B: Section of frontoparietal cortex stained with myelin in case 06-13. C: A close-up of the bend in area 3b. White arrowheads indicate a myelin-light septum which marks the forearm-face border. D: Schematic outline of borders identified in case 06-27. Stars in D represent lesions made during microstimulation mapping, and were not visible in case 06-13. E: Section of frontoparietal cortex stained with cytochrome oxidase in case 06-27. F: More superficial section of frontoparietal cortex stained with cytochrome oxidase in case 06-27. Every-third section was stained for cytochrome oxidase, thus E and F are 80 μm apart. In A-E, rostral is to the left, medial is up. Scale bar in A is 2 mm and also applies to B, D, E, and F. Scale bar in C is 2 mm.

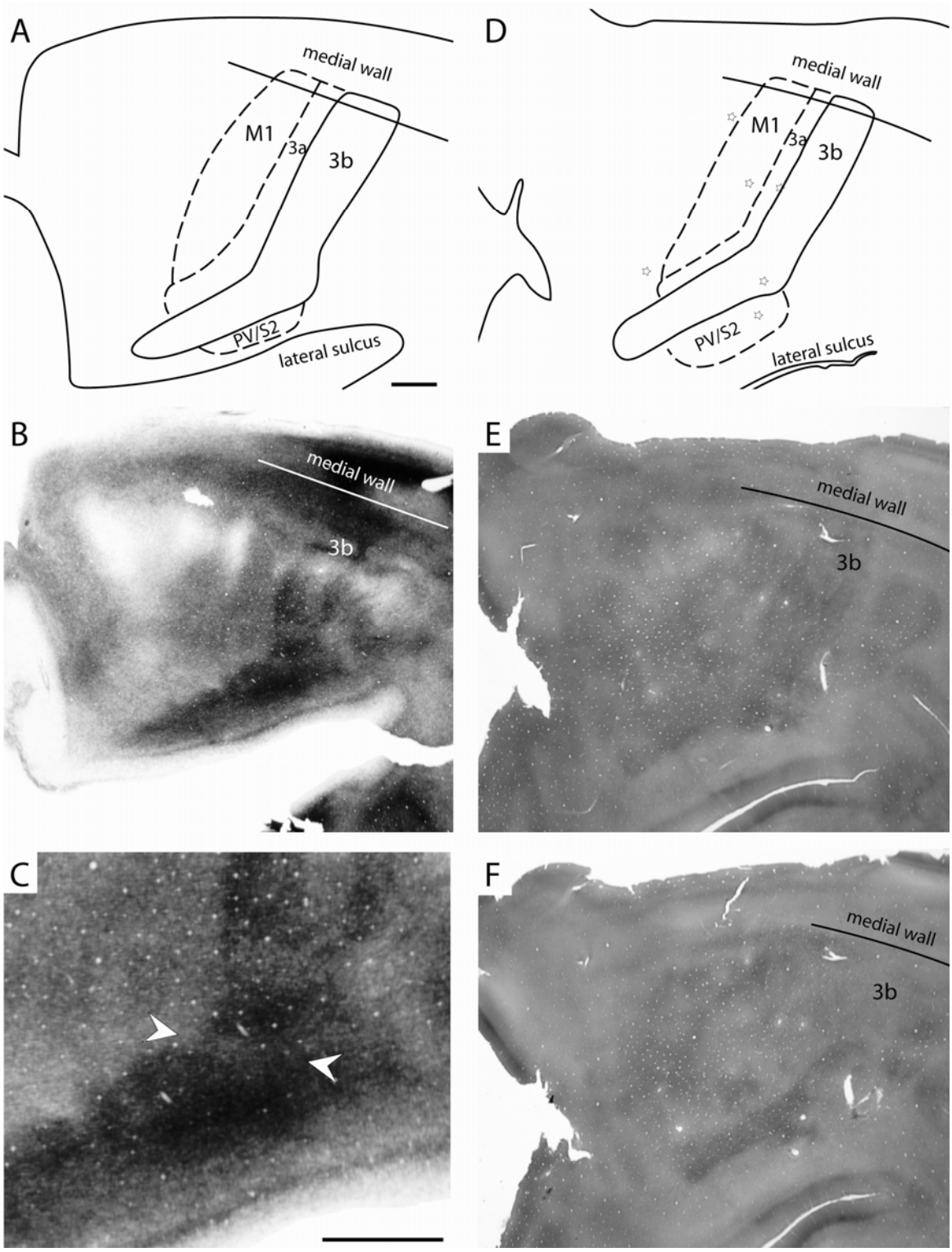
A
medial wall
M1
3a
3b
PV/S2
lateral sulcus
D
medial wall
M1
3a
3b
PV/S2
lateral sulcus
B
medial wall
3b
E
medial wall
3b
C
F
medial wall
3b

immediately rostral to area 3b. This band of lighter cortex, however, was not always distinct in our material. Because the rostral border of area 3b was consistently identified in sections from flattened cortex, the border with area 3a was reliably demonstrated. Area 3a was less myelinated and expressed less cytochrome oxidase than area 3b (Fig. 7). However, differences between area 3a and M1 were not always obvious in sections cut parallel to the cortical surface. Area 3a has been identified as a myelin-light region in sections cut parallel to the surface in one previous study (Huffman and Krubitzer, 2001a) but not in another (Krubitzer and Kaas, 1990b). To reflect this uncertainty, our 3a/M1 border is identified with a dashed line in sections from flattened cortex. The M1/PMC border could be distinguished by darker myelin staining and lighter cytochrome oxidase staining in M1 for some flattened sections but not others, and is thus also marked with a dashed line. Although a previous study has described SMA as a myelin-dense region (Krubitzer and Kaas, 1990b), we could not distinguish SMA from the dorsolateral premotor cortex in flattened sections, nor could we identify a premotor/prefrontal border. As in previous studies (Krubitzer and Kaas, 1990b; Qi et al., 2002), the lateral somatosensory areas PV and S2 were difficult to distinguish in surface-view sections. A similar pattern to that of myelin was observed in sections stained for acetylcholinesterase (not shown), where area 3b was easily identifiable but areas 3a and M1 were more difficult to distinguish.

Discussion

We used intracortical microstimulation and histological staining to examine the organization of frontoparietal cortex in common marmosets. Our focus was primary

motor cortex, but we also examined evoked movements and architecture for several somatosensory areas (3a, 3b, PV, S2, and presumptive area 1) and premotor areas (6m, 6d, 6v, and 6dr). We now review our findings and compare them to architectonic and recording studies of frontoparietal cortex in marmosets, as well as microstimulation studies of frontoparietal cortex in other primates.

Electrophysiology and architectonics of primary motor cortex

The values of stimulating current needed to evoke just noticeable (threshold) movements of body parts were lower for M1 than any other area examined, although they were not significantly lower than area 3a. Primary motor cortex showed a full range of body movements from head to toe, consisting mostly of single-joint movements of the contralateral body. The mediolateral topography of M1 was organized broadly into regions devoted to the hindlimb, trunk, forelimb, and face, but within each region movements were scattered. Cytoarchitectonically M1 in common marmosets is an agranular region with large layer V pyramidal cells (Betz cells). Although there appear to be no modern stimulation studies of motor cortex in marmosets, an early architectonic study of neocortex in marmosets (Hapale) included results of stimulating frontal cortex with surface electrodes in two animals (Mott et al., 1909). The results provided little information about the location or organization of M1, as movements were evoked from scattered sites across most of frontal cortex, with most of the movements involving the eyes, face, or mouth. Architectonically, Mott et al. (1909) defined a motor area with large pyramidal cells that included our present M1, but was considerably larger (perhaps

influenced by their physiological results). Their motor area B, with a "distinct band of granule cells," overlaps the lateral parts of the present areas 3b and 3a.

Other early architectonic studies of motor and other areas of neocortex of marmosets include those of Brodmann (1909) and Peden and von Bonin (1947). Brodmann (1909) described an area comparable to our area 3b (primary somatosensory cortex) as a composite of areas 1-3, concluding that areas 3,1, and 2 of other anthropoid primates were combined in marmosets. An area 3a was not recognized, and Brodmann's area 4 overlapped our M1 but was considerably larger medially, where it would include regions we excluded as belonging to PMD or SMA. Peden and von Bonin (1947) demonstrated an area PB that corresponds well to Brodmann's areas 1-3 and our area 3b, a "transition zone" with granular cells and pyramidal cells that corresponds to our area 3a, and a frontal area FA of large pyramidal cells that would include our M1 but is also somewhat larger medially, though less so that Brodmann's area 4. Clearly, these early investigators recognized the M1 region and other areas in marmosets, although the rostral border of medial M1 may have been misplaced.

In more modern studies, the architectonic border between M1 and premotor cortex was defined by Burman et al. (2006) in a location that closely corresponds to that of the present study. An area 3a of dysgranular cortex with larger layer V pyramidal cells and reduced myelination was outlined by Huffman and Krubitzer (2001a) in close agreement with present results. Modern studies have also identified M1 of marmosets as a region rostral to somatosensory cortex and have described connections of M1 with areas of somatosensory cortex, as well as motor nuclei of the thalamus (Huffman and Krubitzer, 2001a; Huffman and Krubitzer, 2001b; Krubitzer and Kaas, 1990b; Qi et al.,

2002). All these results indicate that M1 in common marmosets is homologous to primary motor cortex described in other primate species (Gould et al., 1986; Qi et al., 2000; Waters et al., 1990; Wu et al., 2000; Wu and Kaas, 1999), and suggest that the boundaries proposed in the present study are at least approximately accurate. However, some differences were noted between M1 in marmosets and other species, as presented below.

Threshold values of primary motor cortex. The threshold for movements evoked from M1 in marmosets has a median value of 55μA and an average value of 60 ± 2 μA (mean ± standard error of the mean), thus higher than those found in owl monkeys (Stepniewska et al., 1993) or galagos (Wu et al., 2000). Very low threshold values are also present in M1 of marmosets, as we were able to obtain some responses below 10μA, but many penetration points gave responses that were much higher than expected. One possibility is that we were not stimulating in layer V, but multiple depths were often tested for each penetration point, and the very low thresholds for some penetration points suggests that our range of depths included layer V. Another possibility is choice of anesthetic. However, ketamine and xylazine were also used in owl monkey motor experiments in similar dosages (Preuss et al., 1996; Stepniewska et al., 1993), and in marmosets ketamine and xylazine have been used successfully in somatosensory, visual, and auditory experiments (de la Mothe et al., 2006a; de la Mothe et al., 2006b; Huffman and Krubitzer, 2001a; Huffman and Krubitzer, 2001b; Kajikawa et al., 2005; Lyon and Kaas, 2001; Qi et al., 2002; Rosa et al., 2005). The level of anesthetic is another possibility, although our criteria for maintaining proper anesthetic level closely follow the previous experiments in owl monkeys (Preuss et al., 1996; Stepniewska et al., 1993). Other

considerations, such as the density of pyramidal cells in layer V, the size of pyramidal cells in layer V, or the nature of corticospinal projections from M1, have not been investigated. A small number of primates, including prosimians and common marmosets, may not have direct corticomotoneuronal connections, suggesting a fundamental difference in motor organization and dexterity (for review see Lemon and Griffiths, 2005). Whether this paucity of corticomotoneuronal inputs is related to increased threshold values in M1 is not clear, as the prosimian galago has lower threshold values than the common marmoset.

Organization of forelimb and face movements in M1. Previous studies in Old World primates have proposed a horseshoe organization in the forelimb region, with proximal movements located externally and distal movements internally (Kwan et al., 1978; Sessle and Wiesendanger, 1982). However, this finding has not been found in other studies (Donoghue et al., 1992; Gould et al., 1986; Huntley and Jones, 1991; Stepniewska et al., 1993; Waters et al., 1990). We found no such horseshoe pattern in the forelimb region of marmosets. Instead, the results better fit the mosaic pattern of repetition and mixing of representation modules as proposed by Gould et al. (1986).

The border between forelimb and face was well-defined, and in all cases unresponsive points were found near this border. In one case (Fig. 4) there appeared to be a thin, largely unresponsive strip of cortex in between the face and forelimb in both M1 and area 3a. In our other cases, however, this thin strip of unresponsive cortex was not found. A previous study on Old World primates suggested the existence of an unresponsive patch of cortex between the forelimb and face in M1 (Waters et al., 1990),

but this has not been found in other studies (Gould et al., 1986; Huntley and Jones, 1991; Sessle and Wiesendanger, 1982; Stepniewska et al., 1993).

Finally, while we observed a variety of face movements, no movements of the oral cavity were seen in our experiments. Movements of the tongue have been elicited from primary motor cortex in the prosimian galago (Wu et al., 2000), the New World owl monkey (Gould et al., 1986; Preuss et al., 1996), and New World squirrel monkey (Wu and Kaas, 1999). Additionally, a cortical region evoking tongue movements has been identified near the lateral sulcus in the saddle-backed tamarin *Sanguinus fuscicollis* (Alipour et al., 2002), a species belonging to the same New World family as the common marmoset. A more detailed examination of the lateral regions of motor cortex is necessary to examine potential tongue movements in common marmosets.

Are there subdivisions of M1 in the marmoset? The cortical cytoarchitecture of marmoset brains, specifically the size of layer V pyramidal cells, appears more homogenous in M1 than in other New World or Old World primates. Clear borders subdividing M1 into halves or thirds were not apparent. However, there was a tendency for pyramidal cell size to be larger caudally and gradually decrease rostrally. Additionally there were significant differences in threshold values comparing the caudal third of M1 to the intermediate and rostral thirds, although no significant differences were found when comparing the rostral third to the intermediate third. Other features of M1 subdivisions, such as differences in proprioceptive and cutaneous inputs (Strick and Preston, 1982) or premotor and somatosensory connections (Stepniewska et al., 1993), cannot be addressed here. Our architectonic and physiologic data suggest a more subtle rostrocaudal difference in M1 than architectonic and physiologic data in other New

World or Old World primates. However, our data is insufficient, and additional information on connectivity patterns is essential for a complete characterization of subdivisions in M1.

Evidence of premotor areas in marmosets

In all cases we were able to elicit responses from cortex rostral to the primary motor area. These responsive points were high threshold, sparse, and generally close to the M1 border. The most medial points appeared to have a full body representation organized rostrocaudally. The more lateral points consisted mainly of shoulder, elbow, and trunk movements, while the most lateral points consisted entirely of forearm and face movements. In a recent cytoarchitectural study, Burman et al. (2006) identified subdivisions of area 6 (6m, 6d, 6v), that correspond roughly to our medial, more lateral, and most lateral points.

Studies of motor cortex in New World owl monkeys (Preuss et al., 1996) and prosimian galagos (Wu et al., 2000) have proposed several areas rostral to M1 with higher average thresholds, including: 1) a supplementary motor area with a topographic, rostrocaudal representation of the body (face and forelimb rostral, hindlimb caudal); 2) a dorsal premotor area with a complete body representation and a predominance of proximal (shoulder and elbow) movements in the forelimb region; and 3) a ventral premotor area of orofacial and forelimb movements. The evidence from other primates, when compared to the marmoset frontal cytoarchitecture and stimulation results in this paper, suggest that areas 6m, 6d, 6v in the marmoset may be homologous to the motor areas SMA, PMD, and PMV of other primates. As our responses were sparse and no

responses were recorded in more rostral or medial areas, we cannot comment on the detailed physiology of premotor cortex, on the possible subdivisions of PMD and PMV, on other motor areas such as pre-SMA or cingulate motor areas, or on the nature of area 6dr identified by Burman et al. (2006). Additional investigations, perhaps using other anesthetic parameters or higher levels of stimulation, are needed to characterize other regions of motor cortex in the marmoset.

Movements of the eyes. Although no movements of the eyes were observed in any of our cases, marmosets likely have a cortical area devoted to these movements. A putative frontal eye field (FEF) has been identified based on physiologic responses in common marmosets (Blum et al., 1982; Krubitzer and Kaas, 1990a). Krubitzer and Kaas (1990a) placed FEF immediately rostral to their motor region M. We did not find eye movements immediately rostral to the lateral part of area M1, as would be expected from the proposed map, but threshold values for evoking eye movements in FEF have been found much higher than our limit of 120 μA (Stepniewska et al., 1993; Wu et al., 2000). Additionally, we found area 3a to be smaller and premotor cortex to be larger in rostrocaudal length than proposed by Krubitzer and Kaas (1990a). Based the rostrocaudal lengths of area 3a, M1, and the premotor areas found in our study, and in Burman et al. (2006), we propose that the FEF is located approximately 4 mm rostral to area 3b, as suggested by Krubitzer and Kaas (1990a), and that area 3a, M1, and the premotor areas all lie between area 3b and FEF (Fig. 1).

Electrophysiology and architectonics of somatosensory cortex

Size of area 3a. Area 3a appears to have a similar motor organization to M1, with a mediolateral organization of hindlimb/trunk/forelimb/face regions and a disordered topography within these four regions, where movements of specific joints and specific parts of the face were sometimes scattered into multiple locations. Our stimulation data is consistent with the somatotopy revealed when recording from area 3a of marmosets, which revealed a mediolateral organization from hindlimb to face (Huffman and Krubitzer, 2001a).

While Huffman and Krubitzer (2001a) noted variability between individuals in the rostrocaudal width of area 3a (between 1-2.5 mm), our cytoarchitectonic results outline area 3a as a region approximately 1 mm in rostrocaudal length, approximately half the length of either 3b or M1. We suggest that the rostrocaudal width of area 3a is closer to the minimum width of 1 mm proposed by Huffman and Krubitzer (2001a).

Possibly, some of M1 was included in area 3a by Huffman and Krubitzer (2001a) as a result of recordings in M1 that were similar to that of area 3a. A thalamocortical study of area 3a and M1 by Huffman and Krubitzer (2001b) suggests that M1 has connections to thalamic motor areas, while area 3a appeared to be a hybrid region with connections to somatosensory areas of the thalamus and, unexpectedly, with strong connections to motor areas of thalamus. Injections in rostral area 3a revealed connectivity patterns similar to those of motor areas, with more extensive connections with both the motor thalamus and areas of premotor cortex. This finding suggests that the injections involved M1, and that the M1/3a border was located more caudally than illustrated. Consistent with this interpretation, Huffman and Krubitzer (2001a) show in

some cases that their histologically-defined M1 has some sites with responses to the stimulation of deep (muscle and joint) receptors.

Organization of area 3b. Recording studies indicate that area 3b has a fairly precise somatotopic representation of cutaneous receptors of the contralateral body (Krubitzer and Kaas, 1990b). Sites responding to a certain body part are not scattered as those for evoked movements in M1 or area 3a, but rather adjacent body parts are adjacent to one another. Similar to previous studies, our experiment has found two exceptions to the continuous orderly progression of the body in area 3b. First, there is a transition from the hand to the face near the 3b bend, and this border has been related histologically to a thin rostrocaudal strip of myelin-light tissue that can be seen in flattened sections (Fang et al., 2002; Krubitzer and Kaas, 1990b). In our cases reconstructed from flattened sections (Fig. 3-5), the myelin-light strip of tissue is in the general location of the forelimb/face border, although in our microstimulation experiments elbow movements rather than hand movements were evoked just medial to that border. Second, area 3b has a representation of ipsilateral face in the most rostrolateral part (Iyengar et al., 2007; Kaas et al., 2006). In one of our cases (Fig. 4) we elicited movements of the ipsilateral face in very lateral-most parts of 3b.

Evolution of motor cortex

The organization of motor cortex varies across mammals. In mammals such as opossums (Beck et al., 1996; Frost et al., 2000), motor areas may be completely missing, with cortical motor functions dependent on areas of somatosensory cortex. In most or all Eutherian mammals, M1 is distinct and one or more premotor areas may exist. Rats

(Donoghue and Wise, 1982; Neafsey and Sievert, 1982) and more recently tree shrews (Remple et al., 2006; Remple et al., 2007) both appear to have an M1 and at least one premotor area. Prosimian primates (Wu et al., 2000) have several premotor areas, while New World and Old World primates have M1 and premotor areas that can be subdivided (Kaas, 2004; Stepniewska et al., 1993; Stepniewska et al., 2006). Our data suggests that M1 in marmosets may have some rostrocaudal heterogeneity but it is not clearly subdivided. Marmoset M1, then, may be similar to that of prosimians such as galagos, or possibly intermediate between prosimians and other New World monkeys.

Marmosets were in part chosen because of their intriguing evolutionary position. Some authors propose that marmosets have undergone dwarfism, with a reduced size ideal for an arboreal, insectivore lifestyle in the fine branches that would not support larger primates (Bloch and Boyer, 2002; Ford and Davis, 1992; Soligo and Martin, 2006; Sussman and Kinzey, 1984). This view would suggest that marmosets represent a line of New World monkeys that have lost subdivisions of M1. Formerly, some authors regarded marmosets as a primitive line of monkeys morphologically similar to the first New World primates (Herschkovitz 1977, Beattie 1927), but this view is no longer widely held. Nevertheless, the division of M1 into rostral and caudal portions may have occurred during the evolution of some New World monkeys and not others. This view would suggest that the subdivision of M1 occurred independently in New World and Old World primates, and may explain why a different set of subdivisions has been proposed for macaque M1 than for owl monkey M1 (Preuss et al., 1997; Stepniewska et al., 1993).

Acknowledgments

We thank Charnese Bowes and Tiffanie Markus for assistance with the microstimulation, Laura Trice and Mary Varghese for assistance with histology, Mary Feurtado for assistance with anesthesia, Troy Hackett and Maggie McTighe for assistance with surgical procedures, and Mike Remple for helpful discussion. This work was supported by NINDS/NIH NS16446 (MJB, IS, JHK) and by the Public Health Service award T32 GM07347 from the National Institute of General Medical Studies for the Vanderbilt Medical-Scientist Training Program (MJB).

Addendum

A second study was published which examined the physiology, connectivity, architectonics of marmoset primary motor cortex using similar methods (Burman et al., 1998). The findings of their paper are very similar to ours. Using intracortical microstimulation, both works found marmoset M1 to be an area with an orderly mediolateral organization of hindlimb-trunk-forelimb-face regions, with threshold currents higher than those found in other primate species. Histologically, both works describe M1 as a myelin-dark area with large pyramidal cells in layer V and a small or absent layer IV, area 3b as a myelin-dark area with a well-defined area IV but a small or absent layer V, and area 3a as area intermediate in characteristics between M1 and 3b. Both works propose that M1 has no clear subdivisions, such as M1r and M1c, as found in other New World primates (Stepniewska et al., 1993).

Our work went on to describe the physiology of frontoparietal cortex in greater detail, while the work of Burman et al. (2008) explored the connectivity of M1 with

posterior parietal cortex. Together, these works suggest that areas M1 and 3a have the lowest threshold values of all frontoparietal areas and that premotor cortex can be divided into at least three areas based on physiology and architectonics. Additionally, connections to M1 come mainly from somatosensory regions of posterior parietal cortex, while connections to premotor cortex include visual inputs.

References

Aitkin LM, Kudo M, Irvine DR. 1988. Connections of the primary auditory cortex in the common marmoset, Callithrix jacchus jacchus. J Comp Neurol 269(2):235-248.

Aitkin LM, Merzenich MM, Irvine DR, Clarey JC, Nelson JE. 1986. Frequency representation in auditory cortex of the common marmoset (Callithrix jacchus jacchus). J Comp Neurol 252(2):175-185.

Alipour M, Chen Y, Jurgens U. 2002. Anterograde projections of the motorcortical tongue area in the saddle-back tamarin (Saguinus fuscicollis). Brain Behav Evol 60(2):101-116.

Beattie J 1927. The anatomy of the common marmoset (Hapale jacchus). J Proc Zool Soc London 1927: 543-718.

Beck PD, Pospichal MW, Kaas JH. 1996. Topography, architecture, and connections of somatosensory cortex in opossums: evidence for five somatosensory areas. J Comp Neurol 366(1):109-133.

Bloch JI, Boyer DM. 2002. Grasping primate origins. Science 298(5598):1606-1610.

Blum B, Kulikowski JJ, Carden D, Harwood D. 1982. Eye movements induced by electrical stimulation of the frontal eye fields of marmosets and squirrel monkeys. Brain Behav Evol 21(1):34-41.

Brinkman C, Porter R. 1979. Supplementary motor area in the monkey: activity of neurons during performance of a learned motor task. J Neurophysiol 42(3):681-709.

Brodmann K. 1909. Vergleischende Lokalisationslehre der Grosshirnrinde. Leipzig: Barth.

Burish MJ, Stepniewska I, Kaas JH. 2006. Topographic organization and architectonics of primary motor cortex and the supplementary motor area in marmosets. Soc Neurosci Abstr 806.11.

Burman KJ, Palmer SM, Gamberini M, Rosa MG. 2006. Cytoarchitectonic subdivisions of the dorsolateral frontal cortex of the marmoset monkey (Callithrix jacchus), and their projections to dorsal visual areas. J Comp Neurol 495(2):149-172.

Burman KJ, Palmer SM, Gamberini M, Spitzer MW, Rosa MG. 2008. Anatomical and physiological definition of the motor cortex of the marmoset monkey. J Comp Neurol 506(5):860-876.

Carlson M, Huerta MF, Cusick CG, Kaas JH. 1986. Studies on the evolution of multiple somatosensory representations in primates: the organization of anterior parietal cortex in the New World Callitrichid, Saguinus. J Comp Neurol 246(3):409-426.

Cartmill M. 1974. Rethinking primate origins. Science 184(135):436-443.

de la Mothe LA, Blumell S, Kajikawa Y, Hackett TA. 2006a. Cortical connections of the auditory cortex in marmoset monkeys: core and medial belt regions. J Comp Neurol 496(1):27-71.

de la Mothe LA, Blumell S, Kajikawa Y, Hackett TA. 2006b. Thalamic connections of the auditory cortex in marmoset monkeys: core and medial belt regions. J Comp Neurol 496(1):72-96.

Donoghue JP, Leibovic S, Sanes JN. 1992. Organization of the forelimb area in squirrel monkey motor cortex: representation of digit, wrist, and elbow muscles. Exp Brain Res 89(1):1-19.

Donoghue JP, Wise SP. 1982. The motor cortex of the rat: cytoarchitecture and microstimulation mapping. J Comp Neurol 212(1):76-88.

Dum RP, Strick PL. 1991. The origin of corticospinal projections from the premotor areas in the frontal lobe. J Neurosci 11(3):667-689.

Fang PC, Jain N, Kaas JH. 2002. Few intrinsic connections cross the hand-face border of area 3b of New World monkeys. J Comp Neurol 454(3):310-319.

Fleagle JG. 1999. Primate adaptation and evolution. San Diego: Academic Press. xvii, 596.

Ford SM, Davis LC. 1992. Systematics and body size: implications for feeding adaptations in New World monkeys. Am J Phys Anthropol 88(4):415-468.

Fritsches KA, Rosa MG. 1996. Visuotopic organisation of striate cortex in the marmoset monkey (Callithrix jacchus). J Comp Neurol 372(2):264-282.

Frost SB, Milliken GW, Plautz EJ, Masterton RB, Nudo RJ. 2000. Somatosensory and motor representations in cerebral cortex of a primitive mammal (Monodelphis domestica): a window into the early evolution of sensorimotor cortex. J Comp Neurol 421(1):29-51.

Gabernet L, Meskenaite V, Hepp-Reymond MC. 1999. Parcellation of the lateral premotor cortex of the macaque monkey based on staining with the neurofilament antibody SMI-32. Exp Brain Res 128(1-2):188-193.

Gallyas F. 1979. Silver staining of myelin by means of physical development. Neurol Res 1(2):203-209.

Geneser-Jensen FA, Blackstad TW. 1971. Distribution of acetyl cholinesterase in the hippocampal region of the guinea pig. I. Entorhinal area, parasubiculum, and presubiculum. Z Zellforsch Mikrosk Anat 114(4):460-481.

Geyer S, Zilles K, Luppino G, Matelli M. 2000. Neurofilament protein distribution in the macaque monkey dorsolateral premotor cortex. Eur J Neurosci 12(5):1554-1566.

Gould HJ, 3rd, Cusick CG, Pons TP, Kaas JH. 1986. The relationship of corpus callosum connections to electrical stimulation maps of motor, supplementary motor, and the frontal eye fields in owl monkeys. J Comp Neurol 247(3):297-325.

Herculano-Houzel S, Collins CE, Wong P, Kaas JH. 2007. Cellular scaling rules for primate brains. Proc Natl Acad Sci U S A 104(9):3562-3567.

Hershkovitz P. 1977. Living New World Monkeys, Vol. 1. Chicago: University of Chicago Press.

Huffman KJ, Krubitzer L. 2001a. Area 3a: topographic organization and cortical connections in marmoset monkeys. Cereb Cortex 11(9):849-867.

Huffman KJ, Krubitzer L. 2001b. Thalamo-cortical connections of areas 3a and M1 in marmoset monkeys. J Comp Neurol 435(3):291-310.

Huntley GW, Jones EG. 1991. Relationship of intrinsic connections to forelimb movement representations in monkey motor cortex: a correlative anatomic and physiological study. J Neurophysiol 66(2):390-413.

Iyengar S, Qi HX, Jain N, Kaas JH. 2007. Cortical and thalamic connections of the representations of the teeth and tongue in somatosensory cortex of new world monkeys. J Comp Neurol 501(1):95-120.

Jerison HJ. 1973. Evolution of the brain and intelligence. New York: Academic Press. xiv, 482 p. p.

Kaas JH. 2000. Why is brain size so important: design problems and solutions as neocortex gets bigger or smaller. Brain and Mind 1(1):7-23.

Kaas JH. 2004. Evolution of somatosensory and motor cortex in primates. Anat Rec A Discov Mol Cell Evol Biol 281(1):1148-1156.

Kaas JH, Qi HX, Iyengar S. 2006. Cortical network for representing the teeth and tongue in primates. Anat Rec A Discov Mol Cell Evol Biol 288(2):182-190.

Kajikawa Y, de La Mothe L, Blumell S, Hackett TA. 2005. A comparison of neuron response properties in areas A1 and CM of the marmoset monkey auditory cortex: tones and broadband noise. J Neurophysiol 93(1):22-34.

Krubitzer LA, Kaas JH. 1990a. Cortical connections of MT in four species of primates: areal, modular, and retinotopic patterns. Vis Neurosci 5(2):165-204.

Krubitzer LA, Kaas JH. 1990b. The organization and connections of somatosensory cortex in marmosets. J Neurosci 10(3):952-974.

Krubitzer LA, Kaas JH. 1992. The somatosensory thalamus of monkeys: cortical connections and a redefinition of nuclei in marmosets. J Comp Neurol 319(1):123-140.

Kwan HC, MacKay WA, Murphy JT, Wong YC. 1978. Spatial organization of precentral cortex in awake primates. II. Motor outputs. J Neurophysiol 41(5):1120-1131.

Lee VM, Otvos L, Jr., Carden MJ, Hollosi M, Dietzschold B, Lazzarini RA. 1988. Identification of the major multiphosphorylation site in mammalian neurofilaments. Proc Natl Acad Sci U S A 85(6):1998-2002.

Lemon RN, Griffiths J. 2005. Comparing the function of the corticospinal system in different species: organizational differences for motor specialization? Muscle Nerve 32(3):261-279.

Lui LL, Bourne JA, Rosa MG. 2006. Functional response properties of neurons in the dorsomedial visual area of New World monkeys (Callithrix jacchus). Cereb Cortex 16(2):162-177.

Lyon DC, Kaas JH. 2001. Connectional and architectonic evidence for dorsal and ventral V3, and dorsomedial area in marmoset monkeys. J Neurosci 21(1):249-261.

Mott FW, Schuster E, Halliburton WD. 1909. Cortical lamination and localization in the brain of the marmoset. Proc Soc London, series B 82:124-134.

Neafsey EJ, Sievert C. 1982. A second forelimb motor area exists in rat frontal cortex. Brain Res 232(1):151-156.

Padberg J, Disbrow E, Krubitzer L. 2005. The organization and connections of anterior and posterior parietal cortex in titi monkeys: do New World monkeys have an area 2? Cereb Cortex 15(12):1938-1963.

Peden JK, von Bonin G. 1947. The neocortex of hapale. J Comp Neurol 86(1):37-63.

Philibert B, Beitel RE, Nagarajan SS, Bonham BH, Schreiner CE, Cheung SW. 2005. Functional organization and hemispheric comparison of primary auditory cortex in the common marmoset (Callithrix jacchus). J Comp Neurol 487(4):391-406.

Preuss TM, Stepniewska I, Jain N, Kaas JH. 1997. Multiple divisions of macaque precentral motor cortex identified with neurofilament antibody SMI-32. Brain Res 767(1):148-153.

Preuss TM, Stepniewska I, Kaas JH. 1996. Movement representation in the dorsal and ventral premotor areas of owl monkeys: a microstimulation study. J Comp Neurol 371(4):649-676.

Purvis A. 1995. A composite estimate of primate phylogeny. Philos Trans R Soc Lond B Biol Sci 348(1326):405-421.

Qi HX, Lyon DC, Kaas JH. 2002. Cortical and thalamic connections of the parietal ventral somatosensory area in marmoset monkeys (Callithrix jacchus). J Comp Neurol 443(2):168-182.

Qi HX, Preuss TM, Kaas JH. 2007. Somatosensory areas of the cerebral cortex: architectonic characteristics and modular organization. In: Gardner EP, Kaas JH, editors. Handbook of the senses. London: Elsevier.

Qi HX, Stepniewska I, Kaas JH. 2000. Reorganization of primary motor cortex in adult macaque monkeys with long-standing amputations. J Neurophysiol 84(4):2133-2147.

Remple MS, Reed JL, Stepniewska I, Kaas JH. 2006. Organization of frontoparietal cortex in the tree shrew (Tupaia belangeri). I. Architecture, microelectrode maps, and corticospinal connections. J Comp Neurol 497(1):133-154.

Remple MS, Reed JL, Stepniewska I, Lyon DC, Kaas JH. 2007. The organization of frontoparietal cortex in the tree shrew (Tupaia belangeri): II. Connectional evidence for a frontal-posterior parietal network. J Comp Neurol 501(1):121-149.

Rizzolatti G, Luppino G, Matelli M. 1998. The organization of the cortical motor system: new concepts. Electroencephalogr Clin Neurophysiol 106(4):283-296.

Rosa MG, Elston GN. 1998. Visuotopic organisation and neuronal response selectivity for direction of motion in visual areas of the caudal temporal lobe of the marmoset monkey (Callithrix jacchus): middle temporal area, middle temporal crescent, and surrounding cortex. J Comp Neurol 393(4):505-527.

Rosa MG, Fritsches KA, Elston GN. 1997. The second visual area in the marmoset monkey: visuotopic organisation, magnification factors, architectonical boundaries, and modularity. J Comp Neurol 387(4):547-567.

Rosa MG, Palmer SM, Gamberini M, Tweedale R, Pinon MC, Bourne JA. 2005. Resolving the organization of the New World monkey third visual complex: the dorsal extrastriate cortex of the marmoset (Callithrix jacchus). J Comp Neurol 483(2):164-191.

Sengpiel F, Troilo D, Kind PC, Graham B, Blakemore C. 1996. Functional architecture of area 17 in normal and monocularly deprived marmosets (Callithrix jacchus). Vis Neurosci 13(1):145-160.

Sessle BJ, Wiesendanger M. 1982. Structural and functional definition of the motor cortex in the monkey (Macaca fascicularis). J Physiol 323:245-265.

Siegel S, Castellan J, N.J. 1988. Nonparametric Statistics for the Behavioral Sciences. New York: McGraw-Hill.

Soligo C, Martin RD. 2006. Adaptive origins of primates revisited. J Hum Evol 50(4):414-430.

Stepniewska I, Preuss TM, Kaas JH. 1993. Architectonics, somatotopic organization, and ipsilateral cortical connections of the primary motor area (M1) of owl monkeys. J Comp Neurol 330(2):238-271.

Stepniewska I, Preuss TM, Kaas JH. 2006. Ipsilateral cortical connections of dorsal and ventral premotor areas in New World owl monkeys. J Comp Neurol 495(6):691-708.

Sternberger LA, Sternberger NH. 1983. Monoclonal antibodies distinguish phosphorylated and nonphosphorylated forms of neurofilaments in situ. Proc Natl Acad Sci U S A 80(19):6126-6130.

Strick PL, Preston JB. 1982. Two representations of the hand in area 4 of a primate. II. Somatosensory input organization. J Neurophysiol 48(1):150-159.

Stoney SD, Jr., Thompson WD, Asanuma H. 1968. Excitation of pyramidal tract cells by intracortical microstimulation: effective extent of stimulating current. J Neurophysiol 31(5):659-669.

Sussman RW, Kinzey WG. 1984. The ecological role of the callitrichidae: a review. Am J Phys Anthropol 64(4):419-449.

Waters RS, Samulack DD, Dykes RW, McKinley PA. 1990. Topographic organization of baboon primary motor cortex: face, hand, forelimb, and shoulder representation. Somatosens Mot Res 7(4):485-514.

Welker WI, Benjamin RM, Miles RC, Woolsey CN. 1957. Motor effects of stimulation of cerebral cortex of squirrel monkey (Saimiri sciureus). J Neurophysiol 20(4):347-364.

Wong-Riley M. 1979. Changes in the visual system of monocularly sutured or enucleated cats demonstrable with cytochrome oxidase histochemistry. Brain Res 171(1):11-28.

Woolsey CN, Settlage PH, Meyer DR, Sencer W, Pinto Hamuy T, Travis AM. 1952. Patterns of localization in precentral and "supplementary" motor areas and their relation to the concept of a premotor area. Res Publ Assoc Res Nerv Ment Dis 30:238-264.

Wu CW, Bichot NP, Kaas JH. 2000. Converging evidence from microstimulation, architecture, and connections for multiple motor areas in the frontal and cingulate cortex of prosimian primates. J Comp Neurol 423(1):140-177.

Wu CW, Kaas JH. 1999. Reorganization in primary motor cortex of primates with long-standing therapeutic amputations. J Neurosci 19(17):7679-7697.

CHAPTER III

CORTICAL PLASTICITY AND BEHAVIORAL EFFECTS OF DORSAL COLUMN INJURIES IN MARMOSETS

This chapter includes contributions from Gharbawie OA, Bowes CP-G, Qi HX, Stepniewska I, and Kaas JH.

Introduction

A lesion of the dorsal columns at the cervical level in primates results in several physiologic and behavioral deficits. Physiologically, long-standing dorsal column lesions result in the reorganization of primary somatosensory cortex (area 3b), where the somatosensory map of the body changes and body parts that still receive peripheral input become overrepresented. Parts of primary somatosensory cortex deprived of inputs begin to respond to parts that are still intact, such as the somatosensory area normally representing the fingers now responding to the face (Jain et al., 1997). This type of plasticity after the loss of peripheral inputs is associated with the sprouting of new connections in the brainstem, such as those from the trigeminal nucleus to the cuneate nucleus (Jain et al., 2000) or from the gracile fasciculus to the cuneate nucleus (Sengelaub et al., 1997). This sprouting in part leads to the reorganization of somatosensory maps in the cuneate nucleus (Churchill et al., 2001; Xu and Wall, 1997) as well as its primary target, the ventroposterior nucleus of the thalamus (Churchill et al., 2001; Florence et al., 2000; Garraghty and Kaas, 1991a). To some extent, then, cortical plasticity reflects reorganization at lower levels, suggesting that cortical areas receiving

similar thalamic connections to area 3b, such as area 1 (Cusick and Gould, 1990; Lin et al., 1979; Mayner and Kaas, 1986; Nelson and Kaas, 1981), would similarly reorganize. The effects of dorsal column injuries on motor cortex organization are incomplete, but preliminary findings suggest that there are few changes in the cortical motor maps (Kaas et al., 2008).

Behaviorally, dorsal column lesions in primates appear to interfere with several somatomotor functions. After dorsal column lesions animals are reluctant to use the affected hand for normal activities such as climbing and grooming (Leonard et al., 1992) and hold the limb in an abnormal position. Tactile discrimination is impaired, especially on tasks requiring temporal resolution such as directional discrimination (Vierck, 1974) and rough versus smooth testing (Vierck and Cooper, 1998). Motor impairments include inaccurate finger placement that interferes with grasping (Glendinning et al., 1993) and the modulation of force applied by the fingers (Glendinning et al., 1992). While some motor impairments may be due to lesions that extended into the lateral column, the dorsal columns appear to play some role in motor tasks, especially those requiring proprioceptive feedback.

The amount of reorganization that occurs in cortical areas other than area 3b, as well as the association between physiologic and behavioral changes, has not been well investigated. The goal of this report is to expand the investigation of plasticity following dorsal column injury. We examine somatosensory reorganization not only in primary somatosensory cortex, but also in other areas receiving somatosensory inputs to the thalamus, such as areas 3a and 1/2. We also characterize changes in somatomotor behavior, specifically a reach and retrieval task. We focus on common marmosets, since

the normal organization of somatosensory areas 3a and 3b (Huffman and Krubitzer, 2001; Krubitzer and Kaas, 1990), and motor cortex (Burish et al., 2008; Burman et al., 2008) have previously been characterized, as well as some aspects of their normal behavior (Przybyszewski et al., 2007) and their behavior after CNS injury (Iwanami et al., 2005; Marshall et al., 2002). Additionally, cortical and behavioral plasticity following dorsal column lesions in the Callitrichidae family of New World monkeys has not yet been investigated. In the discussion section we provide some extra comparative data, with a limited examination of somatosensory cortical reorganization in two other primates (the prosimian galago and the New World squirrel monkey) and a limited examination of motor cortex organization following dorsal column injury in marmosets, galagos, and squirrel monkeys.

Materials and methods

Five adult common marmosets (*Callithrix jacchus jacchus*) were examined in this study. Animals were behaviorally trained on a reaching task, after which a spinal cord lesion was performed. After a recovery period of several days, the animals resumed behavioral training for two to ten weeks. Near the end of behavioral training, animals were injected with the neuroanatomical tracer B-HRP into all ten fingers. Five to six days after tracer injections, multiunit electrode recordings were performed, the animals were perfused, and histological analysis of the tissue was done. This timeline was identical in all animals with two exceptions: tracer injections were not made in one case (07-68), and two spinal lesions spaced ten weeks apart were performed in another case (08-06).

We similarly examined one galago (*Otolemur garnetti*) and one squirrel monkey (*Saimiri sciureus*), which are presented in the discussion section. In both the galago and squirrel monkey, CTB tracer was used in place of B-HRP. In the squirrel monkey one additional manipulation was performed: a dorsal brainstem injection of penicillinase (Sigma, St. Louis, MO), a control enzyme which has been shown to have no effect on CNS tissue (Bradbury et al., 2002; Caggiano et al., 2005; Massey et al., 2006).

In the galago, squirrel monkey, and one marmoset (case 07-53), we additionally performed intracortical microstimulation after multiunit recordings. All procedures were approved by the Vanderbilt University Institutional Animal Care and Use Committee and followed National Institutes of Health guidelines.

Behavioral analysis. Marmosets were transferred to a separate cage for behavioral training on a reach-retrieve task. Reaching boxes were made of clear Plexiglas, with the dimensions 45 cm long x 14 cm wide x 35 cm high. In the center of each front wall was a vertical slit 2 cm-wide, which extended from 2 cm above the floor to a height of 15 cm. On the outside of the wall, in front of the slit and mounted 4 cm above the floor, was a 2 cm-deep shelf. Two indentations on the surface of the shelf were located 3 cm from the inside of the wall and were aligned with the edges of the slit where marmosets could reach. The food target was made of slightly stale and hardened (i.e., not sticky) marshmallows. Each approximated the shape of a 1 mm diameter sphere.

To motivate marmosets to reach for the target, food was removed from the home cage 6-8 hours before reach training. The first week of training consisted of daily 15 minute sessions for each marmoset. Over the following two weeks marmosets still

received daily training sessions, but a session now consisted of 30 food pellets (also considered 30 trials) per session for no longer than 30 min. A session began when a food-deprived marmoset was individually placed in the reaching box and ended when the marmoset was removed from the box and returned to the home cage in which food access was regained.

Successful reaching involved the achievement of three stages, in which a marmoset learned to: 1) orient to the food pellet through the slot, 2) transport its forelimb through the slot to grasp the food pellet, and 3) withdraw its forelimb through the slot to present grasped food to the mouth.

To encourage a naive marmoset to orient to the slot at the front of the reaching box, a number of food morsels were placed on the shelf and directly in front of the slot. The objective was to make the food readily accessible to either hand through the slot. Once a marmoset was successfully taking food from the shelf, pellets were moved further from the slot to encourage forelimb transport for pellet retrieval. Once a marmoset demonstrated a preference for one paw by making more reaching attempts with it, individual morsels were placed into the indentation contralateral to that hand. After retrieving several morsels with a single hand and presenting it to the mouth, the experimenter introduced a delay before presentation of each successive pellet. During the delay, the marmosets were trained to leave the slot, go to the back of the box, and then return to the slot. This provision was introduced to the reaching paradigm to ensure that marmosets properly oriented their body before reaching.

After the lesion the animals were given at least five days to recover before testing resumed. Usually 2-3 sessions were performed each week, with the exception of the first

lesion in case 08-06 in which the sessions were stopped until the week before the second lesion, because the animal did not appear to have a significant impairment. If the animal refused to reach for the target with the impaired hand, the pellet was moved more laterally to make it inaccessible to the unimpaired hand, thus encouraging the animal to use the impaired hand.

Surgery. We performed two separate surgical procedures on each animal: a spinal lesion, followed 2-10 weeks later by a craniotomy for physiologic mapping. In the squirrel monkey, a brainstem injection of penicillinase was also performed during the spinal lesion procedure.

For the spinal lesion procedure, animals were induced anesthetically with an intramuscular injection of ketamine (30 mg/kg) and xylazine (1-2 mg/kg), intubated, and maintained with 1-2% isoflurane gas. Animals were positioned for access to the dorsal cervical spine, and under sterile conditions an incision was made over the midline of the cervical vertebrae and the overlying musculature was dissected. Laminectomy of a single vertebra was performed, the dura removed, and a lesion of the dorsal column ipsilateral to the dominant hand was made with fine scissors. The lesion site was covered with Gelfilm (Pfizer Inc., New York, NY) and Gelfoam (Pfizer Inc., New York, NY), the overlying musculature sutured, and the incision stapled. The animal was then allowed to recover from anesthesia. Naxcel (2.2 mg/kg; Pfizer Inc., New York, NY), Robinul (0.015 mg/kg; Baxter Healthcare Corp., Deerfield, IL), and dexamethasone (1 mg/kg; Phoenix Scientific Inc., St. Joseph, MO) were administered before the initial incision, and

buprenorphine (0.01 mg/kg; Bedford labs, Bedford, OH) was administered after recovery from anesthesia.

For the squirrel monkey only, the spinal lesion procedure was immediately followed by a brainstem injection of pencillinase. The initial incision was extended to the lower portion of head, the overlying musculature dissected, and the dura removed. The medulla was exposed by tilting the head forward, and 750nL of penicillinase (50 U/mL) was injected 0.5 mm below the surface just lateral to the cuneate nucleus, ipsilateral to the spinal lesion. The injection was made using a mechanical microdrive (Nanoliter 2000, World Precision Instruments, Inc., Sarasota, FL), and the animal was then allowed to recover from anesthesia. Unlike previous work in rodents where multiple penicillinase injections are made (Bradbury et al., 2002; Caggiano et al., 2005; Massey et al., 2006), no second injection was made in the squirrel monkey.

For the physiologic mapping procedure, animals were induced anesthetically with an intramuscular injection of ketamine (30 mg/kg) and xylazine (1-2 mg/kg), briefly transferred to 2% isoflurane for surgical preparation and alignment in stereotaxic frame, and transferred to ketamine, either infusion (20 mg/ml) or intramuscular injections, maintaining a surgical anesthetic level. Ketamine was supplemented with intramuscular xylazine (5 mg/kg). Robinul (0.015 mg/kg) and dexamethasone (1 mg/kg) were administered. A portion of the scalp, cranium, and dura was removed over the frontal and parietal lobes and covered with silicone fluid in preparation for electrode recordings and stimulation.

Tracer injections. Animals were anesthetized with an intramuscular injection of ketamine (30 mg/kg). The distal phalanges of the fingers were disinfected with alcohol. A small amount of neuroanatomical tracer (~5 μl per injection site) was injected subcutaneously into the glabrous part of the distal phalange, just below the tip. All 10 fingers were injected, with one injection site per finger. Marmosets were injected with cholera toxin subunit B conjugated to horseradish peroxidase (0.2-0.4% B-HRP, List Biological Labs, Campbell, CA). The galago and squirrel monkey were injected with cholera toxin subunit B (1% CTB, Sigma, St. Louis, MO). After tracer injection, the animals were returned to their home cage for anesthesia recovery.

Microelectrode recordings and stimulation. For multiunit recordings we used low impedance (1 MΩ at 1 kHz) tungsten microelectrodes (Microprobe, Potomac, MD). Electrode penetration sites were marked on a high-resolution photograph of the exposed cortical surface. The electrode was placed perpendicular to the surface and advanced using a stepping microdrive. Recordings were made between 0.6-1.0 mm, aiming for layer IV cells. Marmosets have no central sulcus or dimple, so the location of primary somatosensory cortex was based on bone landmarks and cortical surface vasculature, as well as on the quality of responses. Multiple penetrations were made in a grid, with 0.2-0.5 mm between penetration sites (avoiding surface blood vessels). Receptive fields at each recording site were determined by stimulating the skin using light tapping, q-tips, small glass probes, and brushes for moving hairs. We measured minimal receptive fields, defined as the area of the body evoking a neural response when stimulated at near threshold level (Merzenich et al., 1978; Nelson et al., 1980; Wu and Kaas, 2003). In

addition to these cutaneous receptive fields, we also noted sites that responded to pressure and to joint movements. Points marked as unresponsive were those that did not respond to cutaneous stimulation, pressure, or movement. The entire body (head to tail) was examined.

For intracortical microstimulation we used low impedance tungsten microelectrodes (Microprobe, Potomac, MD). Electrode penetrations were marked on a high-resolution photograph of the exposed cortical surface. The electrode was placed perpendicular to the surface and advanced using a stepping microdrive to a depth of 1.8-2.0 mm, as this depth was optimal in previous studies (Burish et al., 2008; Burman et al., 2008; Wu et al., 2000). The stimulus consisted of a short monophasic train of 60 msec with a single pulse duration of 0.2 msec and a frequency of 300 Hz. The stimulus was delivered with a Master-8 Stimulator (A.M.P.I., Jerusalem, Israel) connected to a stimulus isolation unit (Bak Electronics, Mount Airy, MD). We noted both the type of movement evoked and the amount of current required to evoke it. Evoked movements were classified into four categories: face (jaw, lips, nose, cheek, vibrissae, eyelid, ear, tongue, throat, and some neck movements), forelimb (digit, wrist, elbow, and shoulder movements), trunk (lower trunk, upper trunk, and some neck movements), and hindlimb (toe, ankle, knee, hip, and tail movements). Movements of the eyes were examined but not observed. Some stimulation sites evoked weak or ambiguous movements, which were noted more generally such as "shoulder/upper trunk." We examined the threshold current, defined as the lowest value of current in which visible movements were repeatedly observed (on almost every trial). Unresponsive points were defined as points that did not elicit visible movements at 120 μA or less, with 120 μA chosen as a trade-off

between identifying motor areas with higher thresholds and restricting current spread to approximately 300 μm (Stoney et al., 1968).

At the conclusion of physiological mapping, microlesions of 10 μA direct current were placed at a few penetration sites to mark physiologic borders.

Perfusion and histology. At the end of the electrode recording and stimulation sessions, animals were given a lethal dose of sodium pentobarbital and, when areflexive, the heart was exposed, the right atrium opened, and a needle inserted into the left ventricle for perfusion. Animals were perfused with 0.9% phosphate-buffered saline (PBS, pH 7.4), followed by 2% paraformaldehyde in PBS, followed by 2% paraformaldehyde and 10% sucrose in PBS. The brain and spinal cord were exposed, and dorsal roots of the spinal cord were counted and marked with pins to locate the level of the lesion. The cerebral hemisphere contralateral to the lesion site was flattened, and the brainstem and cervical spinal cord were separated from the rest of the brain. The cortex, brainstem, and spinal cord were postfixed overnight in 2% paraformaldehyde and 10% sucrose in PBS and transferred to 30% sucrose in PBS. The next day the tissue was cut in 40 μl sections: the cortex was cut parallel to the surface, the brainstem was cut coronally, and the spinal cord was cut horizontally.

Sections were serially divided, so that the stains alternated. For cortex, the following stains were used: 1) cytochrome oxidase (Wong-Riley, 1979), and 2) Gallyas myelin stain (Gallyas, 1979). For brainstem the following stains were used: 1) cytochrome oxidase, and either 2) tetramethylbenzidine for visualization of B-HRP tracer (see below), or 3) immunohistochemistry for visualization of CTB tracer (see below).

For spinal cord the following stains were used: 1) acetylcholinesterase (Geneser-Jensen and Blackstad, 1971), 2) Nissl substance, using cresyl violet, and either 3) tetramethylbenzidine for visualization of B-HRP tracer, or 4) immunohistochemistry for visualization of CTB tracer.

For visualization of B-HRP, tetramethylbenzidine (chromagen) and diaminobenzidine (stabilizer) were used following a modified version of a previous protocol (Gibson et al., 1984). For visualization of CTB, we followed previous protocols (Angelucci et al., 1996; Bruce and Grofova, 1992). For CTB immunohistochemistry, tissue sections were washed in 0.1M phosphate buffer (PB, pH 7.4) then 0.5% Triton-X100 (Tx) in 0.05M Tris-buffered saline (TBS, pH 7.5). Sections were blocked in 2.5% normal rabbit serum in TBS/Tx for 2 hours, followed by incubation in a 1:4000 dilution of goat anticholeragenoid (List Biological Labs, Campbell, CA) in 2.5% normal rabbit serum, 2% Tx, and TBS for 4 days at 4°C. Sections were washed in 0.5% Tx in TBS and processed using the Vectastain Elite ABC kit (Vector Laboratories Inc., Burlingame, CA), involving incubation in a 1:200 dilution of biotinylated rabbit anti-goat IgG with 1% Tx in TBS for 2 hours at room temperature, wash in 0.5% Tx in TBS, and incubation in a 1:100 dilution of ABC reagent in 0.5% Tx in TBS for 1 hour at room temperature. Sections were developed with the VIP substrate kit (Vector Laboratories, Inc.).

Cortical sections were used for anatomic reconstruction. Sections were photographed using a Nikon DXM1200F digital camera attached to a Nikon Eclipse E800 microscope (Nikon Inc., Melville, NY). We obtained JPEG images using the Nikon ACT-1 software, and the images were not altered except for uniform changes in contrast using the Adobe Photoshop CS2 levels command (Adobe Systems Inc., San

Jose, CA). Images were imported into Adobe Illustrator CS2, and the borders of somatosensory and motor areas were outlined. Microlesions visible in the cortical sections were used to align multiple tissue sections with each other and with the physiologic data. Cytochrome oxidase and myelin sections were both useful in identifying somatosensory areas, and myelin sections were useful in identifying motor areas.

Brainstem sections were used to analyze the completeness of our dorsal column lesion, specifically the amount of fibers from the fingers that were still present in the cuneate nucleus. Cytochrome oxidase-stained sections were used to identify the location of the cuneate nucleus, and were aligned with adjacent B-HRP or CTB sections to analyze the amount of remaining dorsal column fibers.

Spinal cord sections were used to analyze the extent of our spinal cord lesion, both within and outside of the dorsal columns. The lesion site was readily visible, and the spinal cord was anatomically reconstructed at the level of the lesion by measuring the mediolateral extent of the lesion in each section. The acetylcholinesterase stain was most useful in identifying the dorsal columns, lateral columns, and gray matter.

Results

For each animal we characterized the extent of the spinal cord lesion using spinal architecture and neuroanatomical tracers. We correlated these findings with behavioral performance before and after spinal lesion, as well as with multiunit recordings of the hand area in somatosensory cortex after the lesion. For somatosensory recordings, our focus was area 3b, the adjoining rostral area 3a, and the adjoining caudal area which has

been labeled as either area 1 or area 2 in previous investigations (Burish et al., 2008; Huffman and Krubitzer, 2001; Krubitzer and Kaas, 1990).

We obtained a range of dorsal column lesions, from lesions not involving the finger to lesions that almost completely deprived finger inputs (Table 1). Due to the variability of lesion sizes, level of lesions, and survival times across animals, we consider this work a collection of case studies. The variability, however, allows us to investigate a range of possible changes following long-term dorsal column injuries in marmosets.

Extent of lesion

Spinal cord architecture. The level of spinal cord injury was determined by counting dorsal roots starting at C1, and by placing pins at selected locations around the lesion site. We sectioned the spinal cord horizontally, as this plane would best reveal the mediolateral extent of the injury. Sections of spinal cord were then stained for acetylcholinesterase to delineate spinal gray matter from white matter. We measured the size of the lesion for each section and measured sections systematically through the dorsoventral height of the cord.

Schematic diagrams of the reconstructed lesion sites are shown in Fig. 1. For each case the lesion site is outlined in the acetylcholinesterase-stained sections, one near the central canal and one in the middle of the dorsal horn. In the first case (07-68), the C3 lesion did not involve the dorsal column and instead affected the dorsal horn, dorsolateral white matter, and a portion of the lateral column. In the second case (07-53), the C3 lesion was restricted to the dorsal column but only to the midline portion of the fasciculus gracilis, and did not involve the fasciculus cuneatus. In the third case (07-76),

Table 1. Summary of dorsal column lesions[1]

Case	Sex	Wt. (g)	Lesion level	Survival time (d)
07-68	F	205	C3	13
07-53	M	260	C3	28
07-76	F	315	C3	42
07-86	M	300	C6	35
08-06	M	376	C8/(T1)	35/(70)

[1]Case numbers are ordered as they appear in the paper. Weights (Wt.) are reported in grams. Survival time represents the amount of time between the dorsal column lesion and the somatosensory/motor mapping. In case 07-76, two dorsal column lesions were made, the first at T1 and the second 70 days later at C8.

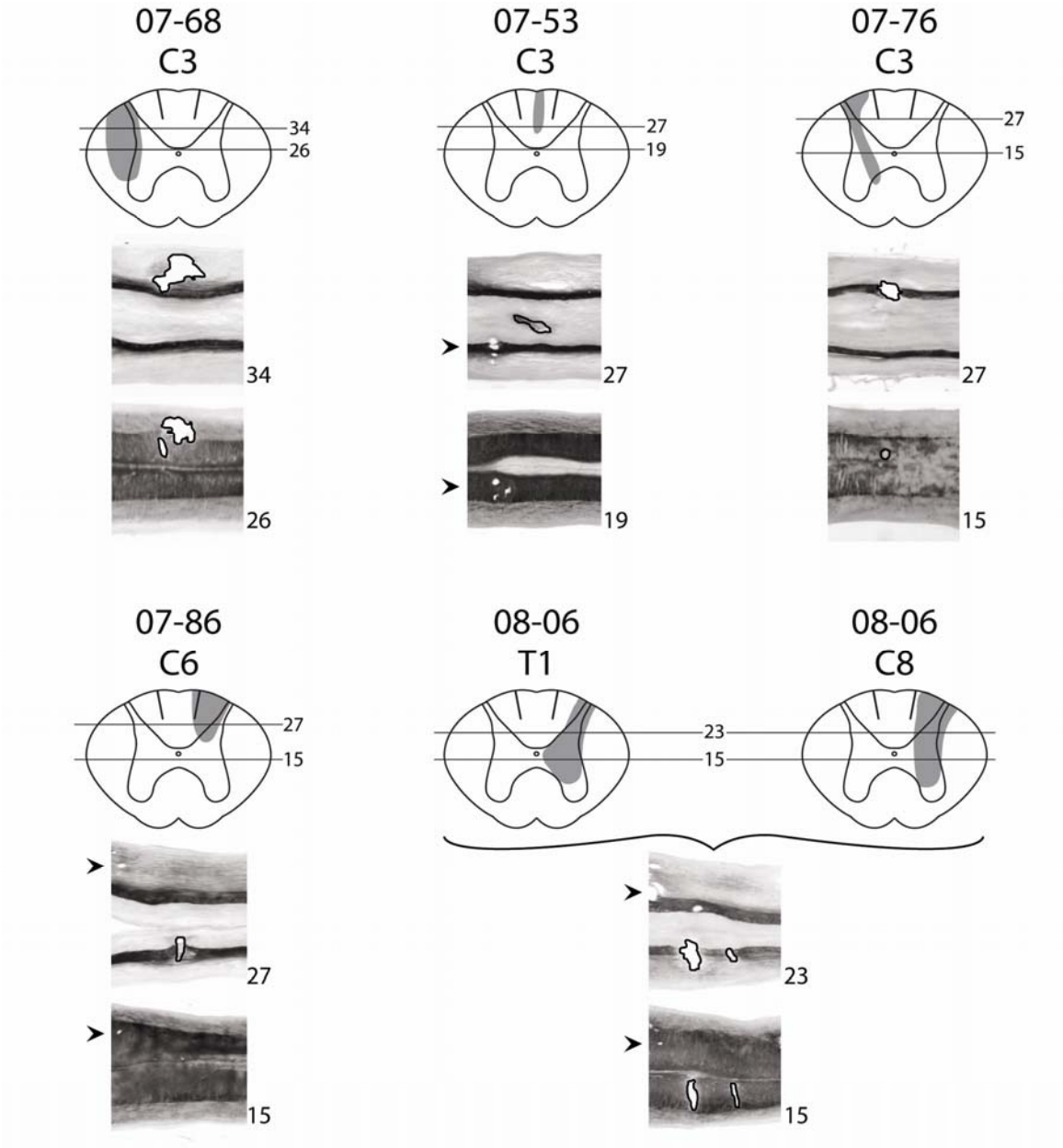

Figure 1. Anatomical reconstructions of spinal lesions. For each case a schematic transverse section of the spinal cord is shown, with the lesioned area shown in gray. The dorsal intermediate sulcus is shown and represents the division between the cuneate and gracile fasciculi, although this division was difficult to distinguish in the stained tissue. Lines running across the schematic represent the horizontal plane of section for the acetylcholinesterase-stained tissue below. In the tissue, the left side of the spinal cord is up, the right side of the spinal cord is down, and the rostral side of the spinal cord is to the right. Lesions are outlined in black; arrowheads mark the location of pins placed in the spinal cord and used for realignment.

the C3 lesion affected a portion of the fasciculus cuneatus, a substantial amount of the dorsal horn, some of the ventral horn, and a very small portion of the ventral white matter. In the fourth case (07-86), the C6 lesion involved the majority of the fasciculus cuneatus, although intact cuneate fibers may still remain in the more ventral portion of the dorsal columns near the central canal. A small portion of the fasciculus gracilis and the dorsal horn also seem to be affected, although the dorsolateral column and the ventral half of the spinal cord were not damaged. In the final case (08-06), two lesions were made, first at T1 and then 70 days later at C8. The T1 lesion affected the lateral-most portion of the fasciculus cuneatus and the medial-most portion of the dorsolateral column, the entire dorsal and intermediate horn, and some of the ventral horn of the gray matter. The C8 lesion involved a substantial amount of the fasciculus cuneatus, most of the dorsal and intermediate horns, and some of the ventral horn and the dorsolateral column.

Our lesions, then, represent a range of dorsal column injuries, from lesions not involving the dorsal column (07-68), to very small dorsal column lesions not involving the cuneate nucleus (07-53), to lesions involving small (07-76), large (07-86), and medium (08-06) proportions of the fasciculus cuneatus.

Transport of neuroanatomical tracer. We injected B-HRP into all ten fingers 5-6 days before perfusion, which has been shown to be sufficient transport time for bigger New World monkeys after spinal cord injury (Jain et al., 1997). As we did not examine the distribution of B-HRP in control marmosets, we are assuming that connections from the fingers to the cuneate nucleus are entirely ipsilateral, as has been proposed for other

primates. Under this assumption, the presence of tracer in the cuneate nucleus ipsilateral to the lesion implies that some fibers from the digits were not lesioned. If our assumption is incorrect we are likely underestimating the extent of the lesion, as the presence of some tracer in the ipsilateral side may instead be from the intact contralateral digits.

We examined the distribution of B-HRP labeled fibers from the upper cervical spinal cord to the lower pons. The extent of intact fibers between the fingertips and the brainstem are shown in Fig. 2. In cytochrome oxidase-stained sections the cuneate nucleus is well delineated as a darkly staining spherical structure in the middle part of the dorsal brainstem. In other primates the internal organization of the cuneate nucleus can be described as cytochrome oxidase-poor septa between darkly staining individual digit and palm areas (Florence et al., 1991; Strata et al., 2003). In common marmosets, however, the use of cytochrome oxidase alone was not sufficient to reveal these subdivisions.

An examination of B-HRP labeling on the non-lesioned side revealed good transport was for three of the cases, with more limited transport in case 07-86. No tracer injections were made in the first case (06-48). In the second case (07-53), the amount of tracer labeling was similar between the non-lesioned/control side and the lesioned side; few if any fibers to the cuneate nucleus were lesioned. In the third case (07-76), slightly more B-HRP labeled fibers were seen on the control side than on the lesioned side, although it is clearly an incomplete lesion and many cuneate fibers remain intact. In the fourth case (07-86) B-HRP transport was lower than in the other cases. Some labeling was seen in the control side, while on the lesioned side only a very small amount of B-HRP label was found in a few of the sections. Despite the low level of transport it still

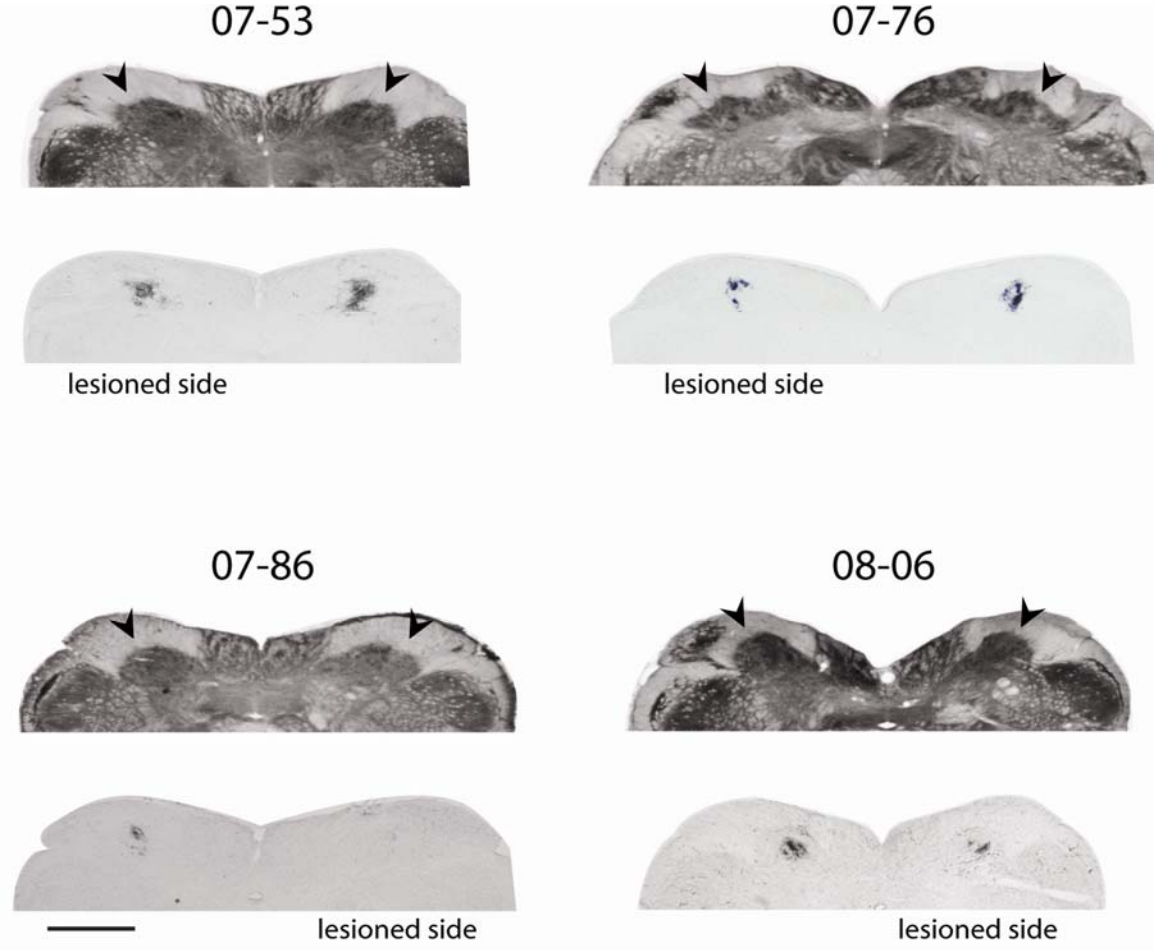

Figure 2. Transport of the neuroanatomical tracer B-HRP from the fingers to the cuneate nucleus. The dorsal halves of brainstem sections are shown for each case in which B-HRP was injected into the fingertips. In the cytochrome oxidase-stained sections (CO), arrowheads mark the location of the cuneate nuclei. In the tetramethylbenzidine-reacted sections for visualization of B-HRP (TMB), the side ipsilateral to the spinal cord lesion is marked. No injections were made in case 07-68 (not shown). Scale bar = 1 mm.

appears that this case has a very limited number of intact fibers from the fingers to the cuneate nucleus. In the final case (08-06), there are more fibers on the non-lesioned side than the lesioned side, although it is also clearly an incomplete lesion. We would expect an incomplete lesion in this animal; the lesions were at C8 and T1 and so digits 1-3 should remain intact. Because of our inability to distinguish the internal organization of the cuneate, however, we cannot say whether B-HRP labeling for digits 4-5 was reduced or completely eliminated.

The cases show a range of incomplete cuneate fasciculus lesions. There seems to be a good correlation between the findings for spinal cord reconstruction and tracer transport as both cases show a range from little-to-no involvement of cuneate fibers (07-53), a small lesion (07-76), an extensive lesion (07-86), and an intermediate lesion (08-06).

Behavioral effects of lesion

The animals were trained on a reach-and-retrieve task, where they extended their arm through a Plexiglas cage for a small pellet of food. The task is similar to that performed in rats (McKenna and Whishaw, 1999; Whishaw and Pellis, 1990) and somewhat similar to the Klüver boards used to assess primate behavioral performance (Friel and Nudo, 1998; Nudo et al., 1992). Unlike the Klüver board, however, the wells on our shelf were only 0.5 mm deep. Thus the majority of the pellet was above the well, presumably making it easier to grasp. Animals were trained before spinal cord injury to provide a baseline level of performance. After a recovery period of 5-7 days following the lesion, behavioral testing resumed. The animals used their entire hand to grasp the pellet,

favoring a power grasp to a precision grasp. We were not able to obtain post-lesional data from case 07-68, and so have omitted this case from our behavioral analysis.

Eventual success. Our first quantitative measure was eventual success (Fig. 3a). For this test a success was scored as any trial in which the animal successfully obtained the pellet off of the shelf. A miss was scored as any trial in which the animal knocked the pellet off the shelf, including into the cage. Before spinal lesion, all animals successfully obtained the pellet over 75% of the time. After spinal lesion, performance on this task did not change for the second case (07-53) or the final case (08-06). For the third and fourth cases (07-76 and 07-86), performance initially worsened, but after a period of weeks returned to near baseline. In the final case, the second lesion occurred after the week 10 data was collected. The week 10 data can thus be considered "prelesion" data for the second lesion, and thus performance after the second lesion did not change.

Single-reach success. For our second quantitative measure, we limited success to any trial in which the animal successfully obtained the pellet off the table using only one flexion of the fingers (Fig. 3b). Before spinal lesion, all animals had a single-reach success over 60%, and all performed slightly worse on this measure than the eventual success measure, meaning that even before the lesion all animals sometimes made multiple finger flexions to obtain the pellet. On this measure three animals performed worse immediately following the spinal lesion (07-53, 07-76, 07-86) although they returned to prelesion levels over a period of weeks. Interestingly, performance in case 07-53 worsened after the lesion, even though histological and tracer transport suggest that

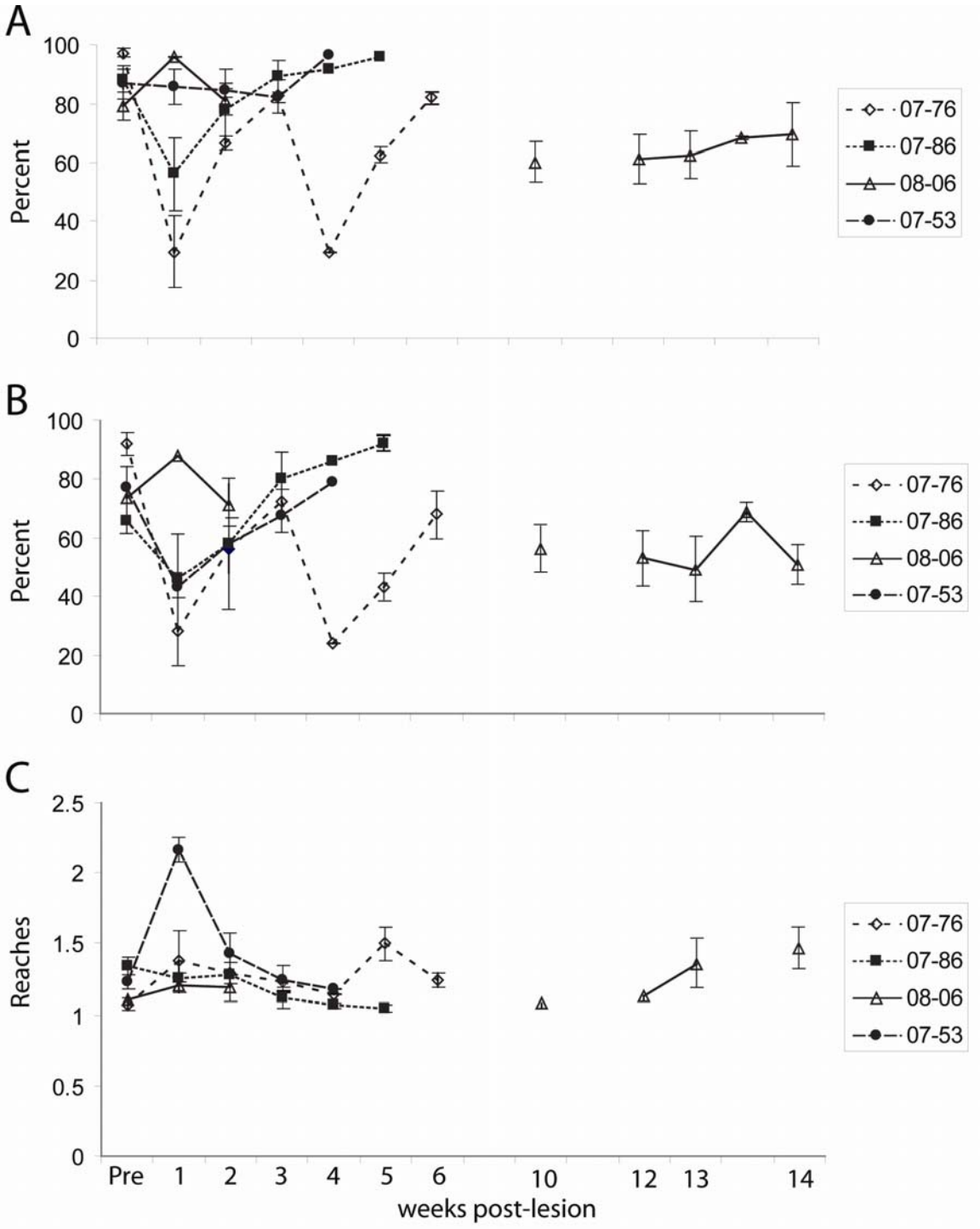

Figure 3. Behavioral performance. Animals were assessed quantitatively on three measures: A) eventual success, or the percentage of trials in which the animal ultimately picked the pellet up from the shelf and placed it in the mouth, B) single-reach success, or the percentage of trials in which the animal obtained the pellet using only a single digit flexion and a single reach, and C) reaches/success, or the average number of reaches necessary to obtain one pellet. Animals were trained before injury ("Pre") and up to four times each week following injury. The data is presented as mean ± SEM.

the animal had little if any cuneate tract lesion. For the final case (08-06), neither the first nor the second lesion affected single-reach success.

Reaches/success. For the third quantitative measure we divided the total number of reaches or finger flexions by the total number of times the animal successfully obtained the pellet, giving us a number of reaches needed for a success. Before spinal lesion, all animals required between 1 and 1.5 reaches per success. In three cases performance did not change after lesion (07-76, 07-86, and 08-06). Again in case 07-53, performance initially got worse, with the animal making more reaches and finger flexions, then returned to prelesion levels.

The behavioral measure that showed the widest range of performance was eventual success. No change in performance was seen in the animal whose lesion did not involve the cuneate tract (07-53) or in the animal with a low cervical lesion in which several digits were likely completely intact (08-06). In contrast the two animals with cuneate tract lesions, 07-76 and 07-86, showed transient impairments in performance on the task. Performance on the single-reach success and the reaches/success measures showed less of a range of performance, and interestingly the animal without a cuneate tract lesion (07-53) showed impairments on both tasks.

Physiologic effects of lesion

We performed somatosensory mapping in frontoparietal cortex, stimulating the entire body surface with light taps, q-tips, probes, and brushes. To identify somatomotor areas,

we correlated our results to the architectonic features of frontoparietal cortex by making microlesions. We used previous descriptions of marmoset frontoparietal architecture (Burish et al., 2006; Burman et al., 2006; Burman et al., 2008; Krubitzer and Kaas, 1990) to delineate borders.

Case 07-68. Only a few electrode penetrations were made in this case and were limited to identification of the hand region and the hand/face border in 3b, as well as the body between the forearm and the leg in area 3a (Fig. 4). In the hand region of 3b the digits were distributed in an orderly fashion, with the thumb most lateral and digit 5 most medial. Digits 2 and 3 were intermingled, and a similar amount of overlap has been seen in previous studies of marmoset area 3b (Huffman and Krubitzer, 2001). At the hand/face border, the thumb is bordered laterally by the chin as seen in studies of marmosets and other New World monkeys (Huffman and Krubitzer, 2001; Kaas et al., 1979; Sur et al., 1980). The mediolateral organization of area 3a from forearm to arm to trunk to leg is similar to that found in a previous study (Huffman and Krubitzer, 2001). For this case, in which the spinal lesion did not involve the dorsal column, the limited somatosensory maps of areas 3b and 3a are similar to the normal organization of these areas seen in previous studies.

Case 07-53. In this study we examined area 3b from face to leg, as well as an extensive amount of adjoining areas 3a and 1/2. In area 3b the somatosensory map again resembled the normal organization of marmoset 3b, with a chin representation immediately lateral to the hand area (Fig.5). Within the hand area the digits were organized mediolaterally from

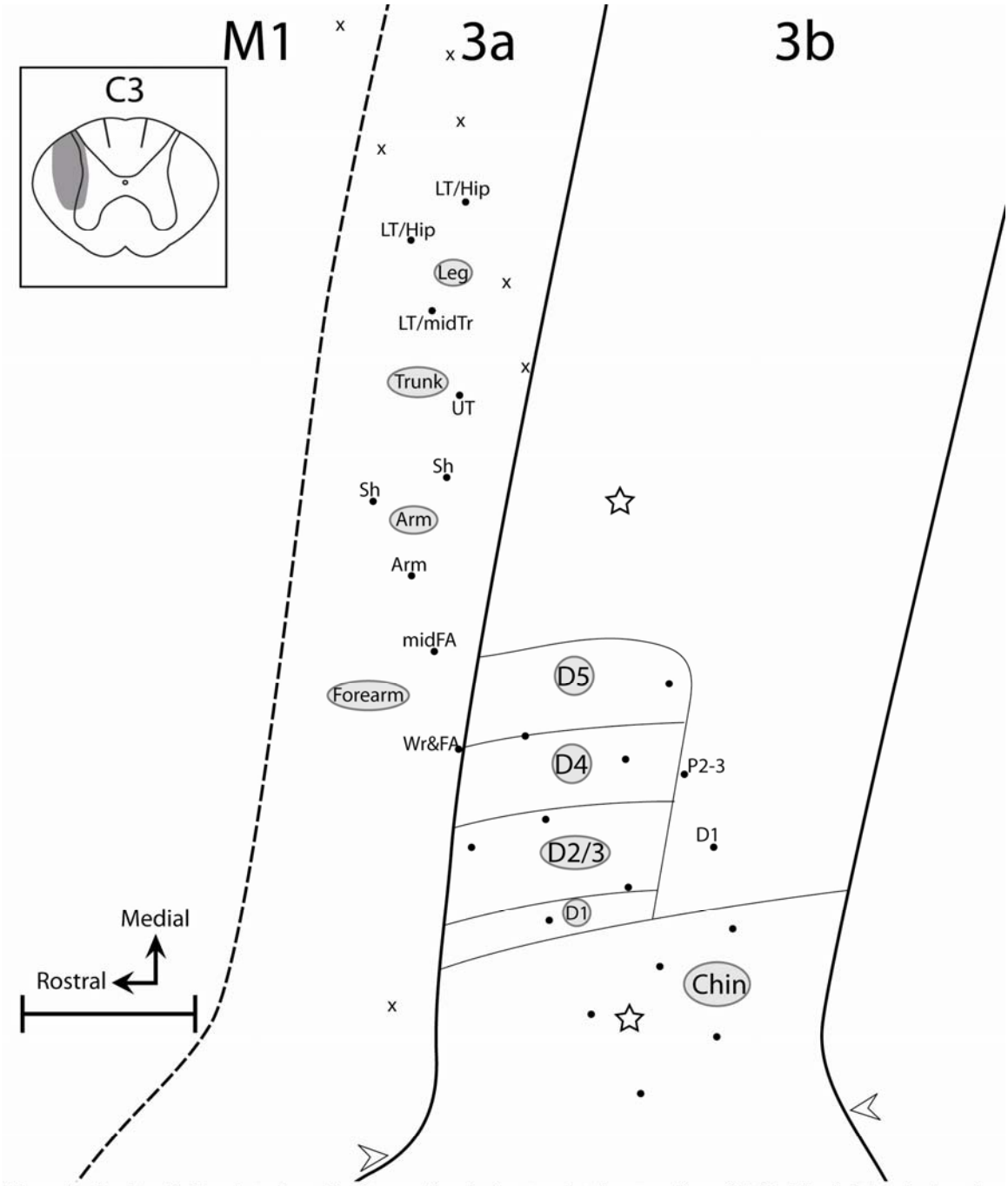

Figure 4. Results of microeletrode multiunit recordings in frontoparietal cortex of case 07-68. The right hemisphere is shown, but the map has been flipped so that in all figures rostral is to the left. A solid line delineates the borders of area 3b, while a dotted line indicates the approximate location of the 3a/M1 border. Thin lines mark the hand region of 3b as well as the hand/face border. Black dots, X's, and stars indicate the locations of responsive penetration points, unresponsive penetration points, and microlesions. When cortical regions were disordered, the location of the receptive field (see abbreviations list) is shown above the responsive point. Two arrowheads near the 3b bend mark the location of a myelin-light septum seen in histological sections. Lesion at top left, orientation at bottom left. Scale bar = 1 mm.

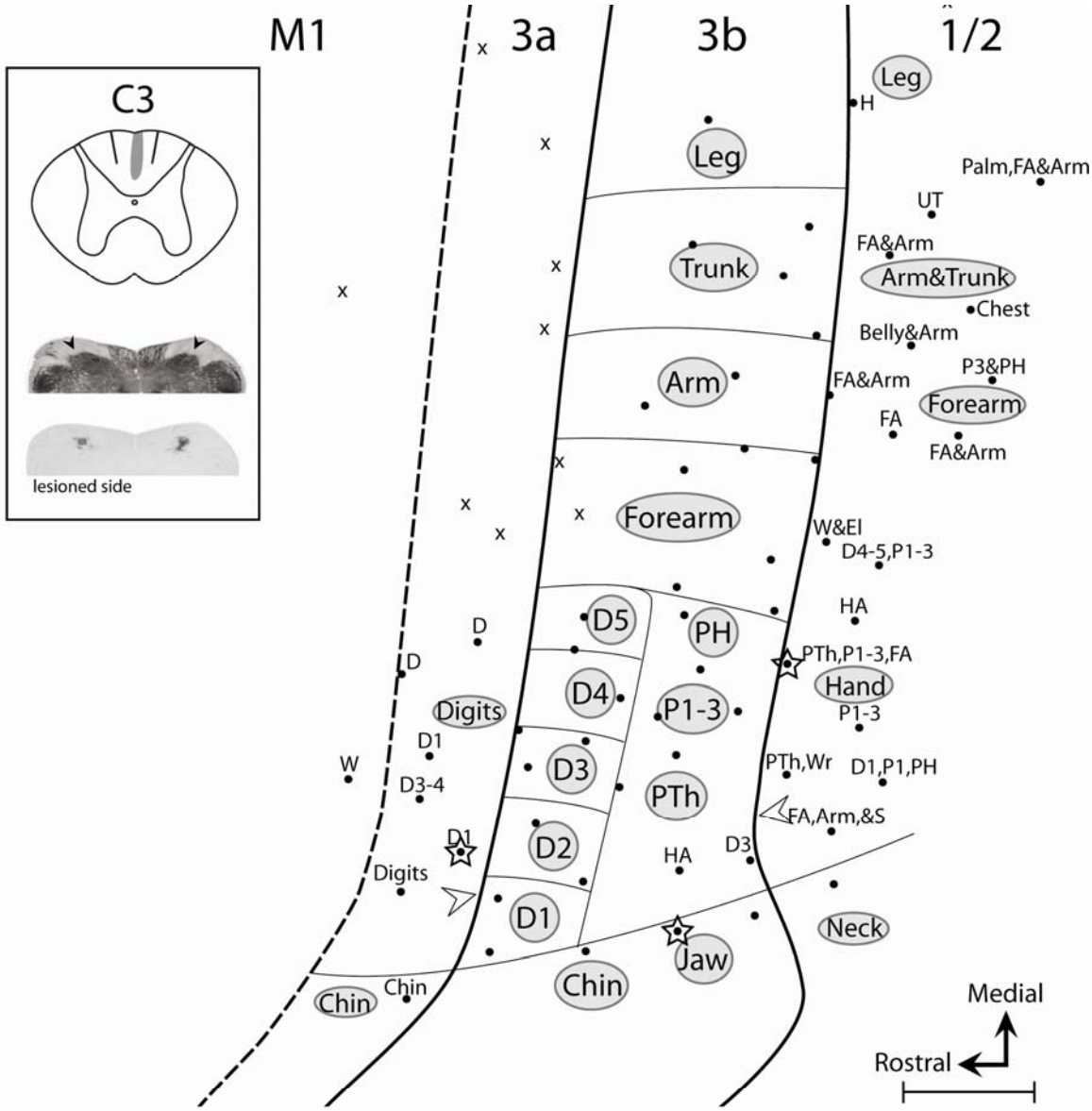

Figure 5. Results of microeletrode multiunit recordings in frontoparietal cortex of case 07-53. The right hemisphere is shown, but the map has been flipped so that in all figures rostral is to the left. A solid line delineates the borders of area 3b, while a dotted line indicates the approximate location of the 3a/M1 border. Thin lines mark the hand region of 3b as well as the hand/face border. Black dots, X's, and stars indicate the locations of responsive penetration points, unresponsive penetration points, and microlesions. When cortical regions were disordered, the location of the receptive field (see abbreviations list) is shown above the responsive point. Two arrowheads near the 3b bend mark the location of a myelin-light septum seen in histological sections. Lesion and tracer uptake at top left, orientation at bottom right. Scale bar = 1 mm.

D5 to D1 and the palm region was located caudally to the digits and organized mediolaterally from the hypothenar pad to the thenar pad. Two points in the lateral-most portion of the palm area were unusually located, representing the hand and digit 3. In more medial regions of area 3b there was an orderly distribution of forearm-arm-trunk-leg, with a few unresponsive points in the forearm region and in the medial-most portion of the leg region. In area 3a the digits were less well organized, but the hand/face border and the digits were both found in approximately the same mediolateral level as in area 3b, as found in previous studies (Huffman and Krubitzer, 2001). Medial to the digit region in area 3a we were not able to elicit responses from the forearm, arm, trunk, or leg regions. In area 1/2, the body parts were again less well organized than in area 3b. Although the somatosensory map of area 1/2 has not been thoroughly investigated in marmosets, a similar organization to the one in this case has been found in other New World primates (Kaas et al., 1979; Sur et al., 1980). The face and hand regions of area 1/2 were again at the same approximate mediolateral level as 3b, except that the hand area extended medially, pushing the forearm and the arm regions more medially than in area 3b.

For this case, in which the spinal lesion involved only a small portion of the gracile tract, the map for area 3b appears to be organized normally, with only a few unusual recording sites. Area 3a, in contrast, has a normal hand and face organization but is largely unresponsive to other parts of the body. Area 1/2 appears to be organized mediolaterally from hand to leg with no unresponsive zones.

Case 07-76. In this case we focused on the hand area and the hand/face border of frontoparietal cortex. The organization of area 3b in this case was much less orderly,

thus the receptive fields for each penetration site are listed (Fig. 6). The representation of the fingers is still located rostrally to the representation of the palm, but in this case the representation of the first three digits is disorganized. Where the thumb is usually represented, there is a site that responds to digits 4-5 and another that responds to a large hand/forearm region. Where digits 2-3 are normally represented, there is an unresponsive point and a large receptive field responding to the first three digits. The more lateral digit 4 representation may reflect the normal location of digit 4, approximately 2 mm from the hand/face border. The palm area of 3b is similarly disorganized, with sites responding to the digits, wrist, and forearm intermixed with sites responding to the palm. The organization of area 3a is again less orderly, and in this case in the hand region there is only one site that responds to the digits and one that responds to the palm; the rest of the sites respond more generally to the hand or the forearm. Area 1/2 was less extensively investigated but again showed a hand representation extending medially.

For this case, in which the spinal lesion affected a small portion of the cuneate tract, the map of the hand in 3b appears to be disorganized, not following the typically orderly progression of digit and palm sites. Area 3a is also disorganized and may show some changes in terms of fewer digit and palm responses.

Case 07-86. In this case we again focused on the hand area and the hand/face border of frontoparietal cortex. In area 3b the finger representation was orderly and resembled the normal organization (Fig. 7). In the palm region there were several unusual receptive fields near the hand/face border. Instead of responding to the thenar pad, penetration sites in this region responded either to the arm and shoulder or to the thumb. More

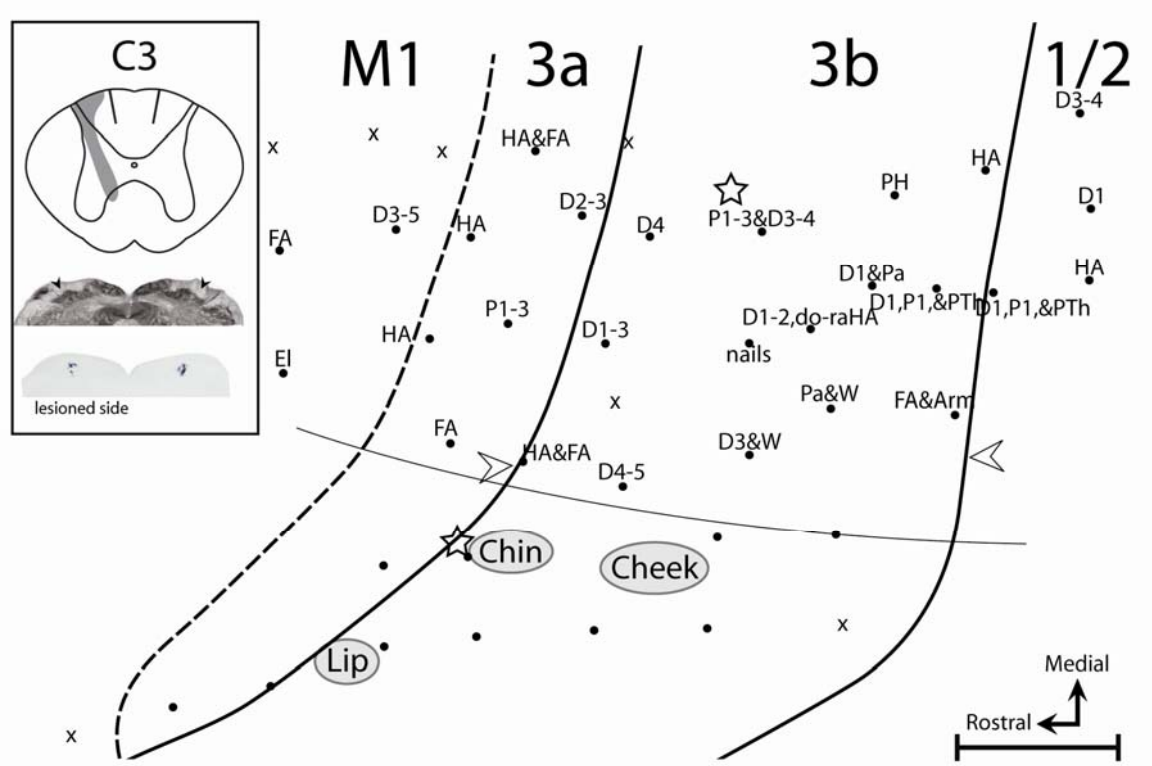

Figure 6. Results of microeletrode multiunit recordings in frontoparietal cortex of case 07-76. The right hemisphere is shown, but the map has been flipped so that in all figures rostral is to the left. A solid line delineates the borders of area 3b, while a dotted line indicates the approximate location of the 3a/M1 border. A thin line marks the hand the hand/face border. Black dots, X's, and stars indicate the locations of responsive penetration points, unresponsive penetration points, and microlesions. When cortical regions were disordered, the location of the receptive field (see abbreviations list) is shown above the responsive point. Two arrowheads near the 3b bend mark the location of a myelin-light septum seen in histological sections. Lesion and tracer uptake at top left, orientation is at bottom right. Scale bar = 1 mm.

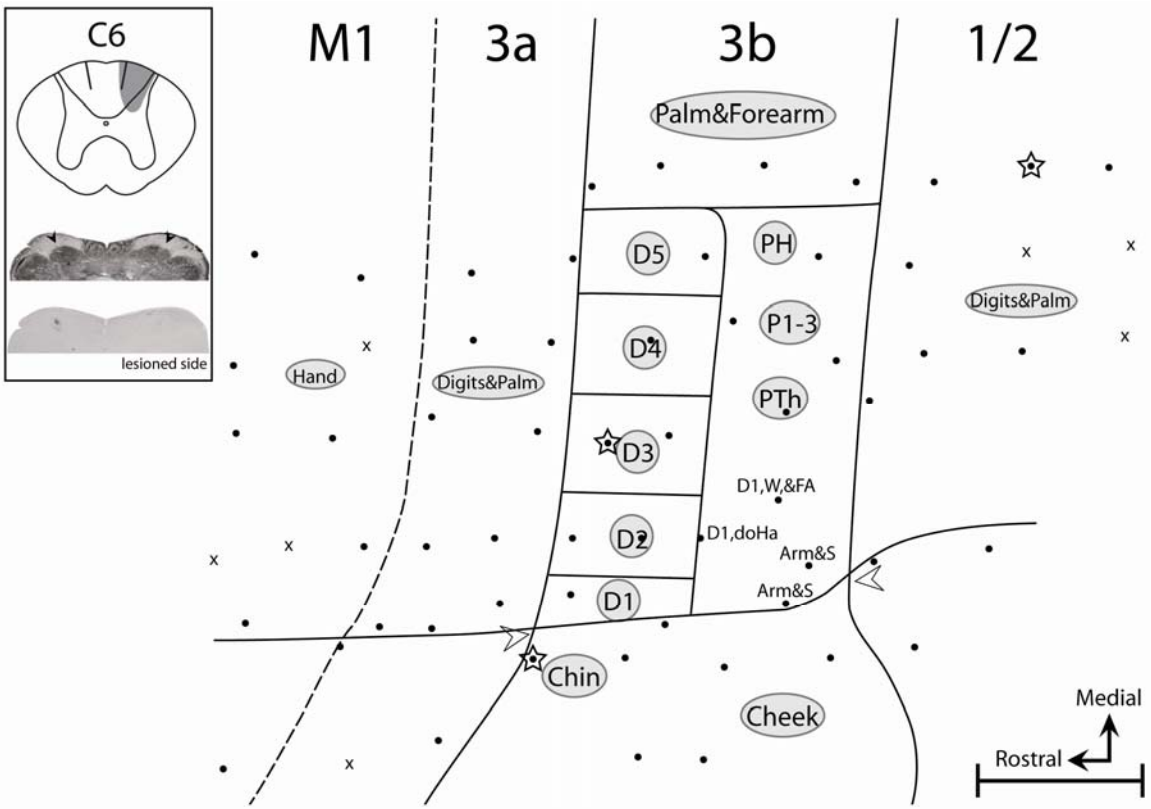

Figure 7. Results of microeletrode multiunit recordings in frontoparietal cortex of case 07-86. The left hemisphere is shown. A solid line delineates the borders of area 3b, while a dotted line indicates the approximate location of the 3a/M1 border. Thin lines mark the hand region of 3b as well as the hand/face border. Black dots, X's, and stars indicate the locations of responsive penetration points, unresponsive penetration points, and microlesions. When cortical regions were disordered, the location of the receptive field (see abbreviations list) is shown above the responsive point. Two arrowheads near the 3b bend mark the location of a myelin-light septum seen in histological sections. Lesion and tracer uptake at top left, orientation is at bottom right. Scale bar = 1 mm.

medially, the palm showed a more orderly mediolateral representation from the thenar to the hypothenar pad, and the palm and forearm were located medial to the hand region. Area 3a and 1/2 appeared to be organized normally, although such a small change in receptive fields in area 3b would be difficult to distinguish in the less ordered areas 3a and 1/2.

For this case, which had a spinal lesion affecting most of the cuneate nucleus, only a small disorganized region was found in the lateral palm region of 3b, while the rest of the map appeared to have a normal organization.

Case 08-06. In this case we performed a more extensive investigation of areas 3b, 3a, and 1/2. In area 3b the hand region was organized normally except for a rostrocaudal strip where digit 4 and pads 1-3 are normally located (Fig. 8). The normal digit and pad representations were replaced mostly by responses from adjacent areas, such as digit 4 being replaced by digits 3 and 5, and pads 1-3 being replaced by the thenar and hypothenar pads. The more medial portions of 3b appeared to have a normal organization, except that several unresponsive points were found near the trunk region. The organization of areas 3a and 1/2 appeared to be organized normally, although again a small change of receptive fields in area 3b would be difficult to distinguish in the less ordered areas 3a and 1/2.

For this case, which had spinal lesions at C8 and T1 affecting most of the cuneate nucleus, a small well delineated strip of area 3b was disorganized, while the rest of the map appeared to have a normal organization.

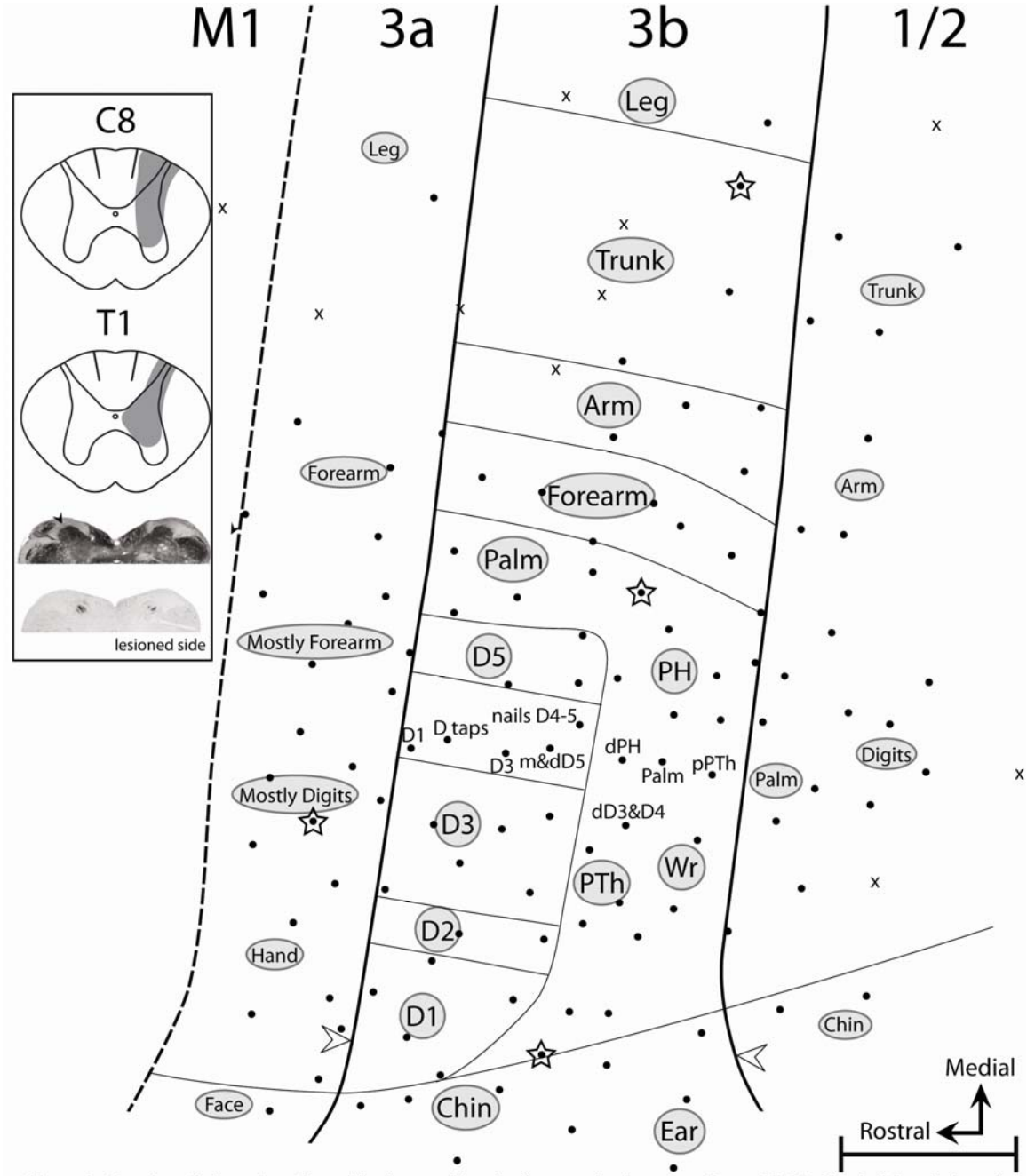

Figure 8. Results of microeletrode multiunit recordings in frontoparietal cortex of case 08-06. The left hemisphere is shown. A solid line delineates the borders of area 3b, while a dotted line indicates the approximate location of the 3a/M1 border. Thin lines mark the hand region of 3b as well as the hand/face border. Black dots, X's, and stars indicate the locations of responsive penetration points, unresponsive penetration points, and microlesions. When cortical regions were disordered, the location of the receptive field (see abbreviations list) is shown above the responsive point. Two arrowheads near the 3b bend mark the location of a myelin-light septum seen in histological sections. Lesion and tracer uptake at top right, orientation is at bottom right. Scale bar = 1 mm.

Receptive field sizes of the fingers. Receptive field sizes in area 3b, especially of the fingers, are normally small, reflecting a single finger or even a single phalange or fingertip (Huffman and Krubitzer, 2001; Kaas et al., 1979). Reorganization of somatosensory maps is often accompanied by a change in receptive field size, either bigger (Calford and Tweedale, 1991) or smaller (Merzenich et al., 1983b). We examined the size of receptive fields for the digit region of area 3b (Fig. 9). In the first and second cases (07-68 and 07-53), receptive field sizes were generally small, with the exception of one forearm point in 07-68 and a movement point and a two-digit point in 07-53. Thus in these cases the receptive field sizes generally corresponded to the normal organization of the somatosensory map. In the third case (07-76), where the somatosensory map was generally disorganized, receptive field sizes in area 3b were likewise abnormal, with unusually large receptive fields throughout the finger region. In the fourth case (07-86), where the somatosensory map of the fingers appeared normal, receptive field sizes were small, with the exception of one large two-digit point. In the final case (08-06), where the digit 4 representation alone was abnormal in the somatosensory map, the receptive field sizes were generally normal, with one unusual movement-related point in the digit 4 region. Thus an alteration in receptive field size generally correlates with the disorderly regions of the somatosensory map.

Discussion

We examined several components of dorsal column lesions in marmosets. We used spinal histology and tracer uptake to classify the extent of the lesion, and a reach-retrieval

Figure 9. Receptive field sizes for the fingers in area 3b. The digit representations of area 3b from Fig. 4-8 have been enlarged. At each penetration point, the body part responding to tactile stimulation is highlighted in orange. Orange arrowheads indicate small receptive fields on the fingertips. Orange waves indicate responsiveness to movement of the fingers.

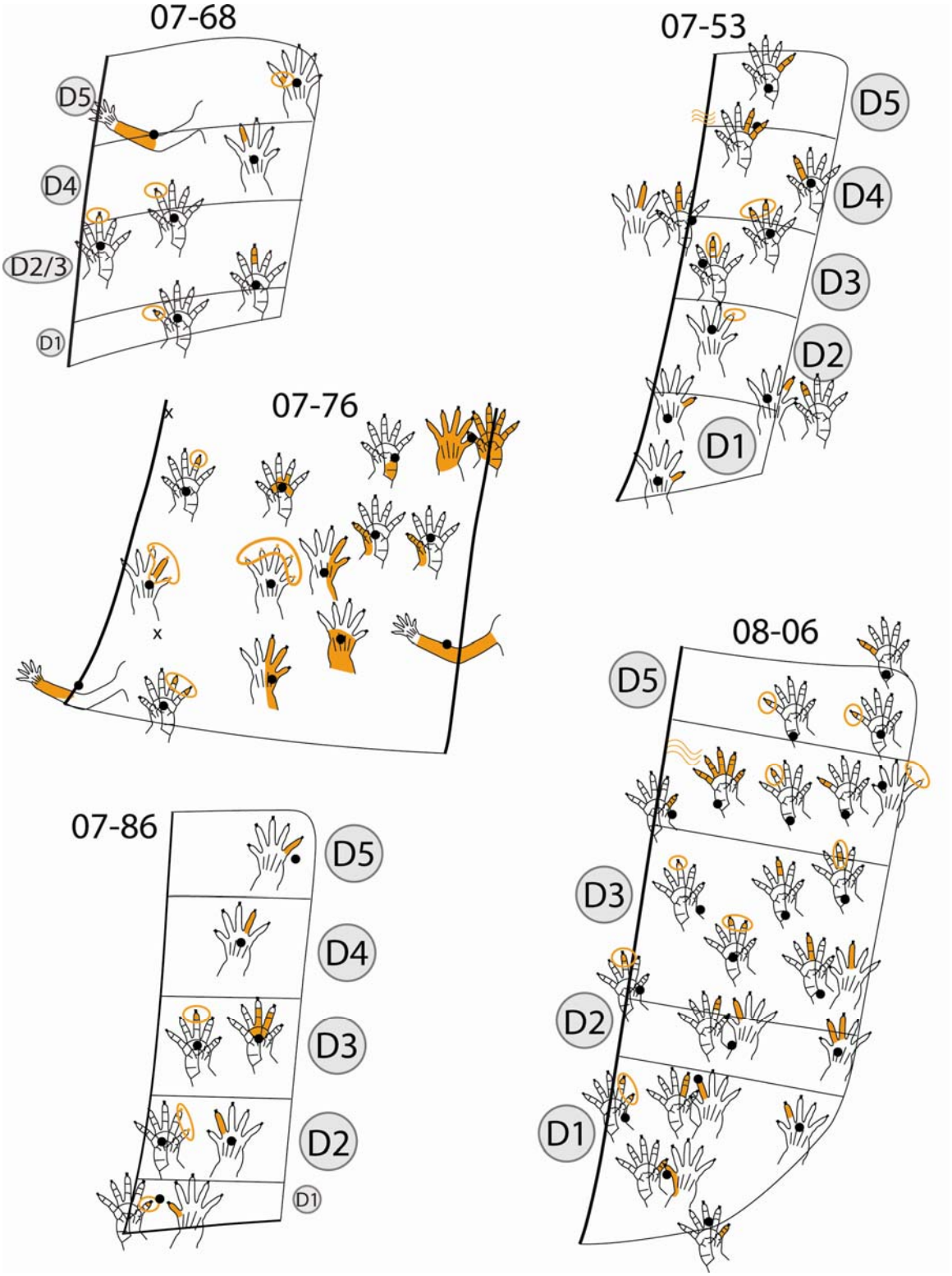
07-68
D5
D4
D2/3
D1
07-53
D5
D4
D3
D2
D1
07-76
07-86
D5
D4
D3
D2
D1
08-06
D5
D3
D2
D1

task and somatosensory mapping to characterize the behavioral and cortical effects. We now review our findings and compare them with other studies of cortical plasticity and behavioral changes following injury. In addition we provide a brief examination of dorsal column injury in two other species, galagos and squirrel monkeys, as well as the effects of motor cortex stimulation following spinal injury.

Our findings suggest that several classical descriptions of the primate spinal cord may hold true for marmosets. First, evidence from our spinal reconstructions and tracer injections suggest that the fasciculus cuneatus is a triangular-shaped region lateral to the fasciculus gracilis in the dorsal horn, and fibers from the fingers are distributed in this area and connect to the cuneate nucleus. We do not have enough information to comment on the organization of forelimb fibers in the fasciculus cuneatus. Second, evidence from our tracer injections and somatosensory mapping suggests the cutaneous innervation of the fingers in marmosets may be similar to that of humans. In humans (Moore and Dalley, 1999), the cervical roots C3 and C4 receive cutaneous innervation from the neck; C5 and T1 from the ventral arm and forearm; C6 from the radial side of the arm, forearm, and hand as well as the thumb; C7 the dorsal arm, forearm, and hand as well as digits 2-3; and C8 the dorsal and ulnar sides of the arm, forearm, and hand as well as digits 4-5. In one case a lesion was made at C6, and there was a nearly complete absence of B-HRP labeled fibers in the lesioned side of the cuneate after injection into all 5 fingers. In another case a lesion was made at C8, and somatosensory mapping revealed that digit 4 in particular was deprived of inputs.

The association between lesion extent, behavior, and physiology

Our five cases show a range of spinal cord lesions. When the dorsal columns were not lesioned (case 07-68), somatosensory cortex was organized normally (we were unable to examine behavior in this case). When the cuneate tract was not lesioned (07-53), the organization of the hand region in areas 3a, 3b, and 1/2 appeared normal, and behavioral performance at least on the eventual success measure was normal. When the cuneate tract was lesioned (07-76, 07-86, and 08-06), reorganization was seen in area 3b, and behavioral changes were seen following lesions at C3 and C6, but not at C8. On this behavioral task, in which the animal uses the entire hand to grasp the pellet, it seems that all of the digits need to be lesioned to show an impairment.

In terms of spinal plasticity, the distribution of B-HRP was limited to the cuneate nucleus; no B-HRP labeling was seen in any other location in the brainstem. This localization of B-HRP suggests that, at least within our post-lesion survival time, dorsal root ganglion axons from the fingers do not sprout collaterals to the gracile nucleus, the spinal trigeminal nucleus, or any other brainstem structure. Our findings are similar to findings of tracer uptake in owl monkeys after dorsal column injury (Jain et al., 1997) and differ from those of injections into the stump of an amputated limb, where more extensive connections to the cuneate and external cuneate nuclei were found (Wu and Kaas, 2002).

We observed that the size of the lesion in the cuneate fasciculus may not correlate with the amount of reorganization in somatosensory cortex. Of the three animals with cuneate tract impairments, animal 07-86 had the largest lesion but the smallest amount of reorganization. We also observed that the size of the lesion in the cuneate nucleus did

not correlate with the behavioral performance. Case 07-76 showed a much smaller lesion than 07-86, nevertheless 07-76 showed a greater behavioral deficit. This issue has been raised in previous studies of dorsal column lesions, in which some cases behavioral changes are found (Nathan et al., 1986), and in others they are not (Wall, 1970). In our study, however, we have the additional confound that the lesions were made at different levels. Nevertheless, it seems that only about 10% of the fibers for any particular body part are necessary to maintain normal behavior (Beck, 1976) and so incomplete lesions can lead to substantial variability between animals.

Also, there is the complication of case 07-53. Despite a normal somatosensory map of the hand and a lesion outside of the cuneate tract, performance on two measures – single-reach success and reaches/success – were abnormal. One possibility is that the animal had a gracile tract lesion, and positioning with the injured leg might have affected behavioral performance. But we would expect this type of deficit to interfere with the eventual success measure too. Another possibility is that the animal was out of practice when allowed a week to recover after the dorsal column lesion and made extra reaches and finger flexions because of it. But if this were true all animals should perform worse after the lesion, and in case 08-06 the animal did not. In the somatosensory map of case 07-53 the animal did seem to have an impairment in the forearm region of area 3a and the rostral portion of area 3b, and perhaps this deficit was sufficient to cause reaching errors but ultimately allow the animal to obtain the pellet.

Finally, there appears to be a relationship between the amount of reorganization in area 3b and behavioral performance. The animal with the largest amount of reorganization, case 07-76, also showed the largest deficit in the eventual success

measure. We ignore case 08-06 because digits 1-3 are presumably still intact, so the next largest amount of reorganization is case 07-86, and this animal showed the next largest deficit in the eventual success measure. Similar to the connection between behavioral deficits and somatosensory reorganization following dorsal rhizotomies (Darian-Smith and Ciferri, 2005), there seems to be an association between the behavioral and physiologic deficits following dorsal column injury.

Behavioral effects following injury.

Performance on reach-and-retrieve tasks. The behavioral task used in this study, with some modifications such as the depths of the wells, has been used for behavioral assessment in rodents (McKenna and Whishaw, 1999; Whishaw and Pellis, 1990), non-human primates (Friel et al., 2005; Friel and Nudo, 1998; Nudo et al., 2000), and humans (Foroud and Whishaw, 2006). The task examines several components of somatomotor performance, including: 1) motor ability in reaching, grasping, and retracting; 2) proprioceptive feedback by aiming for the pellet and bringing the pellet back to the mouth; 3) and tactile discrimination by grasping the pellet when it is being blocked from sight by the hand. Our quantitative measures only score the final result, and so in our analysis deficits in motor, proprioceptive, or tactile abilities, or some combination of the three, could be affected. This task has been performed in rats with dorsal column injuries, and after lesions rats show transient deficits (McKenna and Whishaw, 1999) or no deficits (Schrimsher and Reier, 1993) in the eventual success measure, and more permanent deficits in arm posturing and rotation (McKenna and Whishaw, 1999). It should be noted, however, that in rats the corticospinal tract passes through the dorsal

columns, and so lesions may affect both somatosensory and motor fibers. Nevertheless, our results on the eventual success measure are similar to those in rats, suggesting that a lesion of the dorsal columns leads to similar behavioral deficits in primates and rodents. The results in rats also suggest that endpoint measures alone do not show the full extent of behavioral changes following a dorsal column lesion, and the next step in our investigation is to examine the movement components of marmosets during the reach and retrieve task.

In primates, this behavioral test has been used after lesions of various cortical areas. After lesions of the M1 hand area squirrel monkeys showed transient motor deficiencies such as an increased amount of flexions per reach, proprioceptive deficiencies such as aiming errors, and tactile deficiencies such as checking the paw for pellets on missed trials (Friel et al., 2005; Friel and Nudo, 1998; Nudo et al., 2000). After lesions of posterior parietal cortex using a modified behavioral task, marmosets showed difficulties in reaching towards the contralateral space (Marshall et al., 2002). Our results showed some behavioral deficits in finger flexions as well as changes in somatosensory cortex. It appears, then, that motor and somatosensory cortex both contribute to the motor and the somatosensory aspects of reaching and retrieving.

Somatosensory changes following dorsal column lesions. Our findings suggest that dorsal column injuries lead to many transient deficits in tasks requiring somatosensory and motor functioning, but these deficits improve over a period of weeks after the lesion. Previous investigations of dorsal column injuries have similarly observed deficits in tactile and proprioceptive abilities, with some deficits transient and some more permanent

in nature. In rats dorsal column lesions lead to transient deficits in the reach-and-retrieve task, and more permanent deficits in tactile discrimination (Ballermann et al., 2001) and in checking the paw for pellets (Schrimsher and Reier, 1993). In non-human primates dorsal column lesions lead to transient deficits in the discrimination of touch, joint position, and tactile size (Vierck, 1973; Vierck, 1977), while leading to more permanent deficits in discrimination of motion or items brushed across the skin (Vierck, 1974; Vierck and Cooper, 1998). In humans dorsal column lesions lead to transient impairments in two-point discrimination and proprioceptive sense (Kaas et al., 2008; Nathan et al., 1986), but most impairments appeared to recover over time.

The transient nature of behavioral deficits following dorsal column injury in rats, non-human primates, and humans could be a result of incomplete lesions, as very few fibers appear to be necessary for normal functioning (Beck, 1976). In dorsal rhizotomies, which allow more control over the extent of the lesion by cutting distinct dorsal rootlets (but also involves pain and temperature fibers), animals show substantial deficits in motor control of the digits (Darian-Smith and Ciferri, 2006; Darian-Smith and Ciferri, 2005; Vierck, 1982), although larger movements such as grasping (Taub et al., 1966) and reaching (Bizzi et al., 1984) may not show obvious deficits. Alternatively, the dorsal columns may be injured but the animal compensates by using somatosensory inputs from other pathways, such as proprioceptive inputs from the dorsal and ventral spinocerebellar tracts and tactile information from the anterolateral spinothalamic tracts (Willis and Coggeshall, 1978).

Electrophysiology of somatosensory cortex following injury.

Comparative considerations of cortical plasticity following dorsal column injury. Cortical changes after dorsal column lesions have been found in rodents and in other primates. In rats, lesions of the dorsal columns lead to a similar reorganization of primary somatosensory cortex (Jain et al., 1995). Some deprived zones remain unresponsive for up to three months, suggesting that the extent of plasticity in rats may be limited (Jain et al., 1995; Kaas et al., 2008). In owl monkeys, long-standing lesions of the dorsal columns lead to reorganization of the somatosensory map, with deprived zones eventually entirely responding to adjacent intact regions such as the face or arm (Jain et al., 1997). Finally in humans, referred sensations following spinal injuries have been correlated in fMRI studies to enlarged body representations in the somatosensory map (Moore et al., 2000). In our study area 3b reorganized after only a few weeks, suggesting that cortical plasticity in marmosets is similar to that of other primates.

We also examined the affects of dorsal column injuries on the somatosensory cortex of two other species, a prosimian galago (case 07-48) and a New World squirrel monkey (07-113). The spinal cord architecture and transport of neuroanatomical tracer are shown in Fig. 10. The galago case was a 900g male monkey who received a lesion at C3, injection of CTB tracer into all 10 fingers, and multiunit electrode recordings 21 days after spinal cord injury. The spinal lesion in this case involved a substantial portion of the fasciculus cuneatus and the dorsal horn, as well as a small part of the lateral column and the intermediate and ventral horns. CTB-labeled fibers in the cuneate nucleus were reduced on the lesioned side; five small circles reflecting the five digits could be seen on

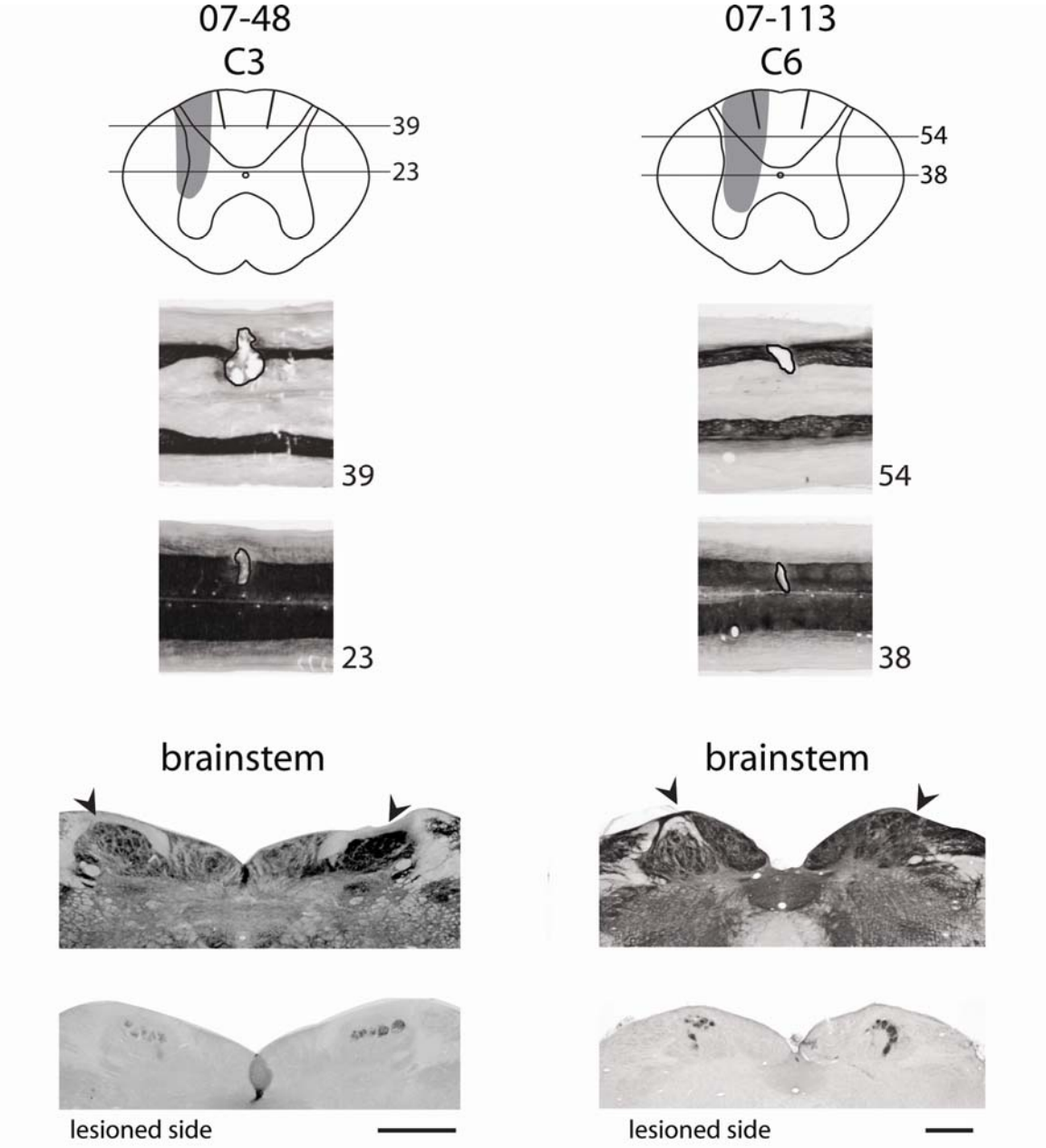

Figure 10. Spinal lesions and tracer transport in the galago and squirrel monkey. Anatomical reconstructions of the spinal lesions in one galago (case 07-48) and one squirrel monkey (case 07-113) are shown at top. A schematic transverse section is shown, with the lesioned area in gray and the lines representing the horizontal plane of section for the acetylcholinesterase-stained tissue below. In the tissue, the left side of the spinal cord is up, the right side of the spinal cord is down, and the rostral side of the spinal cord is to the right; the lesioned area is outlined. At bottom, transport of the neuroanatomical tracer CTB from the fingers to the cuneate nucleus is shown. In the cytochrome oxidase-stained sections, arrowheads mark the location of the cuneate nuclei. In the sections immunoreacted for CTB, the side ipsilateral to the spinal cord lesion is marked. Scale bars at bottom = 1 mm and apply for brainstem sections only.

both sides, suggesting that the lesion was incomplete. CTB-labeled cells were restricted to the cuneate nucleus, and not seen in any other brainstem.

The squirrel monkey case was a 939g male monkey who received a lesion at C6, injection of CTB tracer into all 10 fingers, and multiunit electrode recordings 78 days after spinal cord injury. The spinal lesion in this case involved the majority of the fasciculus cuneatus and the dorsal horn, as well as a small part of the intermediate and ventral horns and the fasciculus gracilis. CTB-labeled fibers in the cuneate nucleus were reduced but not eliminated on the lesioned side, suggesting that the lesion was incomplete. CTB-labeled cells were restricted to the cuneate nucleus, and not seen in any other parts of the brainstem.

The organization of somatosensory cortex in the galago is shown in Fig. 11. The galago somatosensory map of area 3b differs from that of anthropoid primates in that the representation of the radial arm lies between the hand and face representations, and the palm lies in the middle of the hand representation, between the representation of the glabrous digits rostrally and the dorsal digits caudally (Wu and Kaas, 2003). In case 07-48 the radial arm representation was generally unresponsive in both area 3b and area 1/2. There was still a general mediolateral organization of digits 1-5 with the palm in the middle, but there were a few unresponsive points above the fingers and near the forearm representation. These findings suggest that, at least after a period of 3 weeks, reorganization of somatosensory cortex is incomplete. In owl monkeys, reorganization of a similarly sized block of somatosensory cortex was incomplete in 5 days but complete in 36 days. With only one animal investigated, it is unclear whether galagos are more

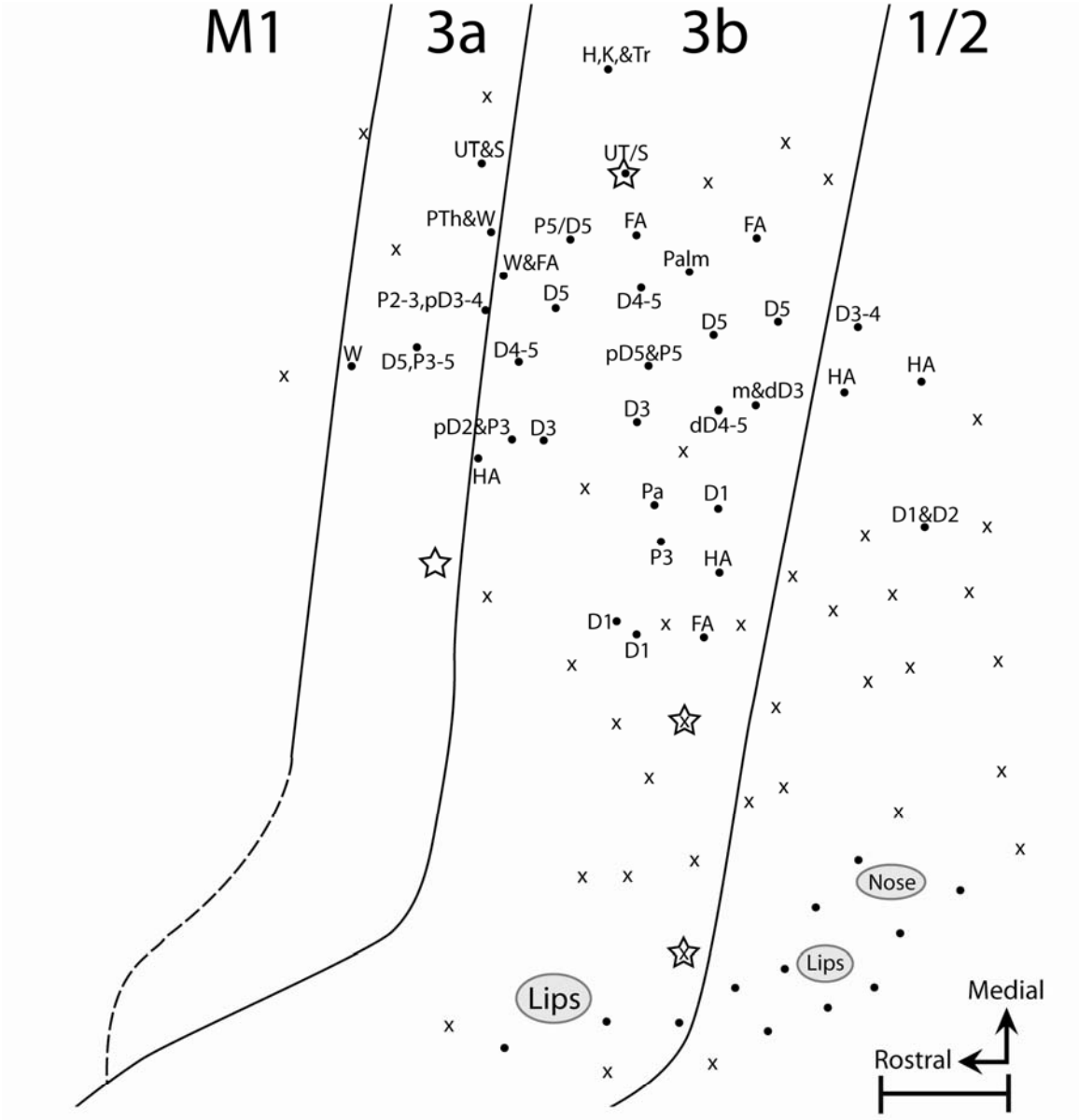

Figure 11. Results of microeletrode multiunit recordings in frontoparietal cortex of case 07-48. The right hemisphere of the galago is shown, but the map has been flipped so that in all figures rostral is to the left. A solid line delineates the borders of area 3b and the upper portion of the 3a/M1 border (from Wu et al 2003), while a dotted line indicates the approximate location of the lateral 3a/M1 border. Black dots, X's, and stars indicate the locations of responsive penetration points, unresponsive penetration points, and microlesions. When cortical regions were disordered, the location of the receptive field (see abbreviations list) is shown above the responsive point. Orientation is at bottom right. Scale bar = 1 mm.

similar to rats with limited plasticity, or are more similar to anthropoid primates and merely need time to reorganize.

The organization of somatosensory cortex in the squirrel monkey is shown in Fig. 12. Despite the size of the lesion, the somatosensory map was normally organized. In area 3b the chin was immediately lateral to the hand region, which had a very orderly mediolateral distribution of the digits and the palm. Areas 3a and 1 were similarly organized, although slightly less orderly than area 3b as seen in the marmosets. These findings suggest that, after an incomplete lesion and long recovery period in a squirrel monkey, somatosensory cortex is generally organized normally.

Reorganization of somatosensory areas. Our marmoset results are similar to those of New World owl monkeys in that reorganization of area 3b occurs after long-standing dorsal column lesions (Jain et al., 1997). Reorganization in area 3b has also been seen following nerve cuts (Garraghty et al., 1994; Garraghty and Kaas, 1991b; Kolarik et al., 1994; Merzenich et al., 1983a; Merzenich et al., 1983b), amputations (Florence and Kaas, 1995; Florence et al., 1998; Merzenich et al., 1984), and dorsal rhizotomies (Darian-Smith, 2004; Darian-Smith and Brown, 2000; Pons et al., 1991). Disruption of somatosensory inputs to the brain at any level, then, seems to result in similar physiologic changes.

The effects of peripheral nerve or dorsal column injuries on areas other than 3b, however, are less well known. After dorsal rhizotomies areas 3, 1, and 2 do not seem to modulate their responses to movements of the limbs while area 4 does (Bioulac and Lamarre, 1979). After dorsal column lesion, one study found that responses in area 3a

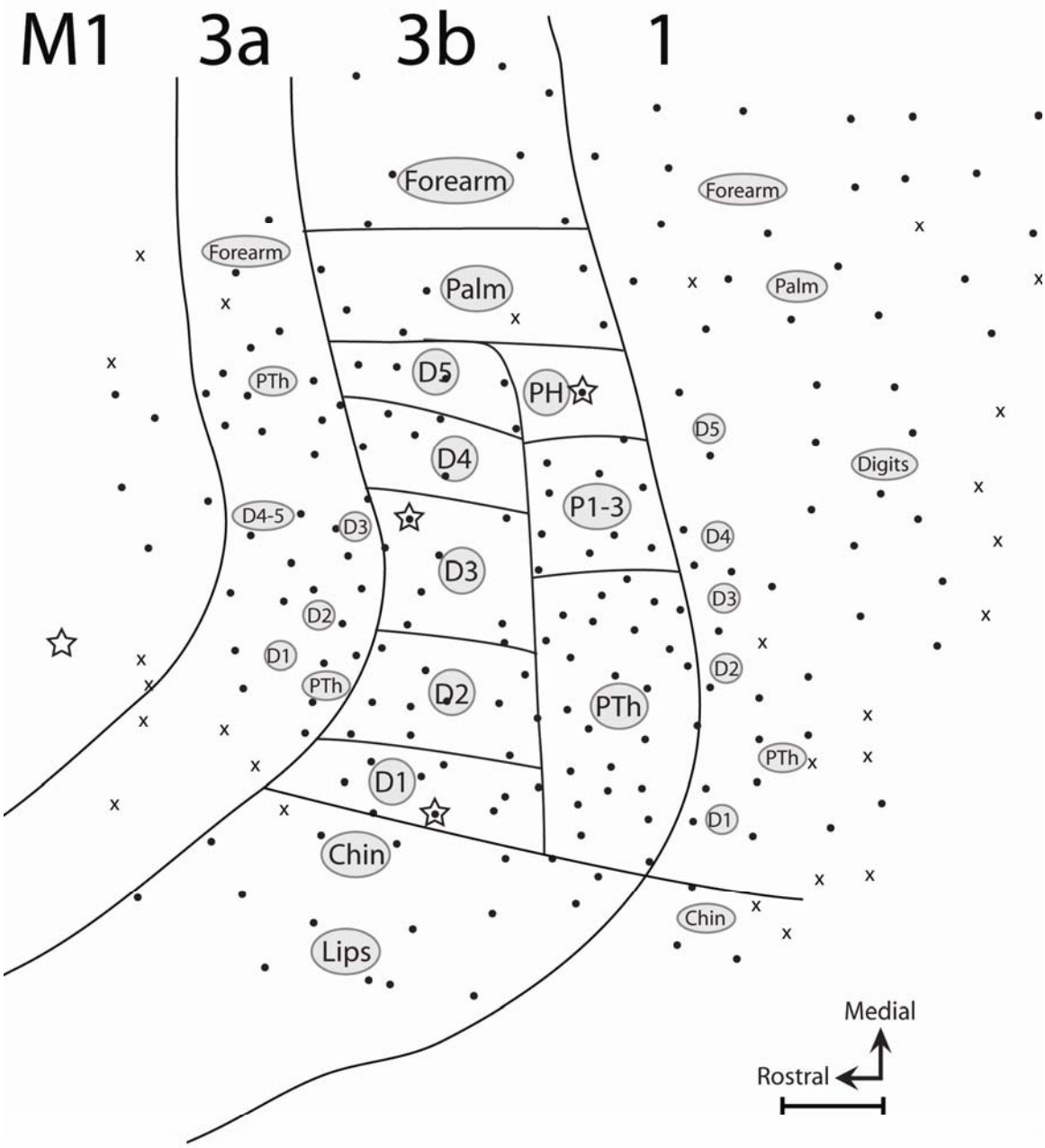

Figure 12. Results of microeletrode multiunit recordings in frontoparietal cortex of case 07-113. The right hemisphere of the squirrel monkey is shown, but the map has been flipped so that in all figures rostral is to the left. Solid line delineates the borders of areas 3b and 3a. Black dots, X's, and stars indicate the locations of responsive penetration points, unresponsive penetration points, and microlesions. When cortical regions were disordered, the location of the receptive field (see abbreviations list) is shown above the responsive point. Orientation is at bottom right. Scale bar = 1 mm.

were abolished (Phillips et al., 1971), and another found that responses in areas 1 and 2 were still intact (Brinkman et al., 1978). In our experiments the disorderly organization normally found in areas 3a and 1/2 made it difficult to tell if reorganization occurred after dorsal column lesion, but in case 07-76 at least, area 3a showed unusual hand and forearm points, correlating with the reorganized map in area 3b. Further investigation is necessary, but other somatosensory areas of anterior parietal cortex may also undergo plasticity following spinal injury.

Effects of dorsal column injury on motor cortex. Motor cortex receives many somatosensory inputs, so there has been some question as to how changes in somatosensory functioning might affect the outputs of the motor system. One previous and incomplete study investigated the changes to motor stimulation in macaques following dorsal column injury, and found little to no change in stimulation thresholds or the organization of the forelimb area (Kaas et al., 2008). We studied the effects of motor stimulation following spinal cord injury in one marmoset (Fig. 13), one galago (Fig. 14), and one squirrel monkey (Fig. 15). In all three cases we performed intracortical microstimulation in the animals after we finished multiunit electrode recordings of somatosensory cortex.

For the marmoset (case 07-53), which had a limited lesion of the fasciculus gracilis and an abnormal area 3a, the motor map of the face and forelimb regions of area 3a and M1 were similar to the normal organization (Burish et al., 2008; Burman et al., 2008), as movements of the shoulder, elbow, wrist, and digits were intermixed in the forelimb area. Two medial shoulder areas, one in area 3a and one in M1, had higher

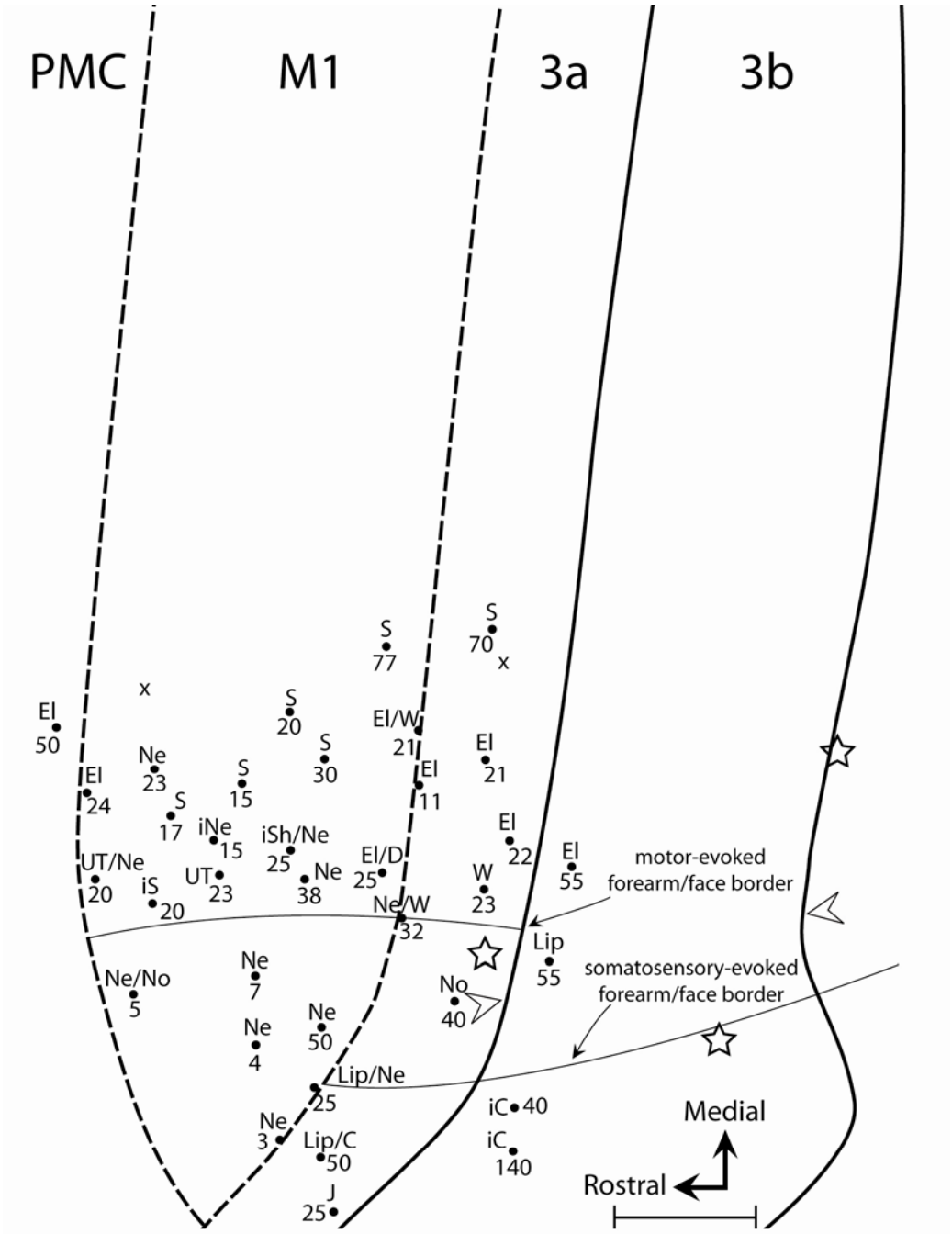

Figure 13. Results of microstimulation mapping in frontoparietal cortex of case 07-53. The right hemisphere of the marmoset is shown, but the map has been flipped so that in all figures rostral is to the left. A solid line delineates the borders of area 3b, while a dotted line indicates the approximate location of the 3a/M1 border. Thin lines mark the motor forearm/face border as defined by intracortical microstimulation and the somatosensory hand/face border evoked by multiunit electrode recordings. Black dots, X's, and stars indicate the locations of responsive points, unresponsive points, and microlesions. Two arrowheads near the 3b bend mark the location of a myelin-light septum seen in histological sections. Orientation is at bottom right. Scale bar = 1 mm.

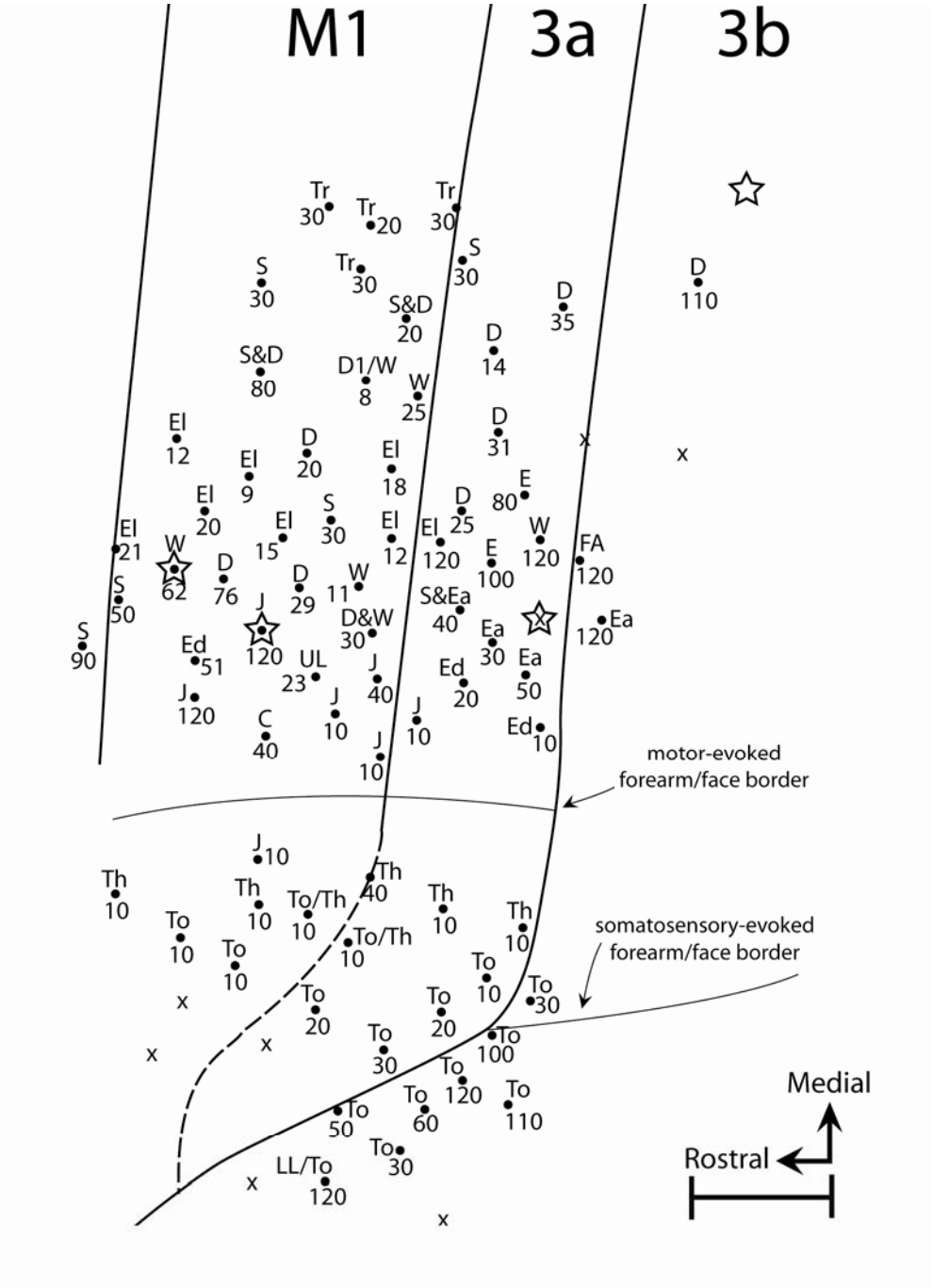

Figure 14. Results of microstimulation mapping in frontoparietal cortex of case 07-48. The right hemisphere of the galago is shown, but the map has been flipped so that in all figures rostral is to the left. Solid lines delineate the borders of area 3a and M1. Thin lines mark the motor forearm/face border as defined by intracortical microstimulation and the somatosensory hand/face border evoked by multiunit electrode recordings. Black dots, X's, and stars indicate the locations of responsive points, unresponsive points, and microlesions. Orientation is at bottom right. Scale bar = 1 mm.

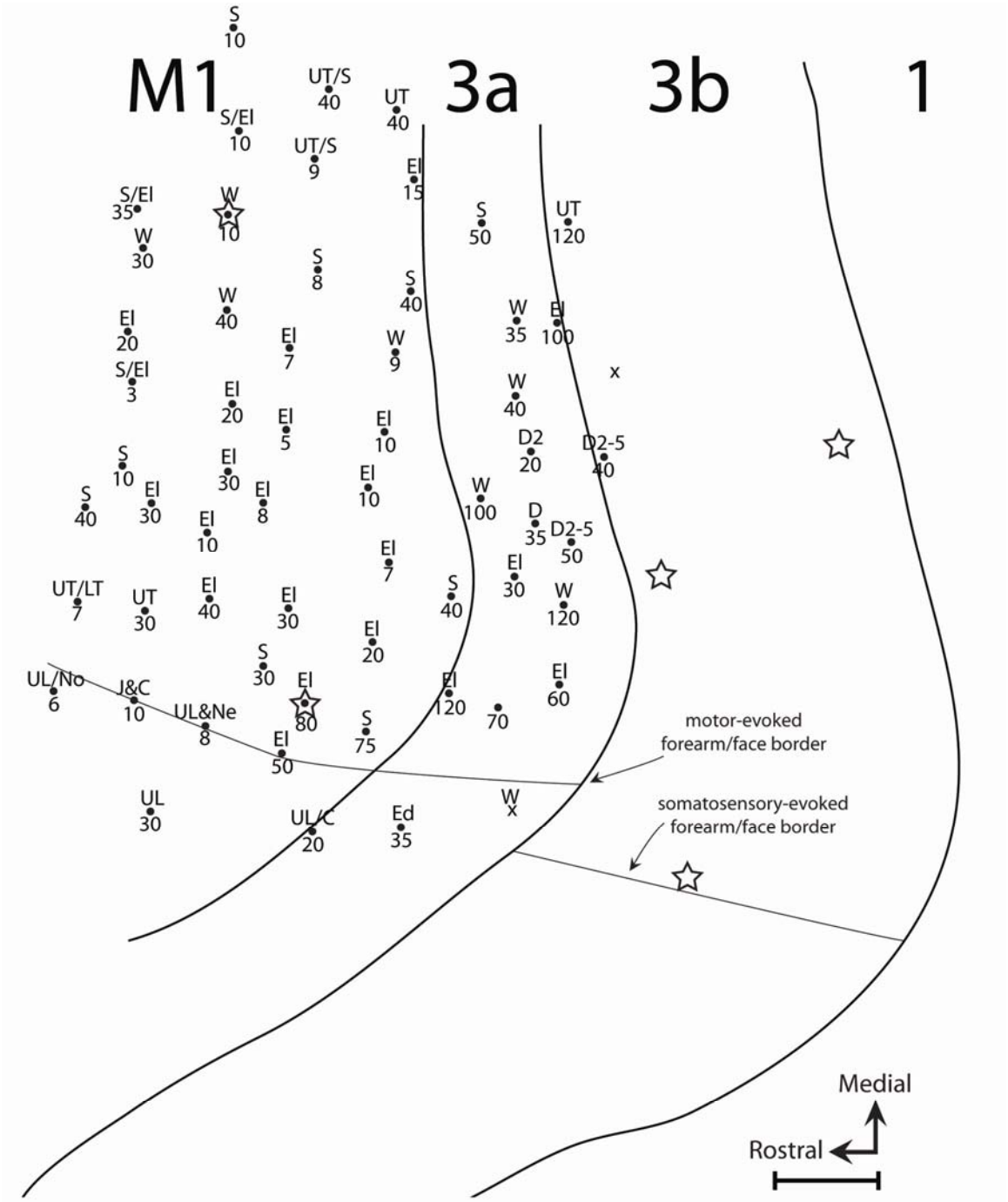

Figure 15. Results of microstimulation mapping in frontoparietal cortex of case 07-113. The right hemisphere of the squirrel is shown, but the map has been flipped so that in all figures rostral is to the left. Solid lines delineate the borders of area 3a and 3b. Thin lines mark the motor forearm/face border as defined by intracortical microstimulation and the somatosensory hand/face border evoked by multiunit electrode recordings. Black dots, X's, and stars indicate the locations of responsive points, unresponsive points, and microlesions. Orientation is at bottom right. Scale bar = 1 mm.

thresholds than other parts of cortex but were within the normal range for areas 3a and M1. For the galago (07-48), which had a substantial cuneate fasciculus lesion affecting the radial forearm, the organization of the forearm and face regions are similar to the normal organization (Wu et al 2003). Threshold values in some but not all locations are higher than those of normal animals, including joints surrounding the radial forearm (elbow and wrist), joints that are farther away (shoulder and digits), and joints whose inputs enter above the lesioned area and thus could not have been lesioned (jaw). For the squirrel monkey (07-113), which had a substantial cuneate fasciculus lesion affecting the majority of the fasciculus cuneatus but a generally normal organization of the somatosensory map, organization of M1 and area 3a appeared to be similar to the normal organization (Donoghue et al., 1992). We observed low threshold values for most penetration points, as well as an intermixing of forearm joints throughout the forearm region. Our very limited results suggest that there are few to no changes in motor cortex following dorsal column lesion in prosimians and New World monkeys, similar to that found in limited results from Old World monkeys. Further investigation, however, is required.

In performing microstimulation and multiunit recordings in the same animal, we noticed that the forelimb/face border defined by intracortical microstimulation was located approximately 1 mm medial to the hand/face border defined by multiunit electrode recordings. Both borders were near but not exactly at the location of the myelin-light septa that represents the forearm/face border in previous studies (Fang et al., 2002; Jain et al., 1998). For area 3a at least, there was a portion of cortex where microstimulation evoked forelimb movements while recordings revealed receptive fields

on the face. A previous study has suggested that each electrode penetration site has homonymous inputs and outputs; if a multiunit recording site shows joint movement or cutaneous stimulation, microstimulation at the same site evokes movements of the same joint or of the joint nearest the cutaneous receptive field (Murphy et al., 1978). A further investigation of this narrow strip of cortex is necessary to describe the relationship between stimulation and recordings in somatomotor cortex. Nevertheless, this difference in borders between stimulation and recording has been found in humans without dorsal column injuries as well (Woolsey et al., 1979). Additional studies on animals without spinal injuries are required, but these findings suggest that different locations for the face/forelimb border may be common to all primates.

Acknowledgments

We thank Laura Trice for assistance with histology, Mary Feurtado for assistance with anesthesia, and Jamie Reed for helpful discussion.

References

Angelucci A, Clasca F, Sur M. 1996. Anterograde axonal tracing with the subunit B of cholera toxin: a highly sensitive immunohistochemical protocol for revealing fine axonal morphology in adult and neonatal brains. J Neurosci Methods 65(1):101-112.

Ballermann M, McKenna J, Whishaw IQ. 2001. A grasp-related deficit in tactile discrimination following dorsal column lesion in the rat. Brain Res Bull 54(2):237-242.

Beck CH. 1976. Dual dorsal columns: a review. Can J Neurol Sci 3(1):1-7.

Bioulac B, Lamarre Y. 1979. Activity of postcentral cortical neurons of the monkey during conditioned movements of a deafferented limb. Brain Res 172(3):427-437.

Bizzi E, Accornero N, Chapple W, Hogan N. 1984. Posture control and trajectory formation during arm movement. J Neurosci 4(11):2738-2744.

Bradbury EJ, Moon LD, Popat RJ, King VR, Bennett GS, Patel PN, Fawcett JW, McMahon SB. 2002. Chondroitinase ABC promotes functional recovery after spinal cord injury. Nature 416(6881):636-640.

Brinkman J, Bush BM, Porter R. 1978. Deficient influence of peripheral stimuli on precentral neurones in monkeys with dorsal column lesions. J Physiol 276:27-48.

Bruce K, Grofova I. 1992. Notes on a light and electron microscopic double-labeling method combining anterograde tracing with Phaseolus vulgaris leucoagglutinin and retrograde tracing with cholera toxin subunit B. J Neurosci Methods 45(1-2):23-33.

Burish MJ, Stepniewska I, Kaas JH. 2006. Topographic organization and architectonics of primary motor cortex and the supplementary motor area in marmosets. Soc Neurosci Abstr 806.11.

Burish MJ, Stepniewska I, Kaas JH. 2008. Microstimulation and architectonics of frontoparietal cortex in common marmosets (Callithrix jacchus). J Comp Neurol 507(2):1151-1168.

Burman KJ, Palmer SM, Gamberini M, Rosa MG. 2006. Cytoarchitectonic subdivisions of the dorsolateral frontal cortex of the marmoset monkey (Callithrix jacchus), and their projections to dorsal visual areas. J Comp Neurol 495(2):149-172.

Burman KJ, Palmer SM, Gamberini M, Spitzer MW, Rosa MG. 2008. Anatomical and physiological definition of the motor cortex of the marmoset monkey. J Comp Neurol 506(5):860-876.

Caggiano AO, Zimber MP, Ganguly A, Blight AR, Gruskin EA. 2005. Chondroitinase ABCI improves locomotion and bladder function following contusion injury of the rat spinal cord. J Neurotrauma 22(2):226-239.

Calford MB, Tweedale R. 1991. Immediate expansion of receptive fields of neurons in area 3b of macaque monkeys after digit denervation. Somatosens Mot Res 8(3):249-260.

Churchill JD, Arnold LL, Garraghty PE. 2001. Somatotopic reorganization in the brainstem and thalamus following peripheral nerve injury in adult primates. Brain Res 910(1-2):142-152.

Cusick CG, Gould HJ, 3rd. 1990. Connections between area 3b of the somatosensory cortex and subdivisions of the ventroposterior nuclear complex and the anterior pulvinar nucleus in squirrel monkeys. J Comp Neurol 292(1):83-102.

Darian-Smith C. 2004. Primary afferent terminal sprouting after a cervical dorsal rootlet section in the macaque monkey. J Comp Neurol 470(2):134-150.

Darian-Smith C, Brown S. 2000. Functional changes at periphery and cortex following dorsal root lesions in adult monkeys. Nat Neurosci 3(5):476-481.

Darian-Smith C, Ciferri M. 2006. Cuneate nucleus reorganization following cervical dorsal rhizotomy in the macaque monkey: Its role in the recovery of manual dexterity. J Comp Neurol 498(4):552-565.

Darian-Smith C, Ciferri MM. 2005. Loss and recovery of voluntary hand movements in the macaque following a cervical dorsal rhizotomy. J Comp Neurol 491(1):27-45.

Donoghue JP, Leibovic S, Sanes JN. 1992. Organization of the forelimb area in squirrel monkey motor cortex: representation of digit, wrist, and elbow muscles. Exp Brain Res 89(1):1-19.

Fang PC, Jain N, Kaas JH. 2002. Few intrinsic connections cross the hand-face border of area 3b of New World monkeys. J Comp Neurol 454(3):310-319.

Florence SL, Hackett TA, Strata F. 2000. Thalamic and cortical contributions to neural plasticity after limb amputation. J Neurophysiol 83(5):3154-3159.

Florence SL, Kaas JH. 1995. Large-scale reorganization at multiple levels of the somatosensory pathway follows therapeutic amputation of the hand in monkeys. J Neurosci 15(12):8083-8095.

Florence SL, Taub HB, Kaas JH. 1998. Large-scale sprouting of cortical connections after peripheral injury in adult macaque monkeys. Science 282(5391):1117-1121.

Florence SL, Wall JT, Kaas JH. 1991. Central projections from the skin of the hand in squirrel monkeys. J Comp Neurol 311(4):563-578.

Foroud A, Whishaw IQ. 2006. Changes in the kinematic structure and non-kinematic features of movements during skilled reaching after stroke: a Laban Movement Analysis in two case studies. J Neurosci Methods 158(1):137-149.

Friel KM, Barbay S, Frost SB, Plautz EJ, Hutchinson DM, Stowe AM, Dancause N, Zoubina EV, Quaney BM, Nudo RJ. 2005. Dissociation of sensorimotor deficits after rostral versus caudal lesions in the primary motor cortex hand representation. J Neurophysiol 94(2):1312-1324.

Friel KM, Nudo RJ. 1998. Recovery of motor function after focal cortical injury in primates: compensatory movement patterns used during rehabilitative training. Somatosens Mot Res 15(3):173-189.

Gallyas F. 1979. Silver staining of myelin by means of physical development. Neurol Res 1(2):203-209.

Garraghty PE, Hanes DP, Florence SL, Kaas JH. 1994. Pattern of peripheral deafferentation predicts reorganizational limits in adult primate somatosensory cortex. Somatosens Mot Res 11(2):109-117.

Garraghty PE, Kaas JH. 1991a. Functional reorganization in adult monkey thalamus after peripheral nerve injury. Neuroreport 2(12):747-750.

Garraghty PE, Kaas JH. 1991b. Large-scale functional reorganization in adult monkey cortex after peripheral nerve injury. Proc Natl Acad Sci U S A 88(16):6976-6980.

Geneser-Jensen FA, Blackstad TW. 1971. Distribution of acetyl cholinesterase in the hippocampal region of the guinea pig. I. Entorhinal area, parasubiculum, and presubiculum. Z Zellforsch Mikrosk Anat 114(4):460-481.

Gibson AR, Hansma DI, Houk JC, Robinson FR. 1984. A sensitive low artifact TMB procedure for the demonstration of WGA-HRP in the CNS. Brain Res 298(2):235-241.

Glendinning DS, Cooper BY, Vierck CJ, Jr., Leonard CM. 1992. Altered precision grasping in stumptail macaques after fasciculus cuneatus lesions. Somatosens Mot Res 9(1):61-73.

Glendinning DS, Vierck CJ, Jr., Cooper BY. 1993. The effect of fasciculus cuneatus lesions on finger positioning and long-latency reflexes in monkeys. Exp Brain Res 93(1):104-116.

Huffman KJ, Krubitzer L. 2001. Area 3a: topographic organization and cortical connections in marmoset monkeys. Cereb Cortex 11(9):849-867.

Iwanami A, Yamane J, Katoh H, Nakamura M, Momoshima S, Ishii H, Tanioka Y, Tamaoki N, Nomura T, Toyama Y, Okano H. 2005. Establishment of graded spinal cord injury model in a nonhuman primate: the common marmoset. J Neurosci Res 80(2):172-181.

Jain N, Catania KC, Kaas JH. 1997. Deactivation and reactivation of somatosensory cortex after dorsal spinal cord injury. Nature 386(6624):495-498.

Jain N, Catania KC, Kaas JH. 1998. A histologically visible representation of the fingers and palm in primate area 3b and its immutability following long-term deafferentations. Cereb Cortex 8(3):227-236.

Jain N, Florence SL, Kaas JH. 1995. Limits on plasticity in somatosensory cortex of adult rats: hindlimb cortex is not reactivated after dorsal column section. J Neurophysiol 73(4):1537-1546.

Jain N, Florence SL, Qi HX, Kaas JH. 2000. Growth of new brainstem connections in adult monkeys with massive sensory loss. Proc Natl Acad Sci U S A 97(10):5546-5550.

Kaas JH, Nelson RJ, Sur M, Lin CS, Merzenich MM. 1979. Multiple representations of the body within the primary somatosensory cortex of primates. Science 204(4392):521-523.

Kaas JH, Qi HX, Burish MJ, Gharbawie OA, Onifer SM, Massey JM. 2008. Cortical and subcortical plasticity in the brains of humans, primates, and rats after damage to sensory afferents in the dorsal columns of the spinal cord. Exp Neurol 209(2):407-416.

Kolarik RC, Rasey SK, Wall JT. 1994. The consistency, extent, and locations of early-onset changes in cortical nerve dominance aggregates following injury of nerves to primate hands. J Neurosci 14(7):4269-4288.

Krubitzer LA, Kaas JH. 1990. The organization and connections of somatosensory cortex in marmosets. J Neurosci 10(3):952-974.

Leonard CM, Glendinning DS, Wilfong T, Cooper BY, Vierck CJ, Jr. 1992. Alterations of natural hand movements after interruption of fasciculus cuneatus in the macaque. Somatosens Mot Res 9(1):75-89.

Lin CS, Merzenich MM, Sur M, Kaas JH. 1979. Connections of areas 3b and 1 of the parietal somatosensory strip with the ventroposterior nucleus in the owl monkey (Aotus trivirgatus). J Comp Neurol 185(2):355-371.

Marshall JW, Baker HF, Ridley RM. 2002. Contralesional neglect in monkeys with small unilateral parietal cortical ablations. Behav Brain Res 136(1):257-265.

Massey JM, Hubscher CH, Wagoner MR, Decker JA, Amps J, Silver J, Onifer SM. 2006. Chondroitinase ABC digestion of the perineuronal net promotes functional collateral sprouting in the cuneate nucleus after cervical spinal cord injury. J Neurosci 26(16):4406-4414.

Mayner L, Kaas JH. 1986. Thalamic projections from electrophysiologically defined sites of body surface representations in areas 3b and 1 of somatosensory cortex of Cebus monkeys. Somatosens Res 4(1):13-29.

McKenna JE, Whishaw IQ. 1999. Complete compensation in skilled reaching success with associated impairments in limb synergies, after dorsal column lesion in the rat. J Neurosci 19(5):1885-1894.

Merzenich MM, Kaas JH, Sur M, Lin CS. 1978. Double representation of the body surface within cytoarchitectonic areas 3b and 1 in "SI" in the owl monkey (Aotus trivirgatus). J Comp Neurol 181(1):41-73.

Merzenich MM, Kaas JH, Wall J, Nelson RJ, Sur M, Felleman D. 1983a. Topographic reorganization of somatosensory cortical areas 3b and 1 in adult monkeys following restricted deafferentation. Neuroscience 8(1):33-55.

Merzenich MM, Kaas JH, Wall JT, Sur M, Nelson RJ, Felleman DJ. 1983b. Progression of change following median nerve section in the cortical representation of the hand in areas 3b and 1 in adult owl and squirrel monkeys. Neuroscience 10(3):639-665.

Merzenich MM, Nelson RJ, Stryker MP, Cynader MS, Schoppmann A, Zook JM. 1984. Somatosensory cortical map changes following digit amputation in adult monkeys. J Comp Neurol 224(4):591-605.

Moore CI, Stern CE, Dunbar C, Kostyk SK, Gehi A, Corkin S. 2000. Referred phantom sensations and cortical reorganization after spinal cord injury in humans. Proc Natl Acad Sci U S A 97(26):14703-14708.

Moore KL, Dalley AF. 1999. Clinically oriented anatomy. Philadelphia: Lippincott Williams & Wilkins. xxxi, 1164 p. p.

Murphy JT, Kwan HC, MacKay WA, Wong YC. 1978. Spatial organization of precentral cortex in awake primates. III. Input-output coupling. J Neurophysiol 41(5):1132-1139.

Nathan PW, Smith MC, Cook AW. 1986. Sensory effects in man of lesions of the posterior columns and of some other afferent pathways. Brain 109 (Pt 5):1003-1041.

Nelson RJ, Kaas JH. 1981. Connections of the ventroposterior nucleus of the thalamus with the body surface representations in cortical areas 3b and 1 of the cynomolgus macaque, (Macaca fascicularis). J Comp Neurol 199(1):29-64.

Nelson RJ, Sur M, Felleman DJ, Kaas JH. 1980. Representations of the body surface in postcentral parietal cortex of Macaca fascicularis. J Comp Neurol 192(4):611-643.

Nudo RJ, Friel KM, Delia SW. 2000. Role of sensory deficits in motor impairments after injury to primary motor cortex. Neuropharmacology 39(5):733-742.

Nudo RJ, Jenkins WM, Merzenich MM, Prejean T, Grenda R. 1992. Neurophysiological correlates of hand preference in primary motor cortex of adult squirrel monkeys. J Neurosci 12(8):2918-2947.

Phillips CG, Powell TP, Wiesendanger M. 1971. Projection from low-threshold muscle afferents of hand and forearm to area 3a of baboon's cortex. J Physiol 217(2):419-446.

Pons TP, Garraghty PE, Ommaya AK, Kaas JH, Taub E, Mishkin M. 1991. Massive cortical reorganization after sensory deafferentation in adult macaques. Science 252(5014):1857-1860.

Przybyszewski AW, Sosale S, Chaudhuri A. 2007. Activity of common marmosets (Callithrix jacchus) in limited spaces: hand movement characteristics. J Comp Psychol 121(3):332-344.

Schrimsher GW, Reier PJ. 1993. Forelimb motor performance following dorsal column, dorsolateral funiculi, or ventrolateral funiculi lesions of the cervical spinal cord in the rat. Exp Neurol 120(2):264-276.

Sengelaub DR, Muja N, Mills AC, Myers WA, Churchill JD, Garraghty PE. 1997. Denervation-induced sprouting of intact peripheral afferents into the cuneate nucleus of adult rats. Brain Res 769(2):256-262.

Stoney SD, Jr., Thompson WD, Asanuma H. 1968. Excitation of pyramidal tract cells by intracortical microstimulation: effective extent of stimulating current. J Neurophysiol 31(5):659-669.

Strata F, Coq JO, Kaas JH. 2003. The chemo- and somatotopic architecture of the Galago cuneate and gracile nuclei. Neuroscience 116(3):831-850.

Sur M, Merzenich MM, Kaas JH. 1980. Magnification, receptive-field area, and "hypercolumn" size in areas 3b and 1 of somatosensory cortex in owl monkeys. J Neurophysiol 44(2):295-311.

Taub E, Ellman SJ, Berman AJ. 1966. Deafferentation in monkeys: effect on conditioned grasp response. Science 151(710):593-594.

Vierck CJ, Jr. 1973. Alterations of spatio-tactile discrimination after lesions of primate spinal cord. Brain Res 58(1):69-79.

Vierck CJ, Jr. 1974. Tactile movement detection and discrimination following dorsal column lesions in monkeys. Exp Brain Res 20(4):331-346.

Vierck CJ, Jr. 1977. Absolute and differential sensitivities to touch stimuli after spinal cord lesions in monkeys. Brain Res 134(3):529-539.

Vierck CJ, Jr. 1982. Comparison of the effects of dorsal rhizotomy or dorsal column transection on motor performance of monkeys. Exp Neurol 75(3):566-575.

Vierck CJ, Jr., Cooper BY. 1998. Cutaneous texture discrimination following transection of the dorsal spinal column in monkeys. Somatosens Mot Res 15(4):309-315.

Wall PD. 1970. The sensory and motor role of impulses travelling in the dorsal columns towards cerebral cortex. Brain 93(3):505-524.

Whishaw IQ, Pellis SM. 1990. The structure of skilled forelimb reaching in the rat: a proximally driven movement with a single distal rotatory component. Behav Brain Res 41(1):49-59.

Willis WD, Coggeshall RE. 1978. Sensory mechanisms of the spinal cord. New York: Plenum. ix, 485 p. p.

Wong-Riley M. 1979. Changes in the visual system of monocularly sutured or enucleated cats demonstrable with cytochrome oxidase histochemistry. Brain Res 171(1):11-28.

Woolsey CN, Erickson TC, Gilson WE. 1979. Localization in somatic sensory and motor areas of human cerebral cortex as determined by direct recording of evoked potentials and electrical stimulation. J Neurosurg 51(4):476-506.

Wu CW, Bichot NP, Kaas JH. 2000. Converging evidence from microstimulation, architecture, and connections for multiple motor areas in the frontal and cingulate cortex of prosimian primates. J Comp Neurol 423(1):140-177.

Wu CW, Kaas JH. 2002. The effects of long-standing limb loss on anatomical reorganization of the somatosensory afferents in the brainstem and spinal cord. Somatosens Mot Res 19(2):153-163.

Wu CW, Kaas JH. 2003. Somatosensory cortex of prosimian Galagos: physiological recording, cytoarchitecture, and corticocortical connections of anterior parietal cortex and cortex of the lateral sulcus. J Comp Neurol 457(3):263-292.

Xu J, Wall JT. 1997. Rapid changes in brainstem maps of adult primates after peripheral injury. Brain Res 774(1-2):211-215.

CHAPTER IV

CELLULAR SCALING RULES FOR PRIMATE SPINAL CORDS

This chapter includes contributions from Peebles JK, Tavares L, Herculano-Houzel S, and Kaas JH.

Introduction

Many studies have examined the relationships between the brain and body and between different parts of the brain (Barton and Harvey, 2000; Changizi, 2001; Finlay and Darlington, 1995; Herculano-Houzel et al., 2007; Herculano-Houzel et al., 2006; Jerison, 1973) and have found that they follow evolutionary trends that can be described mathematically. These allometric scaling rules are expressed by the power function $y = b + x^a$, which can be altered to the logarithmic form $\log(y) = a \log(x) + \log b$. Interestingly, different parts of the brain, such as the cortex and cerebellum, give different values for the slope "a" when compared to the body or total brain, suggesting that parts of the brain scale differently and thus may be exposed to different selection pressures. The purpose of the present study is to extend this examination to another part of the central nervous system, namely the spinal cord.

The spinal cord is an obligatory intermediary for most of the inputs and outputs that pass between the body and brain, and spinal cord size has been used as a measure of the nervous inputs between the brain and body (Passingham, 1975). Some authors have proposed that the spinal cord is merely a "somatic" system of sensorimotor inputs and outputs while the brain is a system with a somatic component plus a non-somatic

component that relates to higher cognitive functions (Krompecher and Lipak, 1966). According to their proposal the spinal cord would have a constant or linear relationship with the body for a slope "a" ~1 in the logarithmic equation. Other authors propose that the sensorimotor inputs and outputs of the spinal cord might relate directly to the surface area of the body, and thus spinal cord size might scale to body size as area to volume, for a slope "a" ~2/3 (Jerison, 1977; MacLarnon, 1996). Still others have proposed that metabolic considerations such as the basal metabolic rate of the mother during gestation (Martin, 1981) or the amount of fat-free body mass (Schoenemann, 2004) push the true slope to "a" ~3/4. Finally, it has been suggested that different orders of mammals follow different scaling rules and that the primate brain scales to body size with a slope of "a" ~1, while the rodent brain scales to body size with an slope of "a" ~3/4 (Herculano-Houzel et al., 2007; Herculano-Houzel et al., 2006). The scaling rules for spinal cords, then, may also be different across mammals.

Previous studies of the spinal cord have focused on whole spinal cord weight and length (MacLarnon, 1996), spinal cord cross-sectional area (Fox and Wilczynski, 1986; MacLarnon, 1995), or specific pathways of the spinal cord (MacLarnon, 1995; Nudo and Masterton, 1990; Towe, 1973). Little is known about the total number of neurons or other cells (non-neurons) in the spinal cord and how they relate to the brain and body. We use the isotropic fractionator (Herculano-Houzel and Lent, 2005), a non-stereological method, to calculate the total number of neurons and non-neurons in the spinal cord. We focus on one subset of mammals, primates and tree shrews. A preliminary description of this work has been presented elsewhere (Burish et al., 2007).

Materials and methods

Animals. We examined the spinal cords of 68 animals from ten species, including eight primates (mouse lemur *Microcebus sp.*, n=1; galago *Otolemur garnetti*, n=15; common marmoset *Callithrix jacchus*, n=1; owl monkey *Aotus trivirgatus*, n=12; squirrel monkey (*Saimiri sciureus*, n=4; rhesus macaque *Macaca mulatta*, n=5; bonnet macaque *Macaca radiata*, n=4; and long-tailed macaque *Macaca fascicularis*, n=1), and two non-primates (tree shrew *Tupaia glis*, n=18 and gray squirrel *Sciurus carolinensis*, n=7) (Table 1). Age was calculated from veterinary records; when only a numerical year was given as date of birth, the last day of the year (December 31st) was used to calculate age. Gender information was obtained from veterinary records when available, and the body mass was measured within the final week before perfusion.

Perfusion and dissection. Animals were given a lethal dose of sodium pentobarbital and, when areflexive, perfused transcardially with 0.1 M phosphate-buffered 0.9% saline (PBS, pH 7.4). Animals were then perfused with either 2% or 4% paraformaldehyde in PBS, usually followed by an equal amount of paraformaldehyde plus 10% sucrose in PBS. In one case (07-119), the animal was perfused with 4% paraformaldehyde, 0.1% glutaraldehyde, and 0.25% picric acid in 0.2 M phosphate buffer (PB, pH 7.4). In another case (07-39), the animal was perfused with PB and then post-fixed in 2% paraformaldehyde in PB. In all animals, the lamina and spinous processes of the vertebrae were removed along the entire length of the cord, the spinal roots were severed, and the spinal cord was removed and immersed in 4% paraformaldehyde for at least 14 days. The dura, brainstem, and cauda equina were removed and discarded. Afterwards the spinal cord was weighed and, in some cases, measured for length.

Table 1: Data set of individual spinal cord measurements

Species	Case	cord mass (g)	body mass (g)	# cells	% neurons	# neurons	# non-neurons	length (mm)	sex	age (years)
Rhesus macaque	07-25	9.814	9750	457500000	3.10	14182500	443317500	unknown	male	5.13
Rhesus macaque	07-29	6.029	4700	326080000	2.39	7793312	318286688	unknown	female	5.48
Rhesus macaque	07-30	9.902	9400	336875000	2.73	9196688	327678313	unknown	male	6.16
Rhesus macaque	07-56	8.871	11000	406250000	2.90	11781250	394468750	247.88	male	7.36
Rhesus macaque	07-119	7.9392	7500	421875000	1.67	7057388	414817612	262.48	female	7.88
Long-tailed macaque	07-44	7.4987	5700	372000000	3.06	11383200	360616800	unknown	male	8.25
Bonnet macaque	07-42	10.1222	10200	445000000	2.42	10769000	434231000	unknown	male	11.33
Bonnet macaque	07-82	5.7329	5400	285000000	2.58	7354839	277645161	unknown	female	unknown
Bonnet macaque	07-90	5.961	8850	304187500	n.a.	n.a.	n.a.	245.94	male	11.69
Bonnet macaque	07-91	9.55	7600	448437500	n.a.	n.a.	n.a.	283.25	male	7.68
Owl monkey	07-03	2.1624	1060	98046875	5.31	5206289	92840586	unknown	male	unknown
Owl monkey	07-26	2.62	1750	117562500	6.34	7456989	110105511	unknown	male	unknown
Owl monkey	07-46	1.7969	800	98906250	6.21	6146034	92760216	unknown	male	unknown
Owl monkey	07-50	1.984	1108	96100000	4.72	4535920	91564080	168.88	female	2.35
Owl monkey	07-77	2.4789	1400	107050781	6.07	6500237	100550544	175.83	male	9.33
Owl monkey	07-85	1.9122	1100	88359375	6.34	5603277	82756098	162.48	male	10.62
Owl monkey	07-87	3.1042	1540	98957031	5.30	5243877	93713154	205.62	male	10.37
Owl monkey	07-88	1.7485	974	80664063	7.09	5716351	74947712	163.88	male	unknown
Owl monkey	07-92	2.4204	1200	96562500	7.55	7291091	89271409	153.01	female	4.84
Owl monkey	07-103	1.9872	1100	87132813	5.64	4916054	82216759	unknown	male	6.80
Owl monkey	07-110	2.3504	1250	123925781	4.50	5582242	118343539	159.43	male	7.27
Owl monkey	07-115	1.4439	1100	68565625	8.28	5674397	62891228	unknown	female	7.91
Squirrel monkey	07-118	1.5768	860	96750000	6.14	5942418	90807582	163.15	male	2.95
Squirrel monkey	08-03	1.7177	915	107144531	5.69	6100756	101043775	172.30	female	1.08
Squirrel monkey	08-05	1.5666	950	89527344	2.27	2034712	87492631	172.98	male	7.91
Squirrel monkey	08-09	1.5477	710	90322917	5.21	4702629	85620287	unknown	female	5.16
Marmoset	07-27	0.6213	340	48195313	7.57	3649831	44545482	unknown	male	3.07
Galago	06-80	1.9345	1408	109375000	5.72	6256250	103118750	unknown	male	8.04
Galago	06-81	1.758	1018	96680000	4.60	4447280	92232720	unknown	male	3.20
Galago	07-08	2.1463	1254	91992188	7.36	6770625	85221563	unknown	male	1.95
Galago	07-40	1.5817	1400	119437500	5.59	6673772	112763728	unknown	male	8.18
Galago	07-51	1.73	1000	109687500	n.a.	n.a.	n.a.	159.23	female	3.62

Table 1 (continued)

Species	Code	sp. cord (g)	body (g)	# cells	% neur	# neurons	# nn	length (mm)	sex	age (years)
Galago	07-52	1.0441	486	75058600	5.65	4239310	70819290	unknown	female	0.84
Galago	07-65	1.4285	1100	88593750	5.45	4829642	83764108	153.40	female	4.45
Galago	07-73	1.7202	1400	101582031	6.32	6419984	95162047	152.23	male	1.58
Galago	07-75	1.3788	1040	107756250	5.78	6224963	101531287	141.73	female	1.93
Galago	07-79	1.4622	1200	75287500	6.46	4865519	70421981	175.21	male	1.83
Galago	07-83	1.395	1400	78890625	9.91	7821635	71068990	147.03	male	3.92
Galago	07-93	1.443	1100	110507813	5.24	5795166	104712647	166.88	female	1.48
Galago	07-105	1.1688	1100	83020833	5.17	4291335	78729498	155.88	male	1.12
Galago	07-111	1.4975	1000	105218750	6.67	7014583	98204167	132.36	female	1.19
Galago	07-120	1.2318	771	75433594	6.11	4612310	70821283	136.02	female	1.43
Mouse lemur	07-39	0.2353	60	22953125	7.33	1682654	21270471	unknown	male	15.61
Tree shrew	07-12	0.6173	231	41750000	6.64	2773453	38976548	unknown	male	0.33
Tree shrew	07-13	0.5297	192	38390625	4.95	1901104	36489521	unknown	male	0.32
Tree shrew	07-14	0.768	193	50121094	5.03	2520089	47601005	unknown	male	0.32
Tree shrew	07-15	0.6632	197	45773438	5.35	2448879	43324559	unknown	male	0.32
Tree shrew	07-16	0.6163	160	50312500	4.94	2485438	47827063	unknown	female	0.27
Tree shrew	07-17	0.4884	188	36351563	5.99	2176732	34174831	unknown	female	0.27
Tree shrew	07-18	0.5527	149	44000000	5.38	2367200	41632800	unknown	male	0.27
Tree shrew	07-19	0.5985	183	50312500	4.89	2460281	47852219	unknown	female	0.27
Tree shrew	07-58	0.6032	144	43699219	5.88	2570542	41128676	103.23	female	3.05
Tree shrew	07-59	0.6472	155	41062500	4.70	1929938	39132563	100.83	female	2.62
Tree shrew	07-60	0.5935	155	43640625	7.62	3324188	40316437	108.00	female	2.62
Tree shrew	07-69	0.735	170	45500000	7.55	3435543	42064457	99.63	male	2.72
Tree shrew	07-108	0.597	unknown	48083333	5.37	2584133	45499200	unknown	female	8.07
Tree shrew	07-109	0.481	144	46119792	10.04	4628510	41491282	unknown	female	5.85
Gray Squirrel	07-02	1.3605	unknown	71250000	5.95	4240800	67009200	unknown	unknown	unknown
Gray Squirrel	07-09	0.9926	387	49531250	7.72	3823813	45707438	unknown	unknown	unknown
Gray Squirrel	07-41	1.3051	486	80000000	10.56	8448000	71552000	unknown	unknown	unknown
Gray Squirrel	07-49	1.5451	unknown	78437500	7.98	6256959	72180541	140.04	unknown	unknown
Gray Squirrel	07-95	1.2367	unknown	71269531	6.91	4924574	66344957	128.85	unknown	unknown
Gray Squirrel	07-97	1.3003	unknown	107187500	5.12	5485974	101701526	144.69	unknown	unknown
Gray Squirrel	07-100	1.2521	unknown	70273438	9.61	6751762	63521676	159.86	unknown	unknown

Histology. The isotropic fractionator method (Herculano-Houzel and Lent, 2005) was used to estimate the total number of cells, neurons, and non-neurons. Each spinal cord was mechanically homogenized in a detergent solution (40 mM sodium citrate and 1% Triton-X100). For analysis of total cell number, we added 4'-6 diamidino-2-phenylindole dihydrochloride (DAPI, Molecular Probes, Eugene, OR), a DNA-specific fluorescent dye, to a final concentration of 0.5-1%. The solution was kept homogenous by agitation and an aliquot of the solution was placed on a hemocytometer. Cells within a known volume were counted under a Nikon Eclipse E800 (Nikon Corp., Tokyo, Japan), a Zeiss Axioskop 20 (Carl Zeiss MicroImaging, Inc., Thornwood, NY), an Olympus BX40F-3 (Olympus America Inc., Center Valley, PA), or a Zeiss Axioplan. This concentration was used to estimate the total number of cells in solution. For analysis of total neuron number, a 1 ml sample of the DAPI-stained solution was centrifuged, washed by resuspension in PBS, centrifuged, then resuspended in PBS and immunoreacted overnight with anti-NeuN mouse IgG (1:300 in PBS, Chemicon, Temecula, CA). The next day the cells were washed then resuspended and incubated in a secondary antibody solution of cyanine 3-conjugated anti-mouse IgG (1:400, Accurate Chemicals, Westbury, NY), 10% goat serum, 40% DAPI, and 50% PBS. Cells were washed then resuspended in a solution of PBS. An aliquot was placed on the hemocytometer, and we counted at least 500 cells, noting which cells were both DAPI-positive and NeuN-positive as well as which cells were DAPI-positive but NeuN-negative. The total number of neurons was calculated by multiplying the percentage of NeuN-positive neurons in our aliquot by the total number of cells, and the total number of

non-neurons was calculated by subtracting the total cell number by the total neuron number.

Data analysis. Statistical analyses were performed in Statview (SAS Institute, Cary, NC) and Microsoft Excel (Microsoft Corporation, Redmond, WA). Adults and juveniles were included in the calculation, but animals less than 2 months of age (tree shrews 07-20, 07-21, 07-22, and 07-23) were excluded. Gray squirrels were excluded from all regression line calculations, since rodents and primates have previously been found to scale differently in their brain components (Herculano-Houzel et al., 2007; Herculano-Houzel et al., 2006). Since tree shrews scale similarly to primates in some comparisons but not others (Herculano-Houzel et al., 2007), we calculated regression lines both with and without the tree shrew data. Correlations between variables were calculated using Spearman's correlation coefficient. For comparisons on smaller portions of the data set, nonparametric statistical tests were calculated using Matlab (The MathWorks, Natick, MA). Mann-Whitney U-tests were used for comparisons between two groups and Kruskal-Wallis tests were used for comparisons of more than two groups.

Results

We obtained 68 spinal cord specimens from eight primate species, one tree shrew species, and one rodent species. Our species list contains three species of closely-related Old World monkeys (*Macaca mulatta, Macaca radiata,* and *Macaca fascicularis*). We also have three species of New World monkeys, including both the Callithricidae radiation (*Callithrix jacchus*) and the Cebidae radiation (*Aotus trivirgatus* and *Samiri sciureus*). We have two species of prosimians, one from the Lorisiform radiation

(*Otolemur garnetti*) and one from the Lemuriform radiation (*Microcebus sp.*). We included the common tree shrew (*Tupaia glis*), a non-primate that is the most closely related species to primates that is available for study. Finally, we list the gray squirrel (*Sciurus carolinensis*), a highly visual arboreal rodent. As a rodent, we exclude it from all comparisons except in the special case of comparing marmosets, tree shrews, and gray squirrels (see below).

Body size in our data set (Table 1) varies 140–fold from the mouse lemur (60g) to the rhesus macaque (~8500g), whereas spinal cord size varies 35–fold from the mouse lemur (0.24g) to the rhesus macaque (8.51g). Looking at cell numbers, total cell number varies 22-fold from the mouse lemur (~18 million cells) to the rhesus macaque (~390 million cells). Specifically, the number of neurons varies 8–fold from the mouse lemur (~1.7 million neurons) to the bonnet macaque (~13 million neurons), and the number of cells that are not neurons ("non-neurons") varies 18–fold from the mouse lemur (~21 million) to the rhesus macaque (~380 million non-neurons). The percentage of cells that are neurons in the spinal cord is 11% or less in every spinal cord examined. This last finding is in stark contrast to the primate brain where, using identical methods, the percentage of cells that are neurons was found to be 45% or greater (Herculano-Houzel et al., 2007).

In larger primates, the spinal cord is proportionately smaller. While bigger primates have larger spinal cords, spinal cord mass does not increase as quickly as body mass (Fig. 1a). Body mass is proportional to spinal cord mass with an exponent of 0.73 (Table 2), and is below linearity (95% confidence interval 0.652-0.814). Removal of the tree shrew

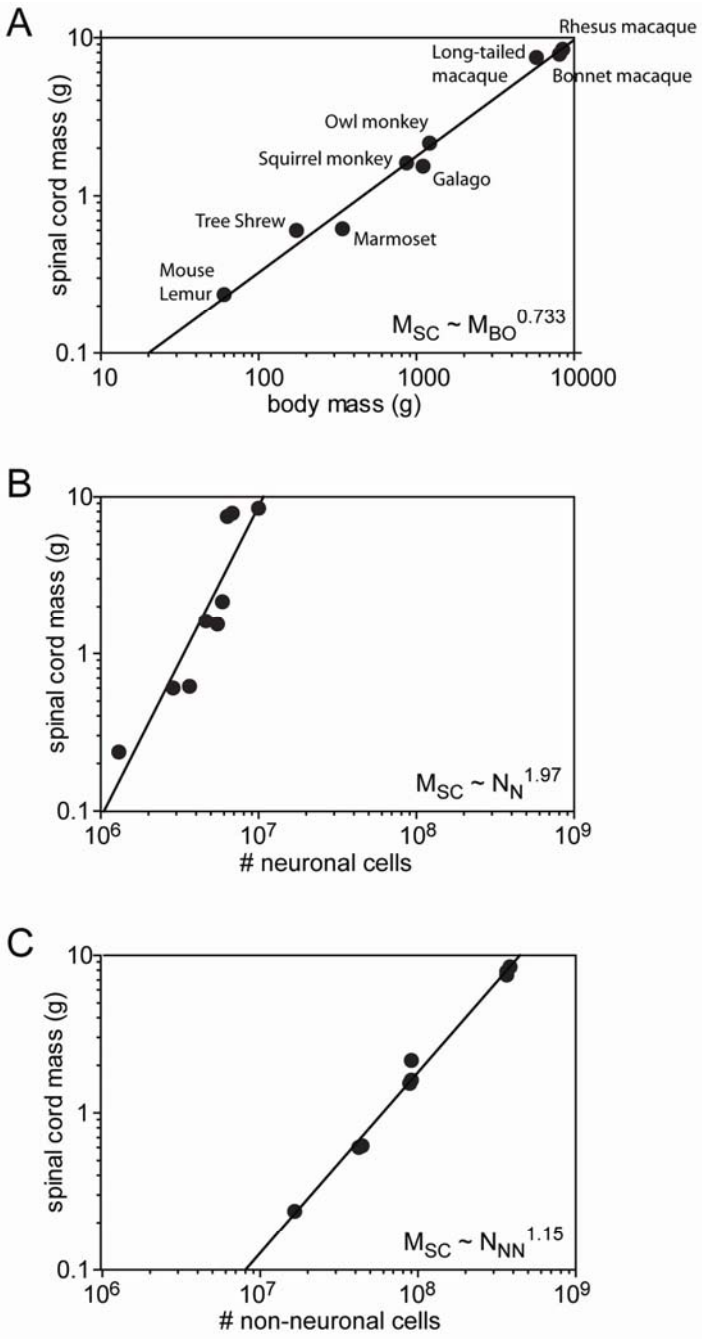

Fig. 1. Relationships between spinal cord mass and A) body mass, B) number of neurons cells, or C) number of non-neurons. Each point represents the mean for a particular species; they are labeled in A. Power functions are shown on the respective graphs; all three comparisons were significant (see text).

TABLE 2. Scaling rules for spinal cords[1]

y variable	x variable	Slope	P value	ρ value	95% C.I.
Spinal cord mass	body mass	0.733	<0.0001	0.983	0.652 - 0.814
Spinal cord mass	Number of N	1.970	0.0005	0.983	1.204 - 2.737
Spinal cord mass	Number of NN	1.150	<0.0001	0.967	1.051 - 1.249
Neuronal density	Spinal cord mass	-0.573	<0.0001	-0.883	-0.739 - -0.407
Non-neuronal density	Spinal cord mass	-0.138	0.0031	-0.850	-0.212 - -0.064
Number of NN/N	Spinal cord mass	0.435	0.0009	0.833	0.249 - 0.622
Number of NN	Number of N	1.693	0.0007	0.933	1.004 - 2.382
Spinal cord mass	Brain mass	0.822	0.0038	0.943	0.408 - 1.237
Spinal cord mass	Cortical mass	0.801	0.0008	1.000	0.513 - 1.088
Spinal cord mass	Cerebellar mass	0.901	0.0058	1.000	0.497 - 1.304
Spinal cord mass	Rest of brain mass	1.223	0.0033	1.000	0.772 - 1.674
Number of cortical neurons	CNS mass	0.966	0.0297	0.700	0.649 - 1.284
Number of cerebellar neurons	CNS mass	0.972	0.0009	1.000	0.743 - 1.200
Number of rest of brain neurons	CNS mass	0.540	0.0023	0.900	0.101 - 0.980
Number of N	CNS mass	0.337	0.0141	0.829	0.113 - 0.562

[1]Variables for "x" and "y" refer to the equation log(y) = a log(x) + log b, with a slope of "a". Significance values (P), correlation coefficients (ρ), and confidence intervals (C.I.) are also show. All calculations include the tree shrew data. N, spinal neurons; NN, spinal non-neuronal cells.

shows only a minor change in the exponent ($M_{BO} \sim M_{SC}^{0.754}$, $p<0.0001$). The mass of the animal, then, increases faster than the mass of the spinal cord.

In larger spinal cords, cell number is proportionately smaller. While animals with larger spinal cords have more neurons and more non-neurons, the spinal cord gains mass faster than it gains neurons or non-neurons (Fig. 1b-c). Spinal cord mass is proportional to the total number of neurons with an exponent of 1.97 (Table 2), and to the total number of non-neurons with an exponent of 1.15. Removal of the tree shrew shows only a minor change in the exponents for number of neurons ($M_{SC} \sim N_N^{1.933}$, $p=0.0018$) or non-neurons ($M_{SC} \sim N_{NN}^{1.140}$, $p<0.0001$). The total number of neurons and non-neurons, then, does not keep up with the mass of the spinal cord.

Cell densities decrease in larger spinal cords. Average density was calculated by dividing the number of neurons or non-neurons by the mass of the spinal cord. Neuronal and non-neuronal densities are smaller in animals with larger spinal cords (Fig. 2a-b). Neuronal density decreases faster in larger spinal cords (with an exponent of -0.573) than non-neuronal density (with an exponent of -0.138), and the confidence intervals do not overlap with an exponent of zero (Table 2). Removing the tree shrew results in only minor changes to the exponents for neuronal density ($D_N \sim M_{SC}^{-0.573}$, $p=0.0004$) and non-neuronal density ($D_{NN} \sim M_{SC}^{-0.131}$, $p=0.0091$). While it must be noted that spinal cord cells, especially neurons, are not uniformly distributed in the cord, the average density does decrease as the spinal cord mass increases.

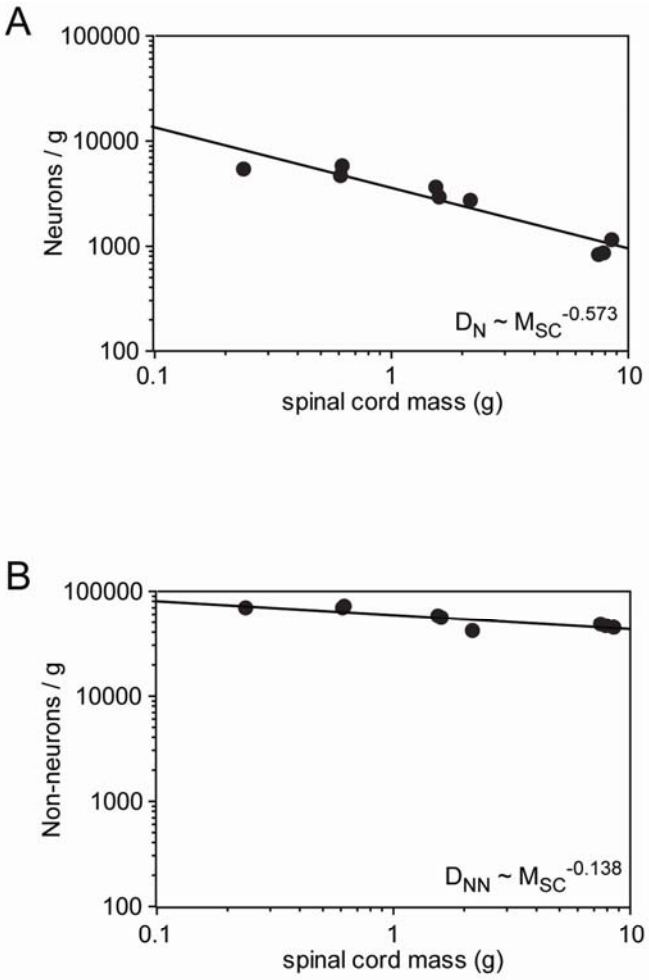

Fig. 2. Relationships between spinal cord mass and A) neuronal density or B) non-neuronal density. Each point represents the mean for a particular species. Power functions are shown on the respective graphs; both comparisons were significant (see text).

Non-neurons increase at a faster rate than neurons. Bigger spinal cords have more neurons and more non-neurons, and the relationship between these cells appears to follow a power function. When plotting the ratio of non-neurons to neurons against spinal cord mass, there is an increase in the ratio in bigger spinal cords, with an exponent of 0.435 (Fig. 3a; Table 2). When comparing non-neurons directly to neurons, more non-neurons are added than neurons, with an exponent of 1.693 (Fig. 3b; Table 2). Removing the tree shrew results in only minor changes to the exponents for the ratio of non-neurons to neurons ($N_{NN}/N_N \sim M_{SC}^{0.442}$, p=0.0026) and for non-neurons versus neurons ($N_{NN} \sim N_N^{1.674}$, p=0.0022).

Spinal cord relationships with the brain. We were interested in comparing our spinal cord data to brain data in these species. For a suitable brain data set we chose that of Herculano-Houzel et al. (2007) because they used identical methods. The spinal cord and brain data sets share six species in common: tree shrew, galago, common marmoset, owl monkey, squirrel monkey, rhesus macaque, and long-tailed macaque, although brain component data was not available for the squirrel monkey or long-tailed macaque. A comparison between brain mass and spinal cord mass shows that they are related with an exponent of 0.822 (Fig. 4a; Table 2). Removing the tree shrew changes the exponent to 0.975 (p=0.0116), which is still within the 95% confidence interval (Table 2). Separating the brain into the cortex, cerebellum, and rest of the brain, it seems that spinal cord mass increases more slowly than cortical mass (exponent of 0.801) or cerebellar mass (exponent of 0.901) but increases more quickly than the mass of the rest of the brain

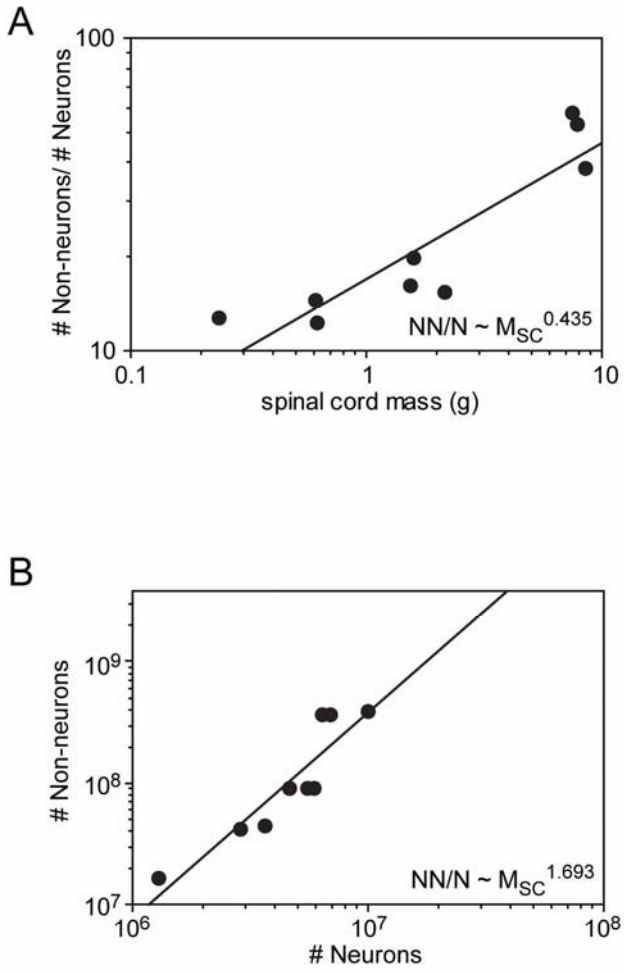

Fig. 3. Relationships between A) ratio of non-neuronal to neuronal number and spinal cord mass, and B) number of non-neurons and number of neurons. Each point represents the mean for a particular species. Power functions are shown on the respective graphs; both comparisons were significant (see text).

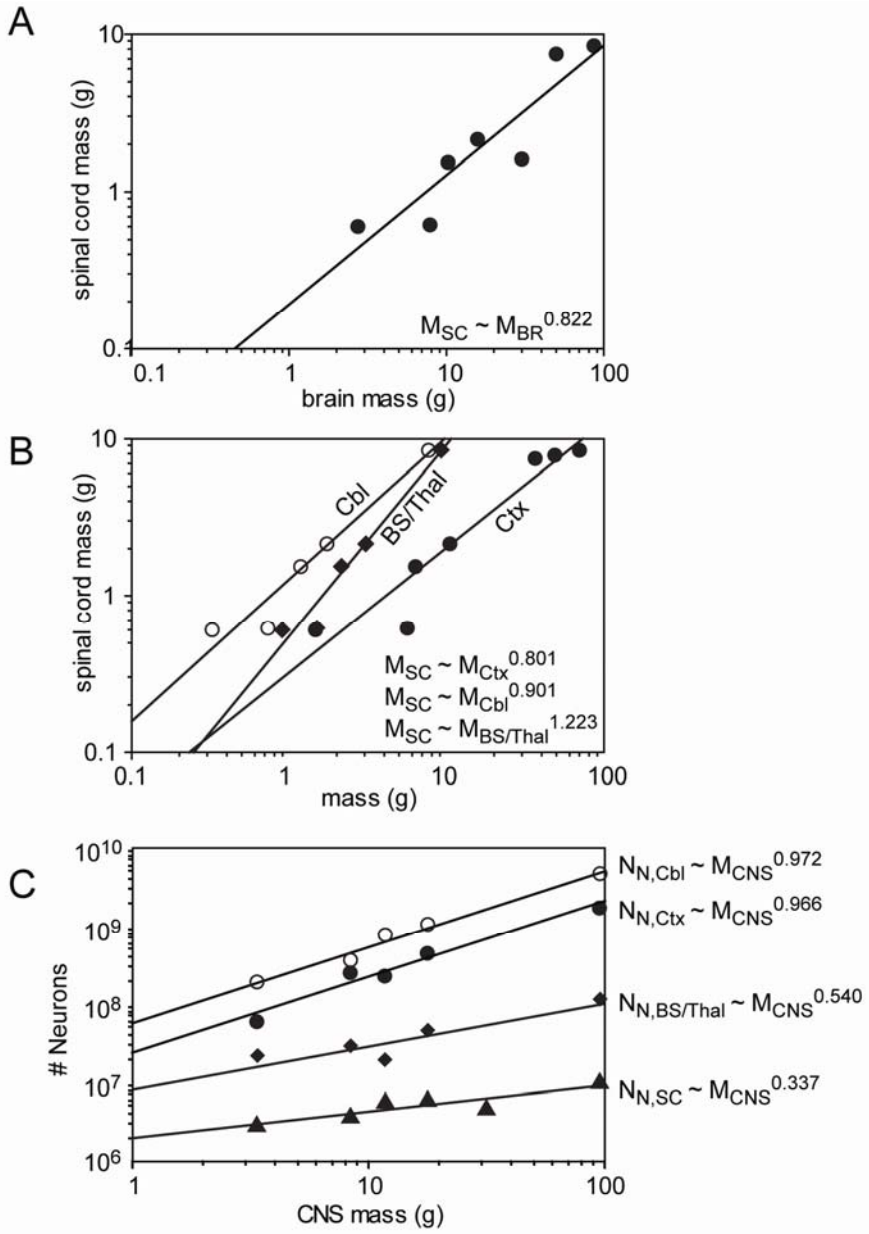

Fig. 4. Mass and cellular scaling rules for the primate central nervous system. Relationships are between A) spinal cord mass and brain mass, B) spinal cord mass and brain component masses, and C) number of neurons for each CNS component and total CNS mass. Filled circles represent cortex (Ctx), Open circles represent cerebellum (Cbl), diamonds represent the rest of the brain consisting mostly of brainstem and thalamus (BS/Thal), and triangles represent spinal cord (SC). Each point represents the mean for a particular species; they are labeled in A. Power functions are shown on the respective graphs; all comparisons were significant (see text).

(exponent of 1.223; Fig. 4b). Removal of the tree shrew only slightly changed the exponents for cortical mass (0.945, p=0.0025), cerebellar mass (1.056, p=0.135), or rest of brain mass (1.361, p=0.0130). When plotting the number of neurons against body mass (Fig. 4c) all values are at or below linearity. Interestingly, the slopes for cortex (0.966) and cerebellum (0.972) are similar, and the slopes for the rest of the brain (0.540) and the spinal cord (0.337) are similar. Removal of the tree shrew only slightly altered the exponents for cortex (0.853, p=0.0145) and cerebellum (0.971, p=0.0140), but the exponents were no longer significant between spinal cord neurons and CNS mass (p=0.0816) or between rest of brain neurons and CNS mass (p=0.0652).

Intraspecies spinal cord comparisons. We collected a substantial number of male and female cords from two species in particular: tree shrews (n=14 animals older than 2 months, 6 male and 8 female), and galagos (n=15, 8 male and 7 female). Significant changes were found in body size between males and females in tree shrews (Mann-Whitney U test, p=0.0390) and galagos (M-W U test, p=0.0034), with males being larger in both species. No significant gender differences were found for spinal cord mass (M-W U test, tree shrew p=0.1812, galago p=0.1206), the total number of neurons (M-W U test, tree shrew p=0.6620, galago p=1.000), the total number of cells (M-W U test, tree shrew p=0.7256, galago p=0.2109), or the percentage of cells that were neurons (M-W U test, tree shrew p=0.7259, galago p=0.2109).

Phylogenic and behavioral comparisons. We performed comparisons on two subsets of the data set. Firstly we compared the three species of closely-related macaques, which

diverged from each other only 2.4 million years ago (Purvis, 1995). No significant differences between the rhesus macaque, long-tailed macaque, and bonnet macaque were seen for body mass (Kruskal-Wallis test, p=0.6643), spinal cord mass (K-W test, p=0.7328), the total number of neurons (K-W test, p=0.1979), the total number of non-neurons (K-W test, p=0.9495), the total number of cells (K-W test, p=0.8725), or the percentage of cells that were neurons (K-W test, p=0.2931).

Secondly we compared marmosets, tree shrews, and gray squirrels, three distantly related species with such similarities in locomotion, diet, and habitat that authors have debated whether they occupy similar niches (Emmons, 2000; Hershkovitz, 1977; Sussman and Kinzey, 1984). A significant difference was seen in body mass (Kruskal-Wallis test, p=0.0328), spinal cord mass (K-W test, p=0.0008), the total number of neurons (K-W test, p=0.0009), the total number of non-neurons (K-W test, p=0.0017), and the total number of cells (K-W test, p=0.0015), with the gray squirrel being the largest in all categories. However, no significant difference was seen in the percentage of cells that were neurons (K-W test, p=0.1329).

Discussion

We examined 68 spinal cords using the isotropic fractionator technique and obtained information on body mass, spinal cord mass, spinal cord number of neurons, and spinal cord number of non-neurons in each animal. In addition, we compared our findings to a similar data set for the brain using the isotropic fractionator, and investigated the variability of spinal cords within the tree shrews and galagos. Our findings suggest that the primate spinal cord follows simple allometric scaling rules

according to the power function $y = b + x^a$, or for our purposes the logarithmic form $\log(y) = a \log(x) + \log b$. We focus on the slope "a," as it indicates how the graphs scale. We largely ignore the coefficient "b," as we are examining a single subset of mammals, and "b" most useful when comparing across subsets (e.g., Jerison, 1973). We now review our findings, as well as the findings of other investigations into spinal cord and brain scaling.

Relationship between spinal cord mass and body mass. We found that spinal cord mass is related to body mass by a power function with an exponent of 0.73. Our 95% confidence interval overlaps with the finding of MacLarnon (1996) of an exponent of 0.66. For the species that the two data sets share, the results are similar: our body weight and spinal cord weights for common marmoset, owl monkey, squirrel monkey, and long-tailed macaque are close to her values for common marmoset (287g body, 0.27g spinal cord), owl monkey (1200g body, 2.320g spinal cord), squirrel monkey (805g body, 1.803g spinal cord), and long-tailed macaque (3610g body, 3.790g spinal cord) (MacLarnon, 1996). Combining the two data sets, the new equation relating body mass and spinal cord mass is $M_{BO} \sim M_{SC}^{0.681}$ ($p<0.001$, $\rho=0.986$, 95% C.I.=0.646-0.717) and accounts for a wide range of body sizes in the primate lineage (Fig. 5). This new equation is closer to the proposed $2/3^{rds}$ exponent relating surface area to body size (Jerison, 1973), than the metabolic exponent of 0.75 (Hofman, 1982; Martin, 1981), and is not close to the exponent of 1.0 that relates brain size to body mass in primates (Herculano-Houzel et al., 2007). Neither data set has taken into account the percentage of fatty tissue, which some authors have suggested skews the spinal cord/body relationship (Schoenemann,

2004). We cannot rule out the possibility that all of these factors and more may play a role in the relationship of spinal cord mass to body mass.

Cell body distributions in the spinal cord. The isotropic fractionator technique allows us to quantify the number of cell bodies of neurons and non-neurons in our sample, and thus this study only examines cells in which the soma is contained within the spinal cord. Therefore most of the neurons in our data set come from the dorsal, intermediate, and ventral horns of the gray matter, which include cells related to crude touch, pain, temperature, the sympathetic system, the motor system, intrinsic spinal systems such as reflex arc neurons and spinal pattern generators, and a portion of the proprioceptive inputs for the body (Willis and Coggeshall, 1978). The majority of neurons in the corticospinal and dorsal column tracts, however, are not included, as their soma are located in the cortex and dorsal root ganglia, respectively. In contrast, soma for supporting cells such as glia and vascular cells are found in both the gray and the white matter of the spinal cord. Thus neurons of the corticospinal tracts and dorsal columns are not counted, but their non-neurons are. This disparity of non-neurons to neurons in the dorsal columns and corticospinal tracts at least in part explains why, in bigger spinal cords, more non-neurons are added to the spinal cord than neurons. Other factors, however, may also play a role in the disproportionate addition of non-neurons. One possibility is that, in bigger spinal cords, neurons increase in size, and more glia are necessary to support larger neurons (see below). This study cannot comment on the scaling of neurons in the dorsal columns or corticospinal tracts, which contain a substantial amount of somatosensory inputs and motor outputs.

A complete examination of white matter neurons would require an extensive analysis of axons. That analysis would have its own complications in calculating neuron number in the spinal cord, as it would be difficult to locate the origins of each axon (from intrinsic or extrinsic spinal neurons) or the presence of axon collaterals. Previous studies have instead examined cross-sectional area of component parts of the white matter, and have found that the corticospinal tract decreases in size relative to body mass (Towe, 1973) and that the size of the dorsal columns in the cervical and lumbar enlargements may be related to forelimb/hindlimb dominance (MacLarnon, 1995). Additionally, tracer labeling studies into the C1/C2 vertebrae suggest that the corticospinal system decreases in size relative to body weight but is a linear function of brain weight (Nudo and Masterton, 1990), while the tectospinal tract is highly variable between species (Nudo and Masterton, 1989).

Why does cell density decrease, and why do cell numbers proportionately decrease?

Cell density is lower in larger primates, and the number of neurons and non-neurons do not increase as rapidly as spinal cord mass (Table 2). Although we do not understand all of the factors involved, we can propose testable hypotheses for the biological significance of these scaling rules.

There are several possibilities for why cell density and cell size decrease in our data set, including an increase in cell size and the enlargement of fiber pathways. For the first possibility, if cells increase in size in larger spinal cords, then the number of cells per volume would decrease (cell density decreases) and relatively fewer cells would fit in the spinal cord (cell number decreases). This decrease in neuronal density was not seen in

primate brains (Herculano-Houzel et al., 2007), but has been observed in the brains of other mammals (Haug, 1987; Herculano-Houzel et al., 2006; Stolzenburg et al., 1989; Tower and Elliott, 1952). Like the primate spinal cord, in rodent brains Herculano-Houzel et al. (2006) found that neuronal density decreases as a function of brain mass, non-neuronal density decreases to a lesser extent, and non-neuronal numbers are added at a faster rate than neurons. Their interpretation is that average neuron size increases, and as a consequence more non-neurons are needed to support each individual neuron. Consistent with this interpretation, at least for corticospinal cells there does appear to be a difference in soma diameter between primates and non-primates (Nudo et al., 1995). Depending on how the gray matter scales relative to the white matter, neuron number could be affected more than non-neuron number.

As a second possibility, another way to decrease cell density and cell size is to increase the proportion of tissue that has few cell bodies, such as the white matter. In the dorsal columns and corticospinal tracts, neuron soma are located outside the spinal cord. If these fiber pathways enlarge faster than the gray matter in larger primates, then cell density would decrease, and neuronal density would decrease more than non-neuronal density. Perhaps the importance of gray matter pathways decreases in larger spinal cords or their functions are relegated to white matter pathways. The dorsal columns contain inputs for touch, vibration, proprioception, visceral pain, and temperature (Willis and Coggeshall, 1978). Perhaps gray matter pathways responsible for crude touch, pain, temperature, or proprioception show a relative decrease in size while the dorsal columns show a relative increase.

The primate spinal cord scales differently than the primate brain. Based on our findings and those of Herculano-Houzel et al. (2007), scaling rules of primate spinal cords are not the same as those of the brain. Spinal cord mass increases more slowly than body mass, whereas brain and body mass are linearly related. Spinal neuronal and non-neuronal densities decrease in larger spinal cords, whereas brain neuronal and non-neuronal densities show no significant change in larger brains. Total numbers for spinal neurons and non-neurons increase more slowly than spinal cord mass, whereas total numbers for brain neurons and non-neurons are linearly related to brain mass. Compared to CNS mass, the number of spinal cord neurons increases much more slowly than any brain component. Even neurons in the 'rest of the brain' increases faster than spinal cord neurons, suggesting that brainstem and thalamic neurons are not simply linked to spinal cord neurons. Previous authors have proposed that the brain and spinal cord face different selection pressures (Fox and Wilczynski, 1986; Jerison, 1973; Krompecher and Lipak, 1966). Perhaps it is the different selection pressures that have lead to different scaling rules.

Addition of the tree shrew to the primate data set. The last common ancestor of all 8 primates lived approximately 55 million years ago (Purvis, 1995), and the last common ancestor of the primates and tree shrews was approximately 85 million years ago (Liu et al., 2001; Murphy et al., 2001; Springer et al., 2003). In an earlier study on brain scaling (Herculano-Houzel et al., 2007), addition of the tree shrew to the primate data set did not significantly alter the values except in the case of the brainstem. In this study removal of the tree shrew resulted in few changes; the slopes with tree shrews removed were still

within the 95% confidence interval for all comparisons except two: CNS mass compared to the number of spinal cord neurons or to the number of 'rest of the brain' neurons. Tree shrew, it appears, scales similarly to primates.

Subset comparisons. We made several comparisons on parts of the data set. For gender comparisons, there is evidence of sexual dimorphism for both tree shrews and galagos in body size, with males being larger, but otherwise there was no dimorphism in the size or cellular components of the spinal cord. For comparisons between the closely related macaques, there were no significant differences, suggesting that the three species are very similar in size and in spinal cord cellular organization. For comparisons between the behaviorally similar marmoset, gray squirrel, and tree shrew, the squirrel was consistently the largest in terms of body size, spinal cord size, and the numbers of neurons, non-neurons, and totals cells. If squirrels are larger in size, it is not surprising that they also have larger spinal cords and more cells in the spinal cord. However, squirrels are not significantly different than marmosets and tree shrews in the percentage of cells that are neurons, suggesting that there may be some conserved or convergent traits in spinal cord cellular organization between the three species.

Acknowledgments

For the generous donation of spinal cords we thank Tom Norton, Jeff Schall, Troy Hackett, Vivien Casagrande, Anna Roe, Christine Collins, Peiyan Wong, Iwona Stepniewska, Omar Gharbawie, Jamie Reed, Huixin Qi, Mary Baldwin, Peter Kaskan,

and Corrie Camalier. We thank Charnese Bowes and Omar Gharbawie for assistance with surgical procedures.

References

Barton RA, Harvey PH. 2000. Mosaic evolution of brain structure in mammals. Nature 405(6790):1055-1058.

Burish MJ, Peebles JK, Kaas JH, Herculano-Houzel S. 2007. Cellular scaling rules for primate spinal cord. Soc Neurosci Abstr 193.4.

Changizi MA. 2001. Principles underlying mammalian neocortical scaling. Biol Cybern 84(3):207-215.

Emmons LH. 2000. Tupai: A Field Study of Bornean Treesrews. Berkeley, CA: University of California Press.

Finlay BL, Darlington RB. 1995. Linked regularities in the development and evolution of mammalian brains. Science 268(5217):1578-1584.

Fox JH, Wilczynski W. 1986. Allometry of major CNS divisions: towards a reevaluation of somatic brain-body scaling. Brain Behav Evol 28(4):157-169.

Haug H. 1987. Brain sizes, surfaces, and neuronal sizes of the cortex cerebri: a stereological investigation of man and his variability and a comparison with some mammals (primates, whales, marsupials, insectivores, and one elephant). Am J Anat 180(2):126-142.

Herculano-Houzel S, Collins CE, Wong P, Kaas JH. 2007. Cellular scaling rules for primate brains. Proc Natl Acad Sci U S A 104(9):3562-3567.

Herculano-Houzel S, Lent R. 2005. Isotropic fractionator: a simple, rapid method for the quantification of total cell and neuron numbers in the brain. J Neurosci 25(10):2518-2521.

Herculano-Houzel S, Mota B, Lent R. 2006. Cellular scaling rules for rodent brains. Proc Natl Acad Sci U S A 103(32):12138-12143.

Hershkovitz P. 1977. Living New World Monkeys (Platyrrhini). Chicago: University of Chicago Press.

Hofman MA. 1982. Encephalization in mammals in relation to the size of the cerebral cortex. Brain Behav Evol 20(1-2):84-96.

Jerison HJ. 1973. Evolution of the brain and intelligence. New York: Academic Press. xiv, 482 p. p.

Jerison HJ. 1977. The theory of encephalization. Ann N Y Acad Sci 299:146-160.

Krompecher S, Lipak J. 1966. A simple method for determining cerebralization. Brain weight and intelligence. J Comp Neurol 127(1):113-120.

Liu FG, Miyamoto MM, Freire NP, Ong PQ, Tennant MR, Young TS, Gugel KF. 2001. Molecular and morphological supertrees for eutherian (placental) mammals. Science 291(5509):1786-1789.

MacLarnon A. 1995. The distribution of spinal cord tissues and locomotor adaptation in primates. J Hum Evol(29):463-482.

MacLarnon A. 1996. The scaling of gross dimensions of the spinal cord in primates and other species. J Hum Evol 30:71-87.

Martin RD. 1981. Relative brain size and basal metabolic rate in terrestrial vertebrates. Nature 293(5827):57-60.

Murphy WJ, Eizirik E, O'Brien SJ, Madsen O, Scally M, Douady CJ, Teeling E, Ryder OA, Stanhope MJ, de Jong WW, Springer MS. 2001. Resolution of the early placental mammal radiation using Bayesian phylogenetics. Science 294(5550):2348-2351.

Nudo RJ, Masterton RB. 1989. Descending pathways to the spinal cord: II. Quantitative study of the tectospinal tract in 23 mammals. J Comp Neurol 286(1):96-119.

Nudo RJ, Masterton RB. 1990. Descending pathways to the spinal cord, IV: Some factors related to the amount of cortex devoted to the corticospinal tract. J Comp Neurol 296(4):584-597.

Nudo RJ, Sutherland DP, Masterton RB. 1995. Variation and evolution of mammalian corticospinal somata with special reference to primates. J Comp Neurol 358(2):181-205.

Passingham RE. 1975. The brain and intelligence. Brain Behav Evol 11(1):1-15.

Purvis A. 1995. A composite estimate of primate phylogeny. Philos Trans R Soc Lond B Biol Sci 348(1326):405-421.

Schoenemann PT. 2004. Brain size scaling and body composition in mammals. Brain Behav Evol 63(1):47-60.

Springer MS, Murphy WJ, Eizirik E, O'Brien SJ. 2003. Placental mammal diversification and the Cretaceous-Tertiary boundary. Proc Natl Acad Sci U S A 100(3):1056-1061.

Stolzenburg JU, Reichenbach A, Neumann M. 1989. Size and density of glial and neuronal cells within the cerebral neocortex of various insectivorian species. Glia 2(2):78-84.

Sussman RW, Kinzey WG. 1984. The ecological role of the callitrichidae: a review. Am J Phys Anthropol 64(4):419-449.

Towe AL. 1973. Relative numbers of pyramidal tract neurons in mammals of different sizes. Brain Behav Evol 7(1):1-17.

Tower DB, Elliott KA. 1952. Activity of acetylcholine system in cerebral cortex of various unanesthetized mammals. Am J Physiol 168(3):747-759.

Willis WD, Coggeshall RE. 1978. Sensory mechanisms of the spinal cord. New York: Plenum. ix, 485 p. p.

CHAPTER V

CONCLUSION

Frontoparietal cortex is the first cortical region to receive inputs from the spinal cord and the last to convey outputs to the spinal cord. The research performed in this dissertation suggests that the organization of frontoparietal cortex and the cellular composition of spinal cords in marmosets are similar to those of other primates.

Marmoset primary motor cortex, as described in this work and independently confirmed (Burman et al., 2008), is so similar in architectonics and physiology to the primary motor cortex of other primates (Gould et al., 1986; Stepniewska et al., 1993; Wu et al., 2000) that we consider it a homologous region. Furthermore our physiological examination of premotor cortex, combined with analyses of architectonics and connectivity (Burman et al., 2006; Burman et al., 2008), suggests that marmosets also have at least three premotor areas. While the smallest mammals such as shrews have only the most basic cortical areas such as primary somatosensory, auditory, and visual areas (Catania et al., 1999), it seems that even the smallest monkeys have preserved the general primate motor plan (Fig. 1). Marmosets appear to be similar to other primates in the differentiation of primary and premotor areas, the amount of cortex devoted to the motor system, and the amount of primary motor cortex devoted to each body part.

The reorganization of somatosensory cortex in marmosets is also similar to other primates. After dorsal column injury regions of somatosensory cortex do not remain silent, but in most cases adopt abnormal receptive fields, often of adjacent digit, palm, or forearm regions. This type of reorganization seems to be characteristic of many

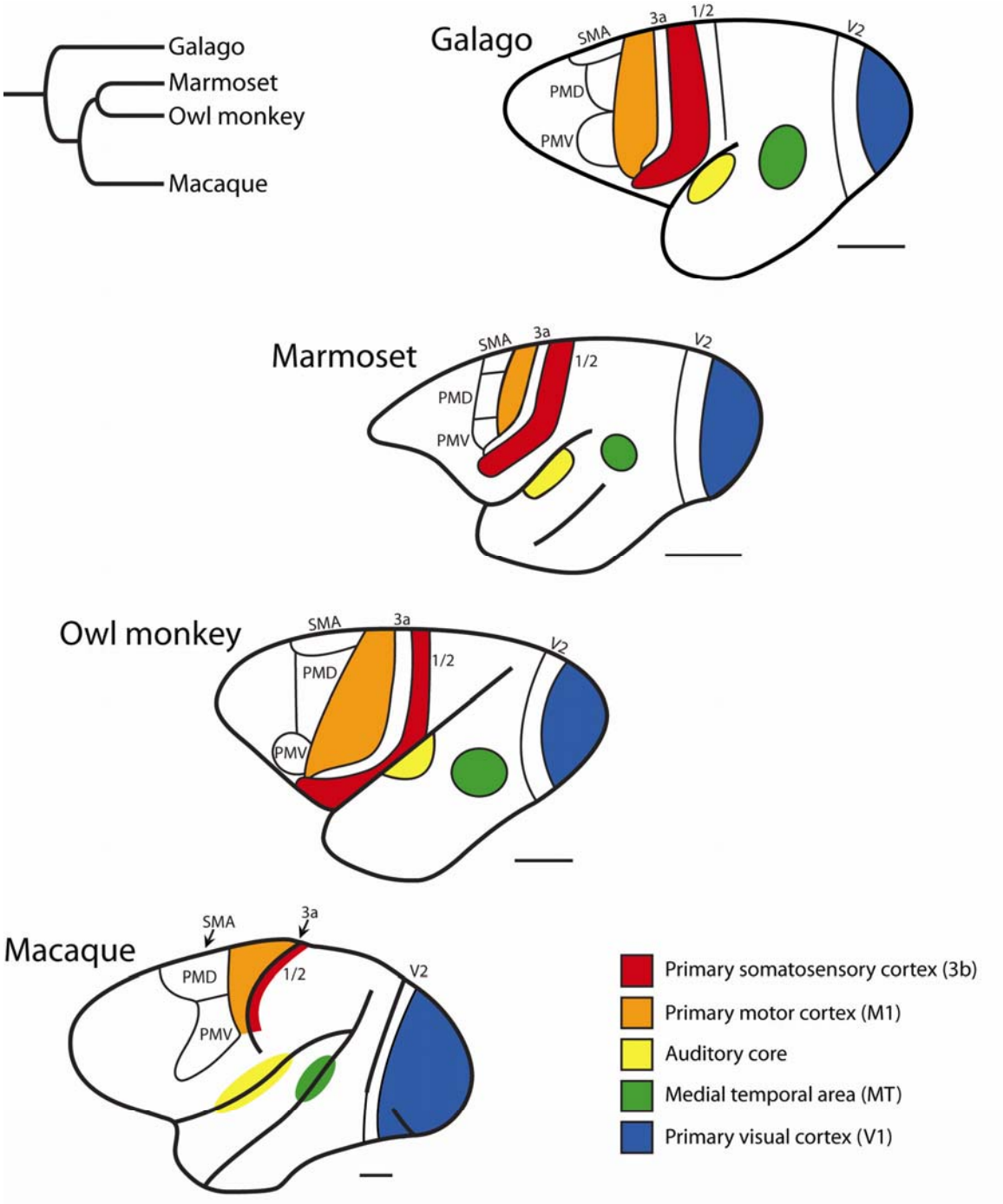

Figure 1. Cortical organization of sensory and motor areas in several primate species. The organization of galago, marmoset, owl monkey, and macaque monkey cortices are based on Burish et al. (2008), Krubitzer and Kahn (2003), and Stepniewska et al. (2006). Several of the macaque areas (V1, V2, MT, 3b, 3a, SMA, and auditory core) are buried within sulci. The phylogenic tree is based on Purvis (1995). Scale bars = 5 mm.

mammals, as a similar amount of somatosensory plasticity is seen in rodents (Jain et al., 1995) as well as primates (Jain et al., 1997). Likewise marmoset behavior after dorsal column lesions is similar to that found in rodents (McKenna and Whishaw, 1999), non-human primates (Vierck, 1973; Vierck, 1974; Vierck, 1977; Vierck and Cooper, 1998), and humans (Kaas et al., 2008; Nathan et al., 1986), in that there are many transient behavioral deficits. The implication for this work is that spinal cord treatments that work in rats are likely to work in non-human primates and humans as well. Rats are an excellent model for initial therapeutic studies, as they are inexpensive and their somatosensory plasticity and behavioral abilities are similar to those of primates (Kaas et al., 2008). However, because motor fibers pass through the dorsal columns in rats, studies of injury repair are in some sense different than similar studies performed in primates. This is one reason that rats are not necessarily the ideal model for human spinal injuries. Along with other concerns, such as the fact that fine motor control of the fingers cannot be tested in rats, potential therapeutic treatments should move from rats to non-human primates and then to human trials (Courtine et al., 2007). The marmoset results in this study, when combined with previous findings in owl monkeys (Jain et al., 1997), show that two different species of New World monkeys have similar reorganizations after dorsal column lesions. The particular species of non-human primate used for testing, then, may not be critical. One caveat that should be added is that animal studies often use a low-dose (1 mg/kg) of the corticosteroid dexamethasone, given approximately 1 hour before spinal cord injury, primarily to prevent CNS swelling. However, it should not be considered the same as the current recommended treatment for

spinal cord injury, a high-dose (5.4 mg/kg/hr for 24-48 hours) of the corticosteroid methylprednisolone (Bracken et al., 1990; Bracken et al., 1997).

Finally, the evolution of tree shrew and primate spinal cords, including marmosets, seems to follow straightforward mathematical plots. Evidence in this study, together with previous investigations of spinal cord scaling (Fox and Wilczynski, 1986; MacLarnon, 1995; MacLarnon, 1996), suggests that selection pressures on the spinal cord are similar throughout the tree shrew and primate lineages. These selection pressures, however, are different than those of the brain, which follow different allometric scaling rules (Herculano-Houzel et al., 2007). One popular interpretation in allometric scaling of cortex is that 1) certain areas of the brain are responsible for social intelligence, 2) an increase in cortical size over the normal brain/body ratio may correlate with increased social intelligence, and 3) natural selection has favored primates capable of increased social complexity. As the spinal cord has not been hypothesized to have any involvement in social intelligence (Krompecher and Lipak, 1966), this may be one fundamental difference as to why brains and spinal cords have different scaling rules.

Unresolved issues

During the course of this research a number of questions were raised that were not completely answered. The more interesting topics from each study will be presented here.

In chapter two, the areas giving the best responses to motor stimulation were M1, 3a, and to some extent 3b. Fewer responses were evoked from premotor areas and from the caudal somatosensory area 1/2, making these two regions the least understood. In

some primates premotor cortex consists of five areas which can all be subdivided based on connectivity patterns, architectonics, and physiology (Luppino and Rizzolatti, 2000; Rizzolatti and Luppino, 2001). Likewise the somatosensory region caudal to area 3b consists of some combination of areas 1, 2, and 5 in different primates (Padberg et al., 2007). Unfortunately our investigation is not extensive enough to comment on these regions in detail. To define an area completely, several lines of evidence are required: a complete topographic representation of the body, a unique pattern of connectivity, a characteristic histology, and a neuronal population with distinct physiological properties (Felleman and Van Essen, 1991). These lines of evidence have for the most part been satisfied for marmoset areas M1, 3a, and 3b (Burish et al., 2008; Burman et al., 2006; Burman et al., 2008; Huffman and Krubitzer, 2001a; Huffman and Krubitzer, 2001b; Krubitzer and Kahn, 2003; Krubitzer and Kaas, 1990; Qi et al., 2002). For premotor cortex and area 1/2, only the architecture of premotor cortex has been well characterized (Burman et al., 2006). An investigation of architectonics in area 1/2 is necessary, as well as additional investigation into the physiology and the connectivity of both of these regions.

In chapter three, an unavoidable factor in all studies of dorsal column injuries is the completeness of the lesion. Since so few fibers appear to be necessary for normal functioning (Beck, 1976), studies which find little to no change after dorsal column injury must always be questioned for completeness of the lesion. Despite the relatively large lesions in some of our cases, relatively small changes were found in behavior and in somatosensory organization. Thus this dissertation focuses on the positive results, that some cortical reorganization and behavioral deficits are found after injury, despite the

fact that the reorganization and deficits were not as extensive as the lesion size would suggest.

The question of motor effects after a dorsal column lesion is also still a matter of debate. We found little change in motor cortex organization, but our lesions were incomplete. Of the three animals whose motor cortices were investigated in this study, only the galago had a large region of somatosensory cortex that was deprived of inputs, and it only represented one side of the forearm. Unpublished results from macaques have also found few motor changes (Kaas et al., 2008). The question is an interesting one, as motor cortex appears to encode several somatosensory-related features such as limb position and speed (Churchland et al., 2006; Georgopoulos, 1995; Graziano et al., 2002a; Graziano et al., 2002b; Kakei et al., 2003; Wang et al., 2007). But additional studies in primates are required, ones that involve extensive lesions of the dorsal columns while leaving the lateral columns completely intact.

In chapter four, a systematic study of the entire spinal cord was performed. This analysis is informative, but in the brain many of the interesting findings come from comparing subdivisions of the brain with each other. Different brain components appear to be subject to different selection pressures (Clark et al., 2001; Stephan et al., 1981), and it would be interesting to perform this type of component analysis on the spinal cord, dividing the spinal cord either by pathway or by vertebral level. Additionally, there is some question how the methods in this dissertation, using a relatively new homogenization technique to count cells (Herculano-Houzel and Lent, 2005), differ the stereologic method of counting cells (Schmitz and Hof, 2005). A direct comparison of the two techniques may be necessary to relate the findings.

References

Beck CH. 1976. Dual dorsal columns: a review. Can J Neurol Sci 3(1):1-7.

Bracken MB, Shepard MJ, Collins WF, Holford TR, Young W, Baskin DS, Eisenberg HM, Flamm E, Leo-Summers L, Maroon J, et al. 1990. A randomized, controlled trial of methylprednisolone or naloxone in the treatment of acute spinal-cord injury. Results of the Second National Acute Spinal Cord Injury Study. N Engl J Med 322(20):1405-1411.

Bracken MB, Shepard MJ, Holford TR, Leo-Summers L, Aldrich EF, Fazl M, Fehlings M, Herr DL, Hitchon PW, Marshall LF, Nockels RP, Pascale V, Perot PL, Jr., Piepmeier J, Sonntag VK, Wagner F, Wilberger JE, Winn HR, Young W. 1997. Administration of methylprednisolone for 24 or 48 hours or tirilazad mesylate for 48 hours in the treatment of acute spinal cord injury. Results of the Third National Acute Spinal Cord Injury Randomized Controlled Trial. National Acute Spinal Cord Injury Study. Jama 277(20):1597-1604.

Burish MJ, Stepniewska I, Kaas JH. 2008. Microstimulation and architectonics of frontoparietal cortex in common marmosets (Callithrix jacchus). J Comp Neurol 507(2):1151-1168.

Burman KJ, Palmer SM, Gamberini M, Rosa MG. 2006. Cytoarchitectonic subdivisions of the dorsolateral frontal cortex of the marmoset monkey (Callithrix jacchus), and their projections to dorsal visual areas. J Comp Neurol 495(2):149-172.

Burman KJ, Palmer SM, Gamberini M, Spitzer MW, Rosa MG. 2008. Anatomical and physiological definition of the motor cortex of the marmoset monkey. J Comp Neurol 506(5):860-876.

Catania KC, Lyon DC, Mock OB, Kaas JH. 1999. Cortical organization in shrews: evidence from five species. J Comp Neurol 410(1):55-72.

Churchland MM, Santhanam G, Shenoy KV. 2006. Preparatory activity in premotor and motor cortex reflects the speed of the upcoming reach. J Neurophysiol 96(6):3130-3146.

Clark DA, Mitra PP, Wang SS. 2001. Scalable architecture in mammalian brains. Nature 411(6834):189-193.

Courtine G, Bunge MB, Fawcett JW, Grossman RG, Kaas JH, Lemon R, Maier I, Martin J, Nudo RJ, Ramon-Cueto A, Rouiller EM, Schnell L, Wannier T, Schwab ME, Edgerton VR. 2007. Can experiments in nonhuman primates expedite the

translation of treatments for spinal cord injury in humans? Nat Med 13(5):561-566.

Felleman D, Van Essen DC. 1991. Distributed hierarchical processing in the primate cerebral cortex. Cereb Cortex 1:1-47.

Fox JH, Wilczynski W. 1986. Allometry of major CNS divisions: towards a reevaluation of somatic brain-body scaling. Brain Behav Evol 28(4):157-169.

Georgopoulos AP. 1995. Current issues in directional motor control. Trends Neurosci 18(11):506-510.

Gould HJ, 3rd, Cusick CG, Pons TP, Kaas JH. 1986. The relationship of corpus callosum connections to electrical stimulation maps of motor, supplementary motor, and the frontal eye fields in owl monkeys. J Comp Neurol 247(3):297-325.

Graziano MS, Taylor CS, Moore T. 2002a. Complex movements evoked by microstimulation of precentral cortex. Neuron 34(5):841-851.

Graziano MS, Taylor CS, Moore T, Cooke DF. 2002b. The cortical control of movement revisited. Neuron 36(3):349-362.

Herculano-Houzel S, Collins CE, Wong P, Kaas JH. 2007. Cellular scaling rules for primate brains. Proc Natl Acad Sci U S A 104(9):3562-3567.

Herculano-Houzel S, Lent R. 2005. Isotropic fractionator: a simple, rapid method for the quantification of total cell and neuron numbers in the brain. J Neurosci 25(10):2518-2521.

Huffman KJ, Krubitzer L. 2001a. Area 3a: topographic organization and cortical connections in marmoset monkeys. Cereb Cortex 11(9):849-867.

Huffman KJ, Krubitzer L. 2001b. Thalamo-cortical connections of areas 3a and M1 in marmoset monkeys. J Comp Neurol 435(3):291-310.

Jain N, Catania KC, Kaas JH. 1997. Deactivation and reactivation of somatosensory cortex after dorsal spinal cord injury. Nature 386(6624):495-498.

Jain N, Florence SL, Kaas JH. 1995. Limits on plasticity in somatosensory cortex of adult rats: hindlimb cortex is not reactivated after dorsal column section. J Neurophysiol 73(4):1537-1546.

Kaas JH, Qi HX, Burish MJ, Gharbawie OA, Onifer SM, Massey JM. 2008. Cortical and subcortical plasticity in the brains of humans, primates, and rats after damage to sensory afferents in the dorsal columns of the spinal cord. Exp Neurol 209(2):407-416.

Kakei S, Hoffman DS, Strick PL. 2003. Sensorimotor transformations in cortical motor areas. Neurosci Res 46(1):1-10.

Krompecher S, Lipak J. 1966. A simple method for determining cerebralization. Brain weight and intelligence. J Comp Neurol 127(1):113-120.

Krubitzer L, Kahn DM. 2003. Nature versus nurture revisited: an old idea with a new twist. Prog Neurobiol 70(1):33-52.

Krubitzer LA, Kaas JH. 1990. The organization and connections of somatosensory cortex in marmosets. J Neurosci 10(3):952-974.

Luppino G, Rizzolatti G. 2000. The Organization of the Frontal Motor Cortex. News Physiol Sci 15:219-224.

MacLarnon A. 1995. The distribution of spinal cord tissues and locomotor adaptation in primates. J Hum Evol(29):463-482.

MacLarnon A. 1996. The scaling of gross dimensions of the spinal cord in primates and other species. J Hum Evol 30:71-87.

McKenna JE, Whishaw IQ. 1999. Complete compensation in skilled reaching success with associated impairments in limb synergies, after dorsal column lesion in the rat. J Neurosci 19(5):1885-1894.

Nathan PW, Smith MC, Cook AW. 1986. Sensory effects in man of lesions of the posterior columns and of some other afferent pathways. Brain 109 (Pt 5):1003-1041.

Padberg J, Franca JG, Cooke DF, Soares JG, Rosa MG, Fiorani M, Jr., Gattass R, Krubitzer L. 2007. Parallel evolution of cortical areas involved in skilled hand use. J Neurosci 27(38):10106-10115.

Qi HX, Lyon DC, Kaas JH. 2002. Cortical and thalamic connections of the parietal ventral somatosensory area in marmoset monkeys (Callithrix jacchus). J Comp Neurol 443(2):168-182.

Rizzolatti G, Luppino G. 2001. The cortical motor system. Neuron 31(6):889-901.

Schmitz C, Hof PR. 2005. Design-based stereology in neuroscience. Neuroscience 130(4):813-831.

Stephan H, Frahm H, Baron G. 1981. New and revised data on volumes of brain structures in insectivores and primates. Folia Primatol (Basel) 35(1):1-29.

Stepniewska I, Preuss TM, Kaas JH. 1993. Architectonics, somatotopic organization, and ipsilateral cortical connections of the primary motor area (M1) of owl monkeys. J Comp Neurol 330(2):238-271.

Vierck CJ, Jr. 1973. Alterations of spatio-tactile discrimination after lesions of primate spinal cord. Brain Res 58(1):69-79.

Vierck CJ, Jr. 1974. Tactile movement detection and discrimination following dorsal column lesions in monkeys. Exp Brain Res 20(4):331-346.

Vierck CJ, Jr. 1977. Absolute and differential sensitivities to touch stimuli after spinal cord lesions in monkeys. Brain Res 134(3):529-539.

Vierck CJ, Jr., Cooper BY. 1998. Cutaneous texture discrimination following transection of the dorsal spinal column in monkeys. Somatosens Mot Res 15(4):309-315.

Wang W, Chan SS, Heldman DA, Moran DW. 2007. Motor cortical representation of position and velocity during reaching. J Neurophysiol 97(6):4258-4270.

Wu CW, Bichot NP, Kaas JH. 2000. Converging evidence from microstimulation, architecture, and connections for multiple motor areas in the frontal and cingulate cortex of prosimian primates. J Comp Neurol 423(1):140-177.